THE ROLE OF ION CHANNELS IN COORDINATING NEURAL CIRCUIT ACTIVITY IN C*AENORHABDITIS ELEGANS*

A Dissertation Presented By

JENNIFER KATHRYN PIRRI

Submitted to the Faculty of the

University of Massachusetts Graduate School of Biomedical Sciences, Worcester
in partial fulfillment of the requirements for the degree of

DOCTOR OF PHILOSOPHY

March 28, 2013

Program in Neuroscience

THE ROLE OF ION CHANNELS IN COORDINATING NEURAL CIRCUIT ACTIVITY IN C*AENORHABDITIS ELEGANS*

A Dissertation Presented By

JENNIFER KATHRYN PIRRI

The signatures of the Dissertation Defense Committee signifies completion and approval as to style and content of the Dissertation

_____

Mark J. Alkema, PhD., Thesis Advisor

_____

Marc R. Freeman, PhD., Member of Committee

_____

Claire Bénard, PhD., Member of Committee

_____

William R. Kobertz, PhD., Member of Committee

_____

Michael Koelle, PhD., Member of Committee

The signature of the Chair of the Committee signifies that the written dissertation meets the requirements of the Dissertation Committee

_____

Michael Francis, PhD., Chair of Committee

The signature of the Dean of the Graduate School of Biomedical Sciences signifies that the student has met all graduation requirements of the school.

_____

Anthony Carruthers, PhD.
Dean of the Graduate School of Biomedical Sciences

Program in Neuroscience
March 28, 2013

Dedicated in memory of my grandfather, Frank Pirri

Acknowledgements

Like many decisions I have made throughout my life, my decision to go to graduate school was impulsive. It's not that I was without passion for science; the truth is I just had no idea what to do with my excitement. I mostly felt that if anything getting a PhD would buy me more time to figure it out. After my first few months as a graduate student I still felt lost, and then I met Mark. Mark has been an amazing mentor to me during my time here. He is an incredible scientist, a dedicated teacher, and a wonderful friend. With his help and guidance I have found my own voice and renewed my faith as a scientist. Without his mentorship I would not be half as successful as I am today. So, Mark, while I feel a simple thank you is not enough to repay for all you have done for me, I am at a loss for another way to show my gratitude. Thank you, from the bottom of my heart.

Mark has the uncanny ability to assemble an amazing group of people. The Alkema Lab has always been a team of people who could not only work together to produce fabulous science, but also get along as good friends. Jamie Donnelly, my good friend and colleague, it was us at the start of it all – we made it through together, good times and bad. I couldn't have done it without all your support and your friendship. I miss our coffee dates and chatting over our microscopes, but am looking forward to the next chapter in our friendship. Chris Clark, sometimes I feel like we are secretly related. I will never forget our movie trailer breaks or our friendly bets (especially since I always win). Your friendship means

a great deal to me, and I am so happy to count you as part of my Worcester family. Sean Maguire, I miss our daily chats and will always remember all laughs and good times we shared as the two man wolf pack. You are a good friend and I am forever grateful for your constant support and cheerleading. Diego Rayes, it was a great experience to get to know you. I appreciate your wisdom and guidance. Thank you for all the help and advice you have given to me over the years. And finally, Yung-Chi Huang, friend and confidant, I am extremely grateful for all our time together, I could not have asked for a better person to work next to.

I would like to thank the members of the Neurobiology Department. Thank you to all the faculty and staff for your support, discussions, and suggestions about science, and life. This has been an amazing place to work and grow and I could not have had a better experience.

Things are always easier to deal with when you realize that “you are not alone”. So, I would like to thank my UMass support system, Tracy Schmidt, Karen Mruk, and Yuly Fuentes-Medel. These strong, inspirational women have been instrumental to my survival of graduate school. I am grateful for our friendship and look forward to all of our future success.

I am eternally grateful for my “Worcester Family”, Megan Potenti, Christina O’Grady, Andrea Clark, Michael O’Grady, and Chris Clark. You guys have been there for me through good times and bad, I have cried and laughed and shared

more with you than with any group of people who are not directly related to me. You have made my experience here in Worcester truly phenomenal. I could not ask for a better group of people to call my friends.

Mat, even though you came into my life at the end of my career as a graduate student, you have made these last few months feel like magic. Your unwavering faith in me has made it possible for me to make it through the final push. You make me happier than I remember. Thank you for being so wonderful.

Finally, I could not have made it through all of this without my mother, Susan, my father, Frank and my sister (and best friend), Laura. I could not feel more proud to have you as my family. I have no idea how to thank you for everything; all I have is because of you. I feel truly blessed to have a family as rich in love as ours. Thank you for everything.

ABSTRACT

Despite the current understanding that sensorimotor circuits function through the action of transmitters and modulators, we have a limited understanding of how the nervous system directs the flow of information necessary to orchestrate complex behaviors. In this dissertation, I aimed to uncover how the nervous system coordinates these behaviors using the escape response of the soil nematode, *Caenorhabditis elegans,* as a paradigm. *C. elegans* exhibits a robust escape behavior in response to touch. The worm typically moves forward in a sinusoidal pattern, which is accompanied by exploratory head movements. During escape, the worm quickly retreats by moving backward from the point of stimulus while suppressing its head movements. It was previously shown that the biogenic amine tyramine played an important role in modulating the suppression of these head movmemetns in response to touch. We identified a novel tyramine-gated chloride channel, LGC-55, whose activation by tyramine coordinates motor programs essential for escape. Furthermore, we found that changing the electrical nature of a synapse within the neural circuit for escape behavior can reverse its behavioral output, indicating that the *C. elegans* connectome is established independent of the nature of synaptic activity or behavioral output. Finally, we characterized a unique mutant, *zf35*, which is hyperactive in reversal behavior. This mutant was identified as a gain of function allele of the *C. elegans* P/Q/N-type voltage-gated calcium channel, UNC-2. Taken together, this work defines tyramine as a

genuine neurotransmitter and completes the neural circuit that controls the initial phases of the *C. elegans* escape response. Additionally, this research further advances the understanding of how the interactions between transmitters and ion channels can precisely regulate neural circuit activity in the execution of a complex behavior.

TABLE OF CONTENTS

LIST OF TABLES

LIST OF FIGURES

LIST OF MOVIES

LIST OF ABBREVIATIONS

<	less than
5HT	serotonin
ADDC	aromatic amino acid decarboxylase
Ca^{2+}	calcium ion
Ca_V2	P/Q type calcium channel
ChR2	channelrhodopsin-2
Cl^-	chloride ion
EC_{50}	half maximal effective concentration
EMS	ethyl methanesulfonate
E_{rev}	reversal potential
FHM	Familial Hemiplegic Migraine
GABA	gamma-aminobutyric acid
gf	gain-of-function
GF	giant fiber
GFP	green fluorescent protein
GPCR	G protein-coupled receptor
hr	hours
K^+	potassium ion
LG	linkage group
LGCC	ligand-gated chloride channel
LGIC	ligand-gated ion channel
mCherry	red fluorescent protein
Na^+	sodium ion

ND96	oocyte storage/recording buffer
NGM	nematode grown media
NMJ	neuromuscular junction
nt	nucleotide
SEM	standard error of the mean
SNP	single nucleotide polymorphism
TEVC	two electrode voltage clamp
UTR	untranslated region
VGCC	voltage gated calcium channel
α	alpha
β	beta
δ	delta

PREFACE

The experimental work written in Chapter II and a portion of the commentary in the Introduction have been published in peer-reviewed journals. References to publications that represent the work and thoughts contained within these chapters:

Pirri, JK., McPherson, AD., Donnelly, JL., Francis, MM., Alkema, MJ. 2009. A tyramine-gated chloride channel coordinates distinct motor programs of a *Caenorhabditis elegans* escape response. *Neuron* 62:526-538.

Pirri, JK and Alkema, MJ. 2012. The neuroethology of *C. elegans* escape. *Curr Opin Neruobiol*. 22(2): 187-193.

The experimental work in Chapter III has been written as a manuscript for publication at the time of this thesis preparation. I generated all mutants and did all the behavioral and imaging experiments. The manuscript and figures were generated by myself and Dr. Diego Rayes. Dr. Diego Rayes will be credited with authorship on this manuscript for his work performing the electrophysiology experiments and his critical feedback and work on the manuscript.

The experimental work written in Chapter IV is a currently unpublished project done in conjunction with Yung-Chi Hunag. Written here is my contributing half of what we expect to be a co-authored paper. Dr. Diego Rayes will also be credited with authorship on this manuscript for his work performing the electrophysiology. Additionally, authorship will be credited to Dr. Yasunori Saheki and Dr. Corneila

Bargmann for their work generating the UNC-2 and UNC-2 GF rescuing constructs.

CHAPTER I

Introduction

"An instinct, like a gene, is a kind of memory, a gift of time. We are born knowing a thousand things we could not reinvent in a lifetime if we had to start from scratch."

- Jonathan Weiner

"Eat but don't get eaten" is the prevailing motto that guides animal behavior. However, this principle presents a dilemma since foraging often increases the risk of predation. Animals can offset part of these risks by trying to survive a confrontation with a predator. Run, dart, jump, fly, burrow and hide can all improve the prey's odds in such life or death encounters. Time is of the essence so the animal needs to quickly translate sensory information about their environment into action. As a consequence, escape responses are typically robust, use dedicated neuronal structures and have a clear evolutionary purpose (Eaton, 1984). One of the critical features of an escape response is the fast translation of sensory information into a coordinated behavioral output. An animal must not only sense the presence of a predator, but also coordinate distinct motor programs to produce an efficient escape. Despite the current understanding that activity of sensorimotor circuits, through the action of transmitters and modulators, controls complex behaviors like the escape response, we have a limited understanding of how the nervous system directs the flow of information necessary to orchestrate these behaviors. This dissertation explores the neural and molecular pathways that translate sensory input into a coordinated behavioral output using escape behavior as a paradigm.

Simple Circuits and the Study of Coordinated Escape Behaviors

The study of relatively simple circuits has provided some of the rare examples where we know the complete path from sensory input to a coordinated

motor output. Often in escape responses, the nervous system must orchestrate multiple motor programs to produce an effective escape behavior. For example, in the tail-flip escape of the crayfish (Figure I-1) touch to the tail induces powerful abdominal flexures that are spatially and temporally controlled to propel the animal through the water away from the stimulus (Edwards, et al., 1999; Herberholz, et al., 2004). In the C-start escape in goldfish (Figure I-1), lateral stimulation causes the animal to coordinate both the strength and the timing of agonist and antagonist muscle contractions on either side of the body to quickly change direction and move away from the stimulus (Foreman and Eaton, 1993; Korn and Faber, 2005). In the *Tritonia* swim reflex response (Figure I-1), upon touch to the body, the animal initiates a series of coordinated dorsal and ventral body flexures to swim away from predators (Willows, et al., 1973; Katz, 1998). Studies of these complex behaviors have provided crucial insights into fundamental neuronal processes as diverse as synaptic transmission, sensory transduction, decision-making, and learning and memory. However, genetic analyses in these organisms are difficult, leaving the molecular coding of these behaviors relatively unexplored.

Studies in genetically tractable organisms, such as the fruit fly *Drosophila melanogatser* and the roundworm *Caenorhabditis elegans*, have provided some insight into the molecular basis of escape behaviors. In the fly, a strong visual stimulus induces fast flight initiation, where the fly couples leg extension and wing depression to quickly fly away (Figure I-1). The critical motor programs that

control leg extension and wing depression critical for fast flight initiation are coordinated by the giant fiber (GF) neurons (Hammond and O'Shea, 2007; Card and Dickinson, 2008). A number of genes have been identified from genetic screens, which play a role in the development of the GF circuit. These genes play a role in regulating the outgrowth of GF axons, and the formation and maturation of synapses (Allen, et al., 2006). Although the neuronal pathway from the GF neurons to motor neurons is well defined, relatively little is known about its sensory inputs. However, in *C. elegans* the transparency of the animal and simple nervous system offers the possibility to study the function of individual neurons and identify complete neural circuits.

The C. elegans escape response

The nematode *C. elegans* has a robust response to anterior touch. This stimulus initiates a stereotyped behavior where the animal must coordinate several motor sequences in order to execute an efficient escape. Gentle touch to the anterior of the body of the worm induces a reversal coupled with the suppression of foraging head movements followed by a deep ventral bend (omega turn) and a 180˚ change in the direction of locomotion (Figure I-1). Given the genetic tractability of this organism, *C. elegans* is an excellent model for the study of how the nervous system coordinates a complex behavior. Additionally, the complete wiring diagram of the *C. elegans* nervous system is

known, and this provides a framework for understanding neural circuits and sensory processing (White, et al., 1986).

C. elegans moves on its side by propagating a sinusoidal wave of dorsal ventral flexures along the length of its body (Croll, 1975a). Locomotion is accompanied by exploratory head movements, in which the head of the animal sways rapidly from side to side (Figure I-1; Movie II-4). Head and body movements are controlled independently by distinct classes of motor neurons and muscles. Although body bends are restricted to the dorsal-ventral plane, the animal can flex its head in three dimensions. Head movements most likely allow the animal to explore its immediate environment and aid in the search for food, as the tip of worm's nose contains the sensory endings that smell, taste and sense touch. Gentle touch to the body of the animal induces a predictable escape response where the animal moves away from the stimulus. Touch to the tail of the animal causes the nematode to speed up; while touch to the anterior half of the animal induces a quick reversal during which foraging head movements are suppressed (Chalfie, et al., 1985; Alkema, et al., 2005; Figure I-1; Movie II-4). Furthermore, optogenetic activation of the mehcanosensory neurons in the anterior or posterior of transgenic animals that express the light activated channelrhodopsin in these cells induces the same behaviors as gentle touch (Stirman, et al., 2011; Leifer, et al., 2011). Much like the coordination of leg extension and wing depression during a fly escape (Card and Dickinson,

2008; Allen, et al., 2006), the worm coordinates backward locomotion with the suppression of foraging head movements in response to anterior touch.

The neural circuit of C. elegans escape

In the worm, gentle touch to the body is sensed by six mechanosensory neurons; a pair of ALM and the AVM neurons sense touch to the anterior half, while a pair of PLM and the PVM neurons sense touch to the posterior half (Chalfie and Sulston, 1981; Figure I-2). All six neurons send anteriorly directed processes that run close to the cuticle and can sense touch over their entire length. Touch reception is mediated by a DEG/ENaC ion channel complex that can sense the application and removal of forces as small as 100 nN with a latency of less than 5 ms, allowing the animal to quickly respond to even the lightest of touches (O'Hagan, et al., 2005; Geffeney, et al., 2011). The touch sensory neurons make chemical synapses and electrical gap junctions with a set of command-like interneurons that control locomotion. The PVC and AVB locomotion command neurons provide inputs into the VB and DB motorneurons which synapse onto body wall muscles and drive forward movement; the AVD and AVA neurons provide inputs into the VA and DA motor neurons that drive backward locomotion (White, et al., 1986, Figure I-2). Laser ablation studies and genetic perturbations indicate that the activity of the interneurons establishes the direction of locomotion (Chalfie, et al., 1985; Zheng, et al., 1999). Recent calcium imaging studies support this notion, indicating that the reciprocal

activation of AVB and AVA command neurons correlates with forward and backward locomotion respectively (Chronis, et al., 2007; Ben Arous, et al., 2010; Kawano, et al., 2011).

Activation of the anterior touch sensory neurons inhibits command neurons that drive forward locomotion (PVC, AVB) and activates those, which promote backward locomotion (AVD, AVA), causing the animal to back away from the stimulus (Figure I-2). During this reversal, the animal also suppresses foraging head movements. The RIM neurons are connected to the backward locomotion circuitry via gap junctions with the AVA command neurons. Optogenetic activation of the RIM neurons causes an increase in intracellular calcium in the AVA, suggesting that the AVA and RIM are co-activated during a backing response (Guo, et al., 2009).

Tyramine and Behavior

The RIM sits in a unique position, making synaptic contacts with the forward locomotion command neurons, AVB, as well as the motor neurons and neck muscles that facilitate foraging head movements (White et al., 1986; Figure I-2). This connectivity, coupled with the data that shows the RIM is activated concurrently with the backward locomotion command neurons, AVA (Guo, et al., 2009) suggests that the RIM is may link the locomotory neural circuit with the neural circuit that controls head movements. The RIM neurons express tyrosine decarboxylase (TDC-1), the biosynthetic enzyme that converts tyrosine into

tyramine (Alkema, et al., 2005). In invertebrates, tyramine was long thought to be the biogenic precursor of octopamine, which is a well-established neurotransmitter (Roeder, et al., 2003). However, the biosynthetic enzyme tyramine β-hydroxylase (TBH-1) that is necessary to convert tyramine to octopamine is not expressed by the RIM neurons (Alkema, et al., 2005; Figure I-3). This suggests that there are distinct cells in the nervous system that might utilize tyramine as a neurotransmitter or a neurohormone.

The role for tyramine as an independent signaling molecule in invertebrate behavior is largely unexplored. G-protein coupled receptors (GPCRs) that respond to tyramine have been found in *Drosophila*, the locust, the honey bee, the silk moth, the freshwater prawn and the nematode (Saudou, et al., 1990; Blenau and Baumann, 2001; Ohta, et al., 2003; Reyes-Colón, et al., 2010; Rex and Komuniecki, 2002; Rex, et al., 2005; Borowsky, et al., 2001; Bunzow, et al., 2001), supporting the notion that tyramine itself might act as a neurotransmitter in invertebrates. Similar to *C. elegans*, distinct tyraminergic cells have been identified in the central complex of the locust and the central nervous system of *Drosophila* (Homberg, et al., *In Press*; Nagaya, et al., 2002). Furthermore, in these insects, tyramine alone has been linked to several physiological processes. It has been shown to change the chloride conductance in the *Drosophila* renal tube, inhibit excitatory junction potentials at both the *Drosophila* and locust neuromuscular junctions (NMJ), affect behavioral responses to cocaine and modulate attraction to ethanol in *Drosophila* (Blumenthal, et al., 2005; Kutsukake,

et al., 2000; Donini and Lange, 2004; McClung and Hirsh, 1999; Schneider, et al., 2012). In *C. elegans,* tyramine deficient animals (*tdc-1*), or animals in which the single pair of tyraminergic RIM neurons are ablated fail to suppress head movements and back up less far in response to touch, behavioral defects that are not shared by octopamine deficient mutants (*tbh-1*) (Alkema, et al., 2005; Figure I-3). Furthermore, recent studies show that tyramine GPCRs may play a role in a modulating the behavioral response to environmental cues and affect decision making (Bendesky, et al., 2011). These studies provide evidence to suggest that tyramine may have an independent role in *C. elegans* behavior.

Although tyramine was often thought of as a metabolic byproduct or precursor to classical biogenic amines in the mammalian nervous system, identification of a family of GPCRs reactive to tyramine and β- phenylethylamine indicates they may also play a more physiological role in the mammalian brain (Borowsky, et al., 2001; Bunzow, et al., 2001). Tyramine is produced in trace amounts in the mammalian nervous system, through the conversion of tyrosine by the biosynthetic enzyme, aromatic amino acid decarboxylase (AADC). AADC is also required for the biosynthesis of dopamine, serotonin and noradrenaline. Evidence suggests that distinct tyraminergic neurons might also exist in the mammalian brain. Within the mammalian CNS there are several regions that express AADC, but do not produce dopamine, serotonin or noradrenaline (Jaeger, et al., 1984; Beltramo, et al., 1993). Tyramine immunoreactivity is strongly observed in the hypothalamus, and only subsets of these cells are

dopaminergic or noradrenergic (Kitahama, et al., 2005). Following stimulation, endogenous tyramine is released from rat striatal slices, indicating that tyramine can be secreted from neurons in an activity dependent manner (Dyck, 1989). These data suggest that distinct populations of tyraminergic cells exist in the mammalian brain, and that tyramine might function as a signaling molecule in mammals as well as invertebrates. Although the role for tyramine in mammalian behavior is currently unknown, deregulation of this trace amine has been implicated in the etiology of a variety of neurological disorders including depression, schizophrenia, attention deficit hyperactivity disorder (ADHD) and migraine (Boulton, 1980; Branchek and Blackburn, 2003; D'Andrea, et al., 2004).

Octopamine and tyramine are often considered the invertebrate counterparts of the structurally related monoamines noradrenaline and adrenaline (Roeder, 2005). In mammals, adrenergic transmitters coordinate the increase in heart rate, muscle tone, oxygen supply to the brain and release of glucose for the increase burst of energy required for the fight-or-flight escape response (Brede, et al., 2004). Similarly, in invertebrates octopamine and tyramine have been implicated in orchestrating the sting response in honeybees, the fight or flight response of locusts, subordinate behavior in lobsters, and aggressive behavior in *Drosophila* and crickets (Burrell and Smith, 1995; Adamo, et al., 1995; Kravitz, 1988; Certel, et al., 2007; Zhou, et al., 2008; Stevenson, et al., 2005). This suggests that monoaminergic signaling might be a universal mechanism for coordinating behaviors during a stress or escape response.

However, how these molecules execute this task remains poorly understood. Previous data has indicated that tyramine plays an important role in coordinating the motor programs of the *C. elegans* escape response (Alkema, et al., 2005). Given that tyramine deficient animals cannot appropriately execute evasion of gentle touch, it is possible that tyramine acts directly as the signaling molecule necessary to orchestrate this response. My research aims to understand how tyramine modulates the escape response and determine the molecular coding and neural circuitry required to coordinate this behavior

Outline of Thesis

My thesis work focuses on the role of tyramine in the coordination of motor programs necessary for the *C. elegans* escape response. To identify receptors and components involved in the tyramine-signaling pathway, we performed a genetic screen to isolate mutants resistant to immobilization induced by the exogenous application of tyramine. Chapter II describes the identification and characterization of the novel ligand-gated chloride channel, LGC-55, which is activated by tyramine. LGC-55 is expressed in neurons and muscle cells that are postsynaptic to the tyraminergic neuron, the RIM, and we found that the activation of LGC-55 by tyramine coordinates the backward locomotion and head movement motor programs during the escape response initiated by touch. This work identifies tyramine as a classical neurotransmitter and delineates the neural circuit that controls the initial phases of the escape response.

Chapter III investigates whether it is possible to change the behavioral outputs of a neural circuit by changing the electrical sign of a synapse. In Chapter II we identified a homomeric receptor, LGC-55, that acts postsynaptically of the tyraminergic neurons to control distinct behaviors. Since there is a single pair of neurons that release tyramine and a single ionotropic postsynaptic receptor, we have a unique opportunity to determine if changing the sign of a receptor can affect the behavioral output of a defined neural circuit. To test this idea we engineered LGC-55 to change its ion selectivity from anions to cations, and generated transgenic animals that expressed the chimeric LGC-55 cation channel. Our experiments show that changing the nature of the synapse within a neural circuit can reverse behavioral output and indicates the *C. elegans* connectome is established independent of the nature of synaptic transmission.

Finally, in a screen for tyramine resistant mutants we isolated a unique hyperactive mutant, *zf35.* Chapter IV describes the identification and characterization of the *zf35* allele. We identified *zf35* as a gain-of-function allele of *unc-2*, which encodes the alpha subunit of a P/Q/N-type voltage-gated calcium channel (Ca_V2). Synaptic activity converges onto presynaptic voltage-gated Ca^{2+} channels (Ca_V) that exert control on neurotransmission within dynamic signaling networks. Neurotransmitters can in turn directly regulate the activity of Ca_V channels by activating GPCRs. $G_{\beta\gamma}$ proteins interact with calcium channels to inhibit their activity, modulating the excitability of postsynaptic neurons (Dascal, 2001; Zamponi and Snutch, 1998). We found that the *zf35* lesion causes an

increase in channel conductance and a shift in the activation voltage, leading to an increase in neurotransmission. Perturbation of Ca_V2 channel function in this manner disrupts the timing and control of distinct motor programs, resulting in the hyperactivity exhibited by *zf35* animals. This mutation causes changes in the biophysical properties of the channel similar to mutations in found in patients with Familial Hemiplegic Migraine (FHM), suggesting *unc-2(zf35)* has the potential to serve as an invertebrate model for the study of FHM.

Figure I-1

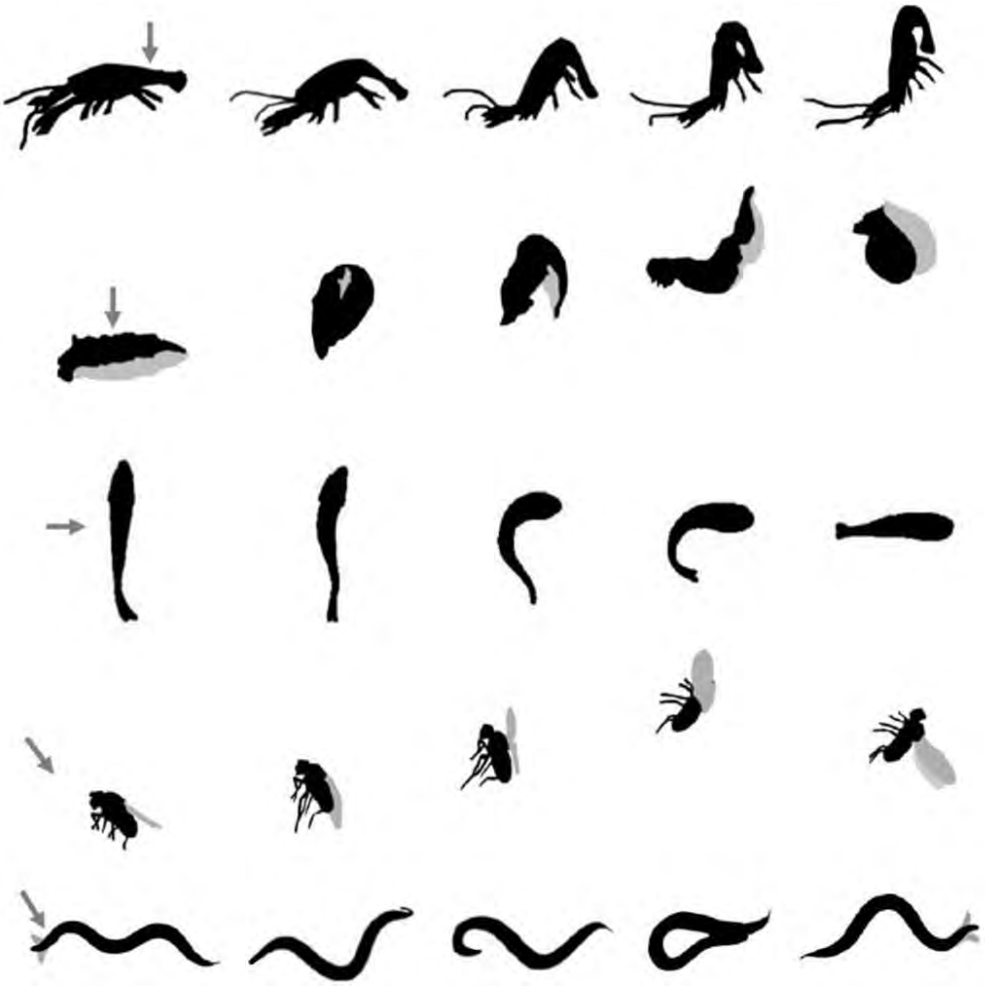

Escape responses.

Silhouettes of animal escape responses. Arrows indicate the direction of the threatening stimulus. Crayfish tail-flip (top): Time from first to last frame is approximately 15 ms (Edwards, et al., 1999; Herberholz, et al., 2004). *Tritonia* swim reflex: Time from first to last frame is approximately 5 s (Willows, et al., 1973). Goldfish C-start: Time from first to last frame is approximately 50 ms (Foreman and Eaton, 1993). *Drosophila* startle response: Time from first to last frame is approximately 25 ms (Card and Dickinson, 2008). *C. elegans* anterior touch response: Time from first to last frame is approximately 10s (Alkema, et al., 2005).

Figure I-2

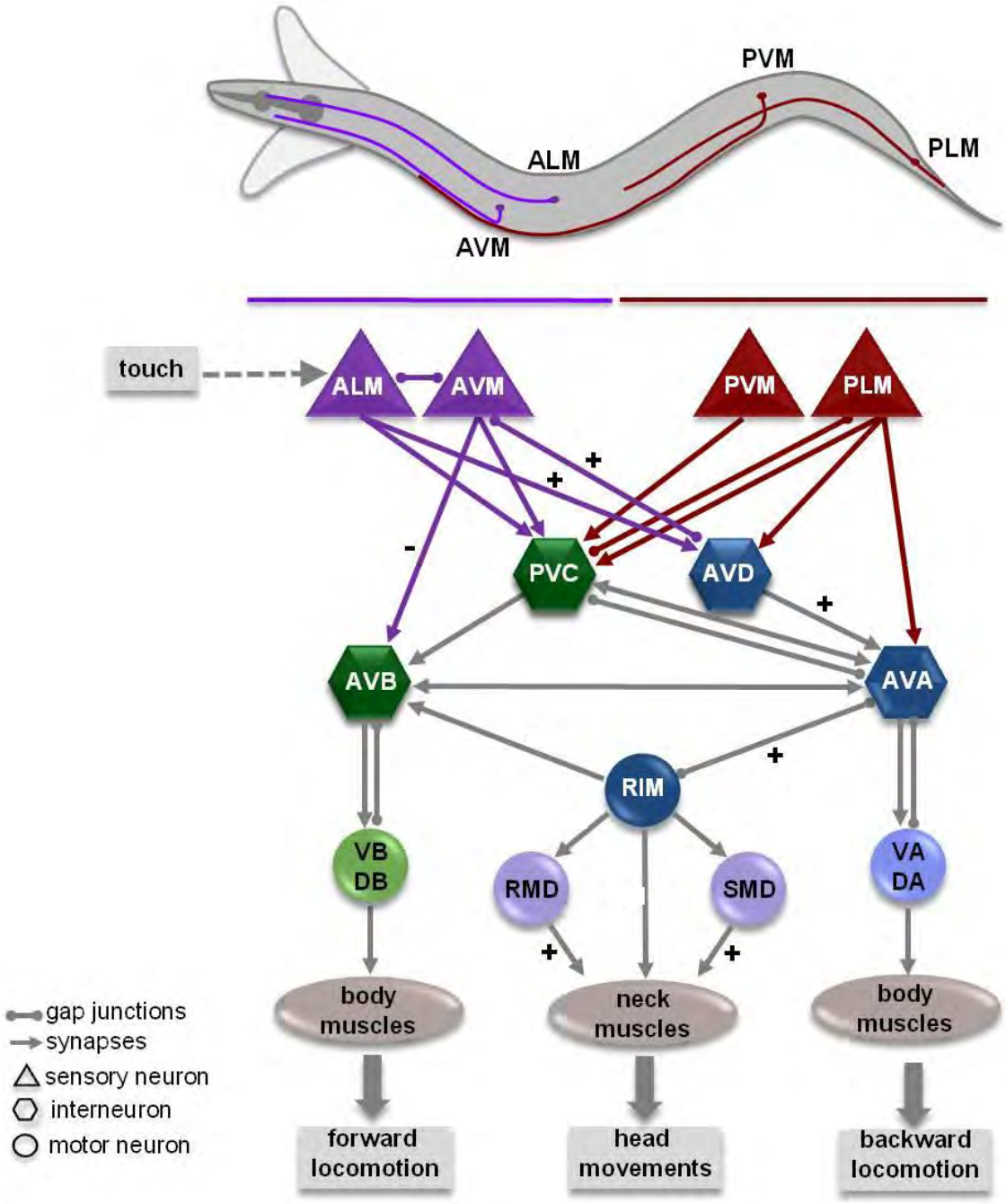
PVM
ALM
PLM
AVM
touch
ALM
AVM
PVM
PLM
+
+
-
PVC
AVD
+
AVB
AVA
+
RIM
VB
DB
RMD
SMD
VA
DA
+
+
body
muscles
neck
muscles
body
muscles
gap junctions
synapses
sensory neuron
interneuron
motor neuron
forward
locomotion
head
movements
backward
locomotion

Figure I-2

***C. elegans* escape circuit.**

Top: *C. elegans* moves its head rapidly from side to side during forward locomotion as indicated by the outline. The relative cell body position and neuronal process of neurons responsible for sensing touch (purple: anterior touch; red: posterior touch) are depicted.

Bottom: The circuit diagram illustrates the connections between the sensory neurons and those that control locomotion and head movements. Synaptic connections (arrows) and gap junctions (spheres) are as described by White, et al. (1986). Sensory neurons are shown as triangles; command neurons required for locomotion are shown as hexagons, and motor neurons as circles. Excitatory (+) and inhibitory (-) connections involved in the anterior touch escape response are noted. Anterior touch activates the AVA backward locomotion command neuron, which in turn activates the tyraminergic RIM motor neuron, which makes synapses on to the AVB forward locomotion command neuron and cells of the head movement circuit: RMD, SMD, and neck muscles (Chalfie, et al., 1985; Alkema, et al., 2005).

Figure I-3

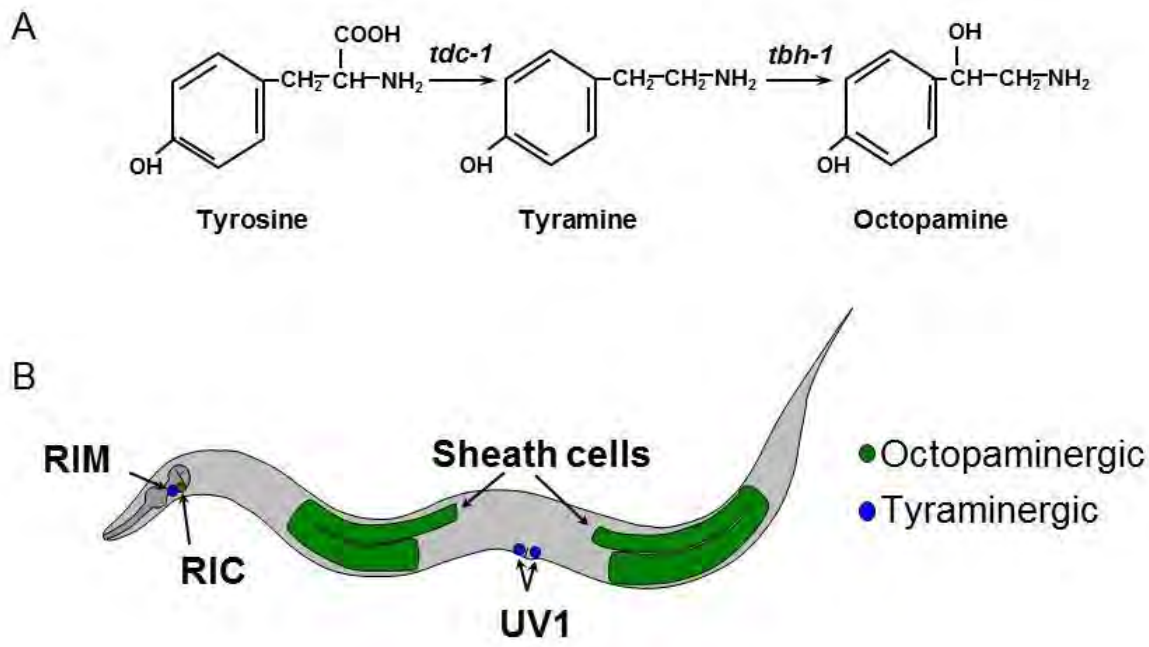

Tyramine acts independently of octopamine in *C. elegans*.

A) Biosynthetic pathway of octopamine in *C. elegans*. Tyramine decarboxylase (TDC-1) converts tyrosine to tyramine; subsequently tyramine β-hydroxylase (TBH-1) converts tyramine to octopamine.

B) Schematic diagram of the location of tyraminergic and octopaminergic cells. RIM and UV1 (blue) express *tdc-1* but not *tbh-1* indicating that tyramine is the end product of the biosynthetic pathway. RIC and the gonadal sheath (green) express both *tdc-1* and *tbh-1*, resulting in the production of octopamine as the final product of the pathway.

CHAPTER II

A Tyramine-Gated Chloride Channel Coordinates Distinct Motor Programs of a *Caenorhabditis elegans* Escape Response

The work in this chapter is reprinted from a published manuscript of the same title, which appeared in *Neuron* (2009) 62. Authorship was given to Adam McPherson for help with cell identifications, to Jamie Donnelly for performing the genetic screen that isolated the *lgc-55* mutants as well as for doing the tyramine dose response experiment in Figure II-2, and to Michael Francis for performing the *in vivo* electrophysiology in Figure II-4.

Abstract

A key feature of escape responses is the fast translation of sensory information into a coordinated motor output. In *C. elegans* anterior touch initiates a backward escape response in which lateral head movements are suppressed. Here we show that tyramine inhibits head movements and forward locomotion through the activation of a tyramine-gated chloride channel, LGC-55. *lgc-55* mutant animals have defects in reversal behavior and fail to suppress head oscillations in response to anterior touch. *lgc-55* is expressed in neurons and muscle cells that receive direct synaptic inputs from tyraminergic motor neurons. Therefore, tyramine can act as a classical inhibitory neurotransmitter. Activation of LGC-55 by tyramine coordinates the output of two distinct motor programs, locomotion and head movements that are critical for a *C. elegans* escape response.

Introduction

Biogenic amines play an important role in the modulation of behaviors in a wide variety of organisms. In contrast to the classical biogenic amines, like dopamine or serotonin, roles for trace amines in the nervous system remain elusive. The trace amine, tyramine is found in the nervous system of animals ranging from nematodes to mammals. Tyramine has often been considered as a metabolic byproduct, or intermediate in the biosynthesis, of the classical biogenic amines. However, the characterization of invertebrate and mammalian G-protein coupled receptors that can be activated by tyramine has peaked new interest in the role of tyramine in animal behavior and physiology. The mammalian trace-amine associated receptor TAAR1, has a high affinity for tyramine and beta-phenylethylamine and is broadly expressed in the mammalian brain (Borowsky et al., 2001; Miller et al., 2005). Tyramine responsive G-protein coupled receptors have been characterized in fruit flies, locusts, honeybees, silk moths and nematodes (Blenau et al., 2000; Ohta et al., 2003; Rex et al., 2005; Rex and Komuniecki, 2002; Saudou et al., 1990). However, it is unclear whether tyramine is the endogenous ligand for these receptors and the role of tyramine in animal physiology and behavior remains relatively unexplored.

Like in mammals, tyramine levels in invertebrates are much lower than those of the classic invertebrate biogenic amines, dopamine, serotonin and octopamine (Cole et al., 2005; Monastirioti et al., 1996). In invertebrates tyramine

is also a precursor in the biosynthesis of octopamine, often considered to be the invertebrate analog of norepinephrine (Roeder et al., 2003). In *C. elegans* tyramine is synthesized from tyrosine by a tyrosine decarboxylase (*tdc-1*), and a tyramine beta-hydroxylase (*tbh-1*) is required to convert tyramine to octopamine (Alkema et al., 2005). TDC-1 and TBH-1 are co-expressed in a single pair of interneurons, the RICs, and in gonadal sheath cells, indicating that these cells are octopaminergic. TDC-1 is also expressed on its own in the RIM motor neurons and the uterine UV1 cells suggesting that these cells are uniquely tyraminergic in *C. elegans*. Furthermore, animals that lack tyramine and octopamine (*tdc-1* mutants) have behavioral defects that are not shared by animals that only lack octopamine (*tbh-1* mutants), indicating a distinct role for tyramine in *C. elegans* behavior (Alkema et al., 2005). *tdc-1* mutants, unlike *tbh-1* mutants, have defects in egg laying, reversal behavior and fail to suppress head movements in response to gentle anterior touch. The *C. elegans* neural wiring diagram (White et al., 1986) and cell ablation studies indicate that the tyraminergic RIM motorneurons link the neural circuits that control locomotion and head movements. In the wild, the suppression of head movements in response to touch may allow the animal to escape nematophagous fungi that trap nematodes with constricting hyphal rings (Barron, 1977).

The study of relatively simple circuits in invertebrates has provided fundamental insights on how biogenic amines change the output of distinct motor programs (Marder and Bucher, 2001; Katz et al., 1994; Nusbaum and

Beenhakker, 2002). In this report, we show that tyramine inhibits head movements and induces long backward runs through the activation of a tyramine-gated chloride channel, LGC-55. *lgc-55* is expressed in cells that are postsynaptic to the tyraminergic RIM neurons and the activation of LGC-55 inhibits the neural circuits that drive head movements and locomotion. Our data firmly establish tyramine as a genuine neurotransmitter in *C. elegans* and suggest that fast inhibitory tyraminergic transmission plays a critical role in coordinating a *C. elegans* escape response.

Experimental Procedures

Genetic Screen, Mapping and Cloning of LGC-55

All strains were cultured at 22˚C on NGM agar plates with the *E. coli* strain OP50 as a food source. The wild-type strain was Bristol N2. All strains were obtained from the *C. elegans* Genetics Center (CGC) unless otherwise noted. Wild-type animals were mutagenized with 50 mM EMS (Brenner, 1974). Young adult F2 progeny of approximately 14.000 mutagenized F1 animals were washed twice with water and transferred to 40 mM tyramine plates. After 10 to 20 minutes animals that displayed sustained head or body movements were picked to single plates. Primary isolates were retested on 30 mM tyramine. Twelve mutants were isolated, of which only *zf11* and *zf53* were sensitive to the inhibitory effects on body movements but resistant to the inhibitory effects on head movements.

We mapped *lgc-55(zf11)* to LG V using the SNP mapping procedure as previously described (Wicks et al., 2001; Davis et al., 2005). Further three factor mapping placed *lgc-55(zf11)* to the left of *rol-9* close to *unc-51.* Full-length *lgc-55* cDNA sequence was obtained from the expressed sequence tag (EST) clone yk1072c.07. Standard techniques for molecular biology were used. ClustalW alignments were carried out using MacVector software (Accelrys). The *lgc-55* deletion allele was obtained from National Bioresource Project and outcrossed four times.

All transgenic strains were obtained by microinjection of plasmid DNA into the germline. At least three independent transgenic lines were obtained and data are from a single representative line. An *lgc-55* rescue construct was made by cloning a *lgc-55* genomic fragment corresponding to nucleotide (nt) -2663 to +3895 relative to the translation start site into the EcoRV site in yk1072c7. For muscle specific rescue an Acc65I/XhoI fragment containing the full-length *lgc-55* cDNA was cloned into pPD95.86 behind the *myo-3* promoter. A 2751 bp genomic fragment upstream of the *sra-11* translation start site was fused to the full-length *lgc-55* cDNA for expression of LGC-55 in the AVB, AIA and AIY, as well as to GFP for expression analysis. A PstI/Acc65I fragment from the vector pV6 containing the *glr-1* promoter was fused to the full-length *lgc-55* cDNA for expression of LGC-55 in head neurons including RMD, SMDD, and SMDV. A 3545 bp genomic fragment upstream *lim-4* translation start site was fused to the full-length *lgc-55* cDNA for expression of LGC-55 in RMD and other head

neurons. LGC-55::GFP translational fusion constructs were made by cloning GFP into an engineered AscI restriction in the genomic rescuing construct in the sequence encoding the intracellular loop between TM3 and TM4 (See Figure II-3C). Transgenic animals for cell specific rescue experiments were made by co-injecting genomic, LGC-55::GFP, *myo-3*::LGC-55, *sra-11*::LGC-55, *glr-1*::LGC-55 or *lim-4*::LGC-55 plasmids at 20 ng/µl along with the *lin-15* rescuing plasmid pL15EK at 80 ng/µl into *lgc-55(tm2913); lin15(n765ts)* animals. *lgc-55::gfp* and *lgc-55::mCherry* transcriptional fusion constructs were made by cloning a genomic fragment corresponding to nt -2663 to +3859 relative to the translational start site into the following vectors pPD95.70 (GFP) and pPD95.70Cherry (mCherry). The membrane targeting signal sequence corresponding to nt +4 to +48 relative to the *lgc-55* translational start site was removed using site directed mutagenesis. GFP and mCherry constructs were microinjected along with the *lin-15* rescuing plasmid, pL15EK, at 80 ng/µl into *lin15(n765ts)* animals.

Cell Identification

Identifications of cells that expressed the *lgc-55::mCherry* reporter were based on cell body positions, axon morphologies and co-expression with previously described cell specific GFP markers. Strains containing the following fusion genes were used to confirm cell identification: IL1: *sEx15005* (*y111b2a.8*::GFP), AVB: *otIs123* (*sra-11::*GFP), RMD, SMDD. SMDV: *kyIs29*

(*glr-1::*GFP), and ALN, SDQ: *otIs107* (*ser-2::*GFP). All strains were examined for co-expression of GFP and mCherry by fluorescence microscopy.

Behavioral Assays

All behavioral analysis was performed with young adult animals (24 hours post L4) at room temperature (22-24°C); different genotypes were scored in parallel, with the researcher blinded to the genotype. To quantify tyramine resistance, young adult animals were transferred to agar plates supplemented with 30 mM tyramine and the percentage of immobilized animals was scored every minute for a 20-minute period. Body and head movements were scored separately. Body movement was defined as sustained locomotion for more than 5 seconds, and head movement was defined as sustained lateral swings of the head (anterior to the posterior pharyngeal bulb) only. Wild-type animals paralyzed on 30 mM tyramine within 3-5 minutes. Tyramine plates were prepared by autoclaving 1.7% agar in water, cooling to ~55°C and adding glacial acetic acid to a concentration of 2 mM and tyramine-HCl (Sigma) to a concentration of 30 mM.

To quantify the effect of tyramine on backward locomotion, animals were transferred in a small drop of water to agar plates with or without 30 mM tyramine (tyramine free plates were made as described above, without the addition of tyramine). The drop of liquid was quickly dried with a KimWipe, with care taken not to disturb the animal. Once the spot was dry, the animals were filmed using

an Imaging Source DMK 21F04 firewire camera and Astro IIDC software, for 5 minutes or until the animal became paralyzed. The length of each reversal was quantified by counting the number of backward body bends. A backward body bend was defined as half of a sine wave and quantified by counting the number of bends made in the posterior body region during backward runs. The data represent the longest average reversal made within the time interval.

Spontaneous reversal frequency was scored on unseeded NGM agar. Animals were transferred from their culture plate to an unseeded plate and allowed to crawl away from any food that might have been transferred. The animals were then gently transferred without food to another unseeded plate and allowed to recover for 1 minute. After the recovery period the animals were filmed for 3 minutes. The reversal frequency was determined as described in Tsalik and Hobert (2003), and reversal length was scored according to Gray et al. (2005). Animals that crawled to the edge of the plate during filming were discarded. To quantify backward locomotion in response to touch, animals were touched gently with an eyelash posterior to the pharynx and the number of backward body bends made in response to the touch was counted. The suppression of head oscillations was scored as described by Alkema, et al. (2005).

Mosaic Analysis

Strains used for mosaic analysis (QW231 and QW232) were made by coinjecting *myo-3::*GFP (50ng/ul)*, lgc-55::*mCherry (30 ng/µl)*,* the *lgc-55* rescuing construct (20ng/µl) and *lin-15* rescuing plasmid pL15EK (80 ng/µl) into *lgc-55(tm2913); lin15(n765ts)* animals. To facilitate the identification of animals that lost the extrachromosomal array in the AB lineage, we selected multivulva (Muv) animals that expressed *myo-3::*GFP. Animals that lost the extragenic array the P1 lineage were selected by picking non-Muv animals that did not express *myo-3::*GFP. Animals that lost the rescuing array in either AB or P1 lineages and non-mosaic controls were tested for the suppression of head oscillations, head paralysis and backward locomotion on exogenous tyramine as described above. Once behavioral assays were completed animals were mounted and examined for the presence of GFP and mCherry using fluorescence microscopy to confirm expression of the array in the appropriate cell type. Animals not expressing the array in all neck muscle or all head neurons were discarded.

Electrophysiology of LGC-55

An EagI/XhoI fragment containing the full length LGC-55 cDNA, including the 5' and 3' UTRs was cloned into the EagI/XhoI site of the vector pSGEM for oocyte expression. Capped RNA was prepared using T7 polymerase from Promega. Stage V and VI oocytes from *X. laevis* were injected with ~50 ng of cRNA. Two electrode voltage clamp experiments were performed 2-3 days post

injection at room temperature (22-24°C). The standard bath solution for dose response and control experiments was ND96: 96 mM NaCl, 2 mM KCl, 1.8 mM $CaCl_2$, 1 mM $MgCl_2$, 5 mM HEPES. For dose response experiments, oocytes were voltage clamped at -60 mV and were subjected to a 10 second application of neurotransmitter (1-1000 μM, in ND96) with 2-3 minute washes between each application. All dose response data were normalized to the mean maximum current observed for tyramine. Data were gathered in 12 independent experiments for each neurotransmitter (totaling 31 eggs), using oocytes from different frogs. Data were consistent between the different batches of oocytes and represent the mean of at least four recordings for each dose of neurotransmitter.

The reversal potential of LGC-55 expressing oocytes was first determined in standard ND96 (as above). For the sodium permeability test, we substituted 96 mM NMDG for NaCl. The Cl^- permeability test was performed in 10% NaCl (9.6 mM NaCl, 86.4 mM sodium gluconate, 2 mM KCl, 1.8 mM $CaCl_2$, 1 mM $MgCl_2$, 5mM HEPES). All points represent the response to an application of 10 μM TA for 10 s at the indicated holding potentials. Data were normalized tyramine current at -60 mV and averaged for 4-5 oocytes per data point. We used 3 M KCl filled electrodes with a resistance between 1-4 MΩ. We used agarose bridges to minimize liquid junction potentials and liquid junction potentials occurring at the tip of the recording electrodes were corrected prior to recording. Currents were recorded using Warner Instrument OC-725 two-electrode voltage clamp (TEVC)

and data were acquired with Digidata 1322A using pClamp 9 (Axon Instruments). Normalized dose response data were fit to the Hill equation $\log(\theta/1-\theta) = n\log[L] - n\log K_A$. Reversal potential ($E_{rev}$) was calculated by determining the x intercept of the linear regression line of each I-V curve and averaged for 4-5 oocytes. Whole-cell voltage-clamp recordings of *C. elegans* muscle cells were performed as previously described in Francis, et al (2005). In short, recording pipettes were filled with an intracellular solution of 25 mM KCl and 115 mM K-gluconate. Muscle cells were voltage clamped at -60 mV and 200 μM tyramine was pressure applied for 250 ms. The reversal potential of LGC-55 in *C. elegans* body wall muscle was determined using voltage steps in 20 mV increments. Data were normalized to the I_{max} for each animal and averaged across 3 to 4 animals. Curve fitting and statistical analyses were performed with Prism version 5.0a for Mac OS X (GraphPad Software).

Results

Exogenous tyramine induces backward locomotion and inhibits head movements.

C. elegans moves on its side in a sinusoidal pattern by propagating dorso-ventral waves of body wall muscle flexures along the length of its body. Locomotion is accompanied by exploratory head movements, where the tip of the nose of the animal moves from side to side. Head movements are controlled independently from body movements by a set of radially symmetric head and

neck muscles. The tyraminergic RIM motorneurons make synaptic connections with neck muscles that control head movements and command neurons that drive locomotion (Figure II-1). To study how tyramine signaling might control head and body movements during locomotion, we developed a simple assay for measuring behavioral responses to tyramine. We found that wild-type animals became immobilized on agar plates containing exogenous tyramine in a dose-dependent manner (Figure II-2). In extended behavioral studies of individual worms in the presence of 30 mM exogenous tyramine, we noted a progressive sequence of behaviors that were nearly invariant from animal to animal (Figure II-1). Wild-type animals displayed a brief period of forward locomotion in which head movements ceased completely, while sinusoidal body movements in the posterior half of the animal persisted. Immobilization of head movements was followed by strikingly long backward locomotory runs (Figure II-1A, Figure II-12D, and Movie II-1). Following this behavioral sequence, most wild-type animals became completely immobilized within 5 minutes of tyramine exposure. Locomotion could still be triggered in immobilized animals by mechanical stimulation with a platinum wire. However, movements were restricted to the posterior half of the animal (body movements) while the head remained paralyzed (Movie II-2). These results support the idea that exogenous tyramine affects head movements and locomotory body movements through distinct tyraminergic signaling pathways.

***lgc-55* mutants are partially resistant to exogenous tyramine.**

To identify genes involved in tyramine signaling we performed a genetic screen for mutants that are resistant to the paralytic effects of exogenous tyramine. We placed F2 progeny of 10,000 mutagenized hermaphrodites on agar plates containing 30 mM tyramine and selected rare mutants that displayed sustained body and/or head movements. Two mutants isolated from this screen, *zf11* and *zf53*, became immobilized slightly more slowly than wild-type animals and continued head movements on plates containing exogenous tyramine (Figure II-1B and II-1C). However, neither *zf11* nor *zf53* mutant animals displayed any body movements posterior to the pharynx (See Movie II-3). Furthermore, exogenous tyramine failed to induce long backward locomotory runs in the *zf11* and *zf53* mutants (See Figure II-12D). *zf11* and *zf53* mutant animals were healthy and viable with normal brood sizes and had no obvious defects in locomotion pattern or head movements in the absence of exogenous tyramine.

We mapped *zf11* using single nucleotide polymorphisms and three-factor mapping to the right of chromosome V close to *unc-51* (Figure II-3A). This genomic region contains a gene, *lgc-55*, which encodes a protein with similarity to members of the cysteine-loop ligand-gated ion channels (Cys-loop LGIC) (Figure II-3B) (Betz, 1990). Sequence analysis revealed single-base transitions in the *lgc-55* coding sequence in *zf11* and *zf53* mutants. The *lgc-55* gene structure

was confirmed by analysis of expressed sequence tagged full-length cDNA clones. The predicted LGC-55 protein is comprised of a large extracellular ligand-binding domain with a characteristic Cys-loop motif, four transmembrane domains (M1-M4) and a large intra-cellular domain between M3 and M4 (Figure II-3C). The *zf11* allele mutates a splice acceptor site of exon 9, which causes a frame shift that would lead to premature truncation of the LGC-55 protein. The *zf53* allele converts the first cysteine codon of the Cys-loop to a tyrosine (C215Y). The cysteines of the Cys-loop motif in the N-terminal extracellular ligand-binding region of each subunit form a disulphide bond that plays a key role in receptor assembly (Green and Wanamaker, 1997) and gating of the ion channel (Grutter et al., 2005). We also obtained an available deletion allele *tm2913,* which deletes parts of both exon 4 and 5 of the *lgc-55* gene. The deletion should prematurely truncate the LGC-55 protein and therefore most likely represents a null allele. Like *lgc-55(zf11)* and *lgc-55(zf53)* mutants, *lgc-55(tm2913)* mutants animals are resistant to tyramine-mediated head paralysis, suggesting that *lgc-55(zf11)* and *lgc-55(zf53)* also represent loss-of-function alleles. We were able to restore tyramine sensitivity by expressing a transgenic *lgc-55* minigene in *lgc-55* mutants (Figure II-1C). These data indicate that *lgc-55* is required for the paralytic effects of exogenous tyramine on head movements.

LGC-55 is an ionotropic tyramine receptor.

Cys-loop LGIC receptors, like nicotinic acetylcholine (nAChR), g-aminobutyric acid ($GABA_AR$), glycine (GlyR) and serotonin ($5HT3_AR$) receptors,

form pentameric complexes in the cell membrane (Betz, 1990). Ligand binding at the N-terminal domain induces a conformational change causing the pore of the channel to open. LGC-55 is most closely related to this family of ligand-gated ion channels, in particular the GABA-, glycine-gated chloride channels as well as the *C. elegans* 5HT-gated chloride channel, MOD-1 (Ranganathan et al., 2000) (Figure II-3B). Additionally, we identified orthologues of LGC-55 in the genomes of the closely related nematode species *C. briggsae* (CBP26358, 94% identity), *C. remanei* (RP28082, 95% identity), *Pristionchus pacificus* (PP01401, 70% identity) and the more distantly related parasitic nematode *Brugia malayi* (EDP32880, 52% identity).

To determine whether LGC-55 can form functional homomeric channels, we expressed *lgc-55* in *Xenopus laevis* oocytes for two-electrode voltage clamp recordings. In *lgc-55* injected oocytes, application of tyramine in concentrations ranging from 1-1000 μM evoked robust and rapidly developing inward currents up to 2.2 μA (Figure II-4A). Application of tyramine to mock injected oocytes showed no such response (data not shown). The EC_{50} (effective concentration for half maximal response) for tyramine activation of LGC-55 receptors was 12.1 ± 1.2 μM, a concentration well within the range of EC50 values defined for neurotransmitters that activate closely related LGIC family members (Figure II-4B). These data indicate that LGC-55 forms a functional homomeric receptor that can be activated by tyramine. The EC_{50} of the structurally related amines, octopamine and dopamine, is approximately 10-fold lower than those for

tyramine (EC_{50} = 215.2 ± 1.1 μM and 158.8 ± 1.1 μM respectively), whereas serotonin only elicited small LGC-55-dependent inward currents at millimolar concentrations. GABA, glycine, acetylcholine, and histamine did not elicit any significant LGC-55-dependent inward currents even at concentrations as high as 1 mM. Although octopamine and dopamine may activate LGC-55 *in vivo*, tyramine is the most potent activator of LGC-55, suggesting that tyramine could function as the native ligand for LGC-55.

LGC-55 is a tyramine gated chloride channel.

The ion selectivity of cys-loop LGICs is determined by the M2 domain, which lines the pore of the ion channel. LGC-55 contains a PAR motif on the cytoplasmic side of the M2 domain, which is conserved in most anion-selective channels (Figure II-4D) (Karlin and Akabas, 1995). To determine the ion selectivity we analyzed the current-voltage (*I-V*) relationship for LGC-55 under a variety of ionic conditions. Under our standard recording conditions (100 mM Cl^-), current responses to tyramine application reversed at -25.7 ± 0.9 mV (Figure II-4C), consistent with the chloride equilibrium potential (E_{Cl}) in *Xenopus* oocytes (Weber, 1999). This is similar to the reported reversal potential of other *C. elegans* chloride selective channels, such as the UNC-49B/GABA receptor (Bamber et al., 1999) and the serotonin-gated chloride channel, MOD-1 (Ranganathan et al., 2000) and significantly different from the near 0 mV reversal potential normally observed for non-selective cation channels. Furthermore, after complete substitution of extracellular sodium with the large impermeant cation *N*-

methyl-D-glucamine (NMDG), we did not observe an obvious change in reversal potential (E_{rev}NMDG = -27.2 ± 1.3 mV), suggesting that sodium ions do not significantly contribute to the current passing through the LGC-55 ion channel (Figure II-4C).

To test how changes in the chloride ion concentration affected the reversal potential of LGC-55, we substituted external chloride with the large anion gluconate. When the chloride concentration was reduced by 10-fold, we observed a rightward shift in reversal potential of approximately 40 mV (E_{rev}gluconate = 14.9 ± 2.6) (Figure II-4C). These data are consistent with corresponding shifts predicted by the Nernst equation and indicate that LGC-55 is a chloride selective channel. To test whether the LGC-55 receptors expressed *in vivo* were also chloride selective, we expressed *lgc-55* in *C. elegans* body wall muscles using the muscle-specific *myo-3* promoter (*myo-3::*LGC-55) and recorded current responses to tyramine using whole-cell patch clamp electrophysiology (Figure II-4E). While we never detected measurable current responses to tyramine in body wall muscles of wild-type worms, we noted robust responses to tyramine in the body wall muscles of transgenic worms expressing LGC-55. Consistent with our results for heterologously expressed LGC-55 receptors, current responses to tyramine reversed at approximately –30 mV (Figure II-4F), near the predicted reversal potential for an anion-selective channel under our conditions (Francis and Maricq, 2006).

LGC-55 is expressed in cells that are postsynaptic to the tyraminergic RIM motorneurons

To determine the expression pattern of *lgc-55* we generated translational fluorescent reporter constructs. A 7 kb *lgc-55* genomic fragment including a 3.5 kb promoter and the first intron was fused to the open reading frame of green (GFP) (Chalfie et al., 1994) and red (mCherry) fluorescent reporters (Shaner et al., 2004). The *lgc-55*::mCherry and *lgc-55*::GFP reporter expression was observed in a subset of neck muscles, and a restricted set of neurons (Figure II-5). We have identified these neurons as the AVB, RMD, SMDD, SMDV, IL1D, IL1V, SDQ, HSN and ALN neurons (Figure II-5A, B, C, and Figure II-6,7,8). In addition, weak *lgc-55* reporter expression was also detected in the UV1 cells and tail muscle cells.

To visualize the localization of the LGC-55 protein we fused the GFP coding sequence between the M3 and M4 coding domain of the minimal rescuing construct. The LGC-55::GFP construct rescued the sensitivity of *lgc-55(tm2913)* mutants to exogenous tyramine and also rescued defects in the suppression of head oscillations (data not shown), indicating that LGC-55::GFP is, at least in part, properly localized to restore tyraminergic signaling. LGC-55::GFP fluorescence was observed in neuronal cell bodies and punctate structures in the nerve ring suggestive of postsynaptic specializations (Figure II-5E). In *C. elegans,* muscles extend cytoplasmic arms that synapse with bundles of motor

neuron processes (White et al., 1986) (Hall and Altun, 2007). Neck muscle arms turn anteriorly into the nerve ring where they make synapses with the head motorneurons including the tyraminergic RIMs. Therefore, the LGC-55::GFP puncta in the nerve ring suggest that LGC-55 receptors cluster at post synaptic sites that may include neuromuscular synapses between the RIMs and the neck muscles. The neck muscles, the AVB, RMD, SMDD and SMDV neurons are postsynaptic to the tyraminergic RIM motor neurons (White et al., 1986), consistent with tyramine being an endogenous ligand of LGC-55. The HSN, IL1, SDQ and ALN neurons send processes to the nerve ring but do not receive direct synaptic input from the RIM suggesting that LGC-55 may also act extrasynaptically. Furthermore, tyramine release from non-neuronal cells, such as the uterine UV1 cells, could activate lgc-55.

lgc-55 **is required in neck muscles to suppress head oscillation in response to anterior touch.**

Gentle touch to the anterior half of the body of *C. elegans* elicits an escape response in which the animal reverses its direction of locomotion (Chalfie et al., 1985). Wild-type animals suppress head oscillations during this backing response (Movie II-4). However, head oscillations are usually not suppressed during spontaneous reversals (Alkema et al., 2005). Mutant animals that lack tyramine, and animals in which the tyraminergic RIM motorneurons are ablated, fail to suppress head oscillations in response to anterior touch (Alkema et al.,

2005). *lgc-55* mutants had no obvious defects in locomotion pattern or head oscillations during normal foraging. However, we found that *lgc-55* mutant animals failed to suppress head oscillations in response to anterior touch (Figure II-9, Movie II-5).

How does the tyramine-gated chloride channel suppress head oscillations in response to anterior touch? We observed strong *lgc-55*::GFP expression in the RMD and SMD neurons as well as 8 radially symmetric neck muscle cells (Figure II-5B and D). Head movements that accompany foraging behavior are controlled by the excitatory cholinergic RMD and SMD neurons and the inhibitory GABAergic RME neurons that provide synaptic inputs to the neck muscles (Hart et al., 1995; Gray et al., 2005). The RMD and SMD neurons are coupled through gap junctions and reciprocal synaptic connections, and innervate contralateral neck muscles (White et al., 1986). The RMD neurons display bistable potentials, which may contribute to the oscillatory head movements (Mellem et al., 2008). The GABAergic RME neurons synapse onto the neck muscles as well as the RMD and SMD neurons and limit the extent of head deflection during head oscillations (McIntire et al., 1993).

We sought to identify the cells in which *lgc-55* acts to suppress head oscillations in response to anterior touch using cell specific rescue and mosaic analysis. For the first approach we expressed the *lgc-55* cDNA under the control of cell specific promoters in the *lgc-55(tm2913)* mutants. We used the following

promoters to drive the expression of *lgc-55* in specific subsets of cells: *lim-4*: the RMD neurons (plus 5 additional neurons) (Sagasti et al., 1999); *glr-1:* the RMD and SMD neurons (plus 14 additional neurons) (Hart et al., 1995; Maricq et al., 1995); *sra-11*: the AVB neurons (plus 2 additional neurons) (Altun-Gultekin et al., 2001) and *myo-3*: body wall muscle (including neck muscle) (Okkema et al., 1993) (Table II-1). Expression of *lgc-55* in the AVB (*sra-11::*LGC-55) or RMD (*lim-4::*LGC-55) neurons failed to rescue the defect in the suppression of head oscillations. Animals that expressed *lgc-55* in the RMD and SMD neurons (*glr-1::*LGC-55) also did not fully rescue the suppression of head oscillations but usually kinked their head to one side while reversing (Movie II-6). However RMD and SMD expression did restore sensitivity to the paralyzing effects of exogenous tyramine in head movement assays (Figure II-10). The expression of *myo-3::*LGC-55 in muscle, on the other hand, fully rescued the defect in the suppression of head oscillations of *lgc-55* mutants (Figure II-9C, Movie II-7) and restored sensitivity to the paralyzing effects of exogenous tyramine in head movement assays (Figure II-10). Animals in which *lgc-55* expression was rescued in body wall muscle displayed normal locomotion and backing in response to touch, suggesting that tyraminergic activation of *lgc-55* mainly occurred synaptically at the RIM-neck muscle neuromuscular junctions.

As a second approach we performed genetic mosaic analysis. The *lgc-55* expressing neurons are derived from the embryonic AB blastomere, whereas the body wall muscles are derived from the P1 blastomere (Figure II-11A). Using

GFP and mCherry markers we selected animals that had lost a rescuing extrachromosomal array in either the descendants of AB blastomere or the descendants of the P1 blastomere. Mosaic animals that lost the array in the P1 lineage failed to suppress head oscillations whereas animals that lost the array in the AB lineage did suppress head oscillations in response to touch (Figure II-11B). Exogenous tyramine could still inhibit head movements in animals that lost the rescuing array in the P1 lineage, albeit to lesser extent than animals that lost the array in the AB lineage. These results indicate that even though LGC-55 expression in the RMD and SMD neurons may contribute to the suppression, LGC-55 expression in neck muscles is necessary and sufficient to fully suppress lateral head movements upon anterior touch. However, *lgc-55* expression in neurons was required to mediate the tyraminergic stimulation of backward locomotion, since exogenous tyramine did not induce long backward locomotory runs in animals that had lost the array in the AB lineage (see below).

lgc-55 acts in the AVB forward locomotion command neurons to modulate reversal behavior.

On agar plates *C. elegans* mainly displays forward locomotion interrupted by brief backward locomotory runs. The neural circuit that controls forward and backward locomotion consists of four pairs of locomotion command interneurons: the PVC and AVB neurons are primarily required for forward locomotion whereas the AVD and AVA neurons are required for backward locomotion (Chalfie et al.,

1985). Electrophysiology, Ca^{2+} imaging and genetic experiments indicate that depolarization of the forward locomotion command neurons results in forward locomotion whereas depolarization of the backward locomotion command neurons drives backward locomotion (Chronis et al., 2007; Zheng et al., 1999). The forward and backward locomotion command neurons make reciprocal synaptic connections, which may link the neural activities underlying these antagonistic behaviors and allow the animal to switch its direction of locomotion. The tyraminergic RIM neurons are electrically coupled through gap junctions with the AVA backward command neurons and have synaptic outputs onto the AVB forward locomotion command neurons. Although tyramine deficient animals normally initiate backward locomotion in response to anterior touch, they back up less far than the wild type. In addition, tyramine deficient animals have a marked increase in the number of spontaneous reversals indicating that tyramine modulates reversal behavior (Alkema et al., 2005).

We tested whether *lgc-55* mutants have defects in reversal behavior. Like *tdc-1* mutants, *lgc-55* mutants initiated backward locomotion normally in response to anterior touch but displayed shorter runs of backward movement (2.4 ± 0.1 body bends) than the wild type (3.3 ± 0.1 body bends) (Figure II-12A and II-13). In addition, we found that *lgc-55* mutants had an increase in spontaneous reversals compared to the wild type, although the increase was less pronounced than that of the *tdc-1* mutants (Figure II-12B). To examine spontaneous reversal behavior in more detail we categorized the reversals

according to the number of backward body bends (Gray et al., 2005). We found that *lgc-55* mutants displayed more short reversals than wild-type worms (Figure II-12C). The increase in short reversals was even more dramatic in the *tdc-1* mutants. An *lgc-55* minigene rescued the defects of *lgc-55* mutants in reversal behavior in both the touch-induced and spontaneous reversal assays.

Where does *lgc-55* act to increase the length of reversals? Cell specific rescue experiments showed that *lgc-55* expression in the RMD (*lim-4::lgc-55*), RMD or SMD neurons (*glr-1::lgc-55*) or body wall muscle (*myo-3::lgc-55*) did not restore normal reversal behavior in *lgc-55* mutants (Figure II-12A, data not shown). However, *lgc-55* expression in the AVB neurons (*sra-11::lgc-55*) restored normal reversal behavior in *lgc-55* mutants. The length of backward runs in response to anterior touch (on average 3.3 ± 0.2 backward body bends), and the number and percentage of long reversals (39.6% short vs 60.4% long) in spontaneous reversal assays were comparable to those observed for wild-type worms (Figure II-12). These data indicate that *lgc-55* expression in the AVB neurons is required to sustain backward locomotion once a reversal is initiated.

Our data support the hypothesis that tyramine inhibits forward locomotion by activating *lgc-55* and hyperpolarizing the AVB forward locomotion command neurons. The *lgc-55* dependent inhibition of the forward locomotion program could dramatically shift the balance towards the backward locomotion program, thus explaining our observation that exogenous tyramine induces extremely long

backward locomotory runs. To further test this hypothesis, we quantified reversal behavior in the presence of exogenous tyramine. The longest average backwards run for wild-type worms in the presence of exogenous tyramine was approximately 15 body bends, compared to 4 body bends in the absence of exogenous tyramine (Figure II-12D). However, exogenous tyramine did not elicit prolonged backward runs in *lgc-55* mutant animals (4.0 versus 2.8 backward body bends, respectively). In contrast, *lgc-55* mutants that carried a rescuing *lgc-55* transgene displayed a dramatic increase in the length of backwards runs in this assay (44 backward body bends), likely due to overexpression of *lgc-55*. Exogenous tyramine also triggered long backward runs (11 backward body bends) in *lgc-55* mutants that express *lgc-55* in the AVB neurons using the *sra-11*::*lgc-55* transgene (Figure II-12D), but failed to do so in animals that express *lgc-55* in the SMD and/or RMD neurons or body wall muscles (data not shown). This result indicates that the effects of exogenous tyramine on backward locomotion are mediated, at least in part, through the activation of *lgc-55* in the AVB forward locomotion neurons.

Discussion

Tyramine acts as a classical neurotransmitter in *C. elegans*.

Although tyramine is found in nervous systems from worms to man, it has remained unclear whether tyramine can act as a genuine neurotransmitter. The data presented further satisfy the six criteria that tyramine must meet to enter the

realm of neurotransmitters (Paton, 1958)(Cowan et al., 2001): (1) the presynaptic neuron contains enzymes to make the substance; (2) the substance is released upon activation of the neuron; (3) exogenous application of the substance to the postsynaptic cell mimics normal synaptic transmission; (4) the postsynaptic cell has receptors for the substance; (5) blocking the receptor disrupts the activity of the substance; (6) there are mechanisms to terminate the action of the substance. First, it was previously shown that the *C. elegans* RIM neurons contain the TDC-1 enzyme that synthesizes tyramine. Second, behavioral analysis of *tdc-1* mutants, vesicular monoamine transporter (*cat-1*) mutants and laser ablation studies indicate that activation of the RIM motor neuron leads to synaptic tyramine release (Alkema et al., 2005). Third, here we show that exogenous tyramine, like endogenous tyramine release, leads to the suppression of head oscillations and stimulates backward locomotion. Fourth, cells that are postsynaptic to the RIM express the tyramine-gated chloride channel, LGC-55. Fifth, genetic disruption of the receptor blocks the tyramine-induced suppression of head oscillations and stimulation of backward locomotion. Sixth, to date no tyramine or octopamine reuptake transporter has been characterized in *C. elegans.* However several of the *C. elegans* sodium neurotransmitter transporter gene family (SNF) (Mullen et al., 2006) have not been characterized. In addition, monoamine-oxidase (MAO) and aryl-alkylamine N-acetyltransferase activities have been detected in nematodes including *C. elegans* (Isaac et al., 1996)

indicating that mechanisms that could terminate tyramine action are present in *C. elegans*.

Metabotropic tyramine receptors have been identified in a wide variety of animals. Three G-protein coupled receptors that are activated by tyramine, SER-2, TYRA-2 and TYRA-3, have been identified in *C. elegans* (Rex et al., 2005; Rex and Komuniecki, 2002; Wragg et al., 2007; Tsalik et al., 2003). *ser-2*, *tyra-2* and *tyra-3*, are expressed in cells that do not receive direct input from the tyraminergic RIMs suggesting that tyramine mainly acts as a neurohormone to activate G-protein coupled tyramine receptors. *ser-2*, *tyra-2* and *tyra-3* mutants have no obvious defects in the suppression of head oscillations or reversal behavior. However, *ser-2* mutants are partially resistant to the inhibitory effects of tyramine on body movements (J.D. and M.J.A, unpublished observations). LGC-55 provides the first example of an ionotropic-tyramine receptor. Ligand-gated ion channels are thought to have arisen from a common ancestor over 2 billion years ago (Ortells and Lunt, 1995). LGC-55 is found in the same clade as the serotonin-gated chloride channel MOD-1, suggesting that an ancestral anion-channel accumulated mutations in its extracellular domain to acquire sensitivity to tyramine. Have tyramine-gated chloride channels evolved in species other than nematodes? Some observations seem to support this idea. Tyramine increases chloride conductance in the *Drosophila* Malpighian (renal) tubules (Blumenthal, 2005). Furthermore in rats, tyramine induces strong inhibitory effects on the firing rate of caudate and cortical neurons (Henwood et al., 1979)

and can induce hyperpolarization in neurons of the subthalamic nucleus (Zhu et al., 2007) of the rat brain.

Tyramine coordinates distinct motor programs in a *C. elegans* escape response.

The analysis of escape responses in flies, crayfish and goldfish have illuminated how neural networks translate sensory input into a motor output (Korn and Faber, 2005; Edwards et al., 2002; Allen et al., 2006). An animal's escape response increases its ability to survive predator-prey encounters. One of the main predators of nematodes is the nematophagous fungi (Barron, 1977). These carnivorous fungi are ubiquitous in the soil and decaying organic material and have developed distinctive trapping devices, including constricting hyphal rings, to catch worms (Thorn and Barron, 1984). When a nematode passes through a hyphal ring, gentle friction induces the cells of the ring to inflate and catch the nematode. In *C. elegans* gentle anterior touch is detected by the ALM and AVM mechanosensory neurons (Figure II-14) (Chalfie and Sulston, 1981). The neural wiring diagram and laser ablation studies support a model by which activation of the ALM and AVM neurons leads to the inhibition of the PVC and AVB forward locomotion command neurons and activation of the AVD and AVA backward locomotion command neurons. This causes the animal to move backward away from the stimulus (Chalfie et al., 1985). Subsequently, the RIM is activated through gap junctions with the AVA neurons triggering the release of tyramine

(Alkema et al., 2005) and the activation of tyramine-gated chloride channel, LGC-55.

In response to anterior touch, *lgc-55* mutants, like tyramine deficient animals, fail to suppress head movements and back up less far than the wild type. This indicates that tyramine modulates the output of two independent motor programs, head movements and locomotion. *lgc-55* is expressed in neck muscles, the RMD and SMD motorneurons and the AVB forward locomotion command neurons that receive postsynaptic inputs from the RIM. Our studies indicate that tyramine hyperpolarizes neck muscles through activation of LGC-55, thus relaxing the muscle and inhibiting head movements. Since *lgc-55* is also expressed in the cholinergic RMD and SMD motor neurons, which regulate head movements, hyperpolarization of these motor neurons may further contribute to the inhibition of head movements. Interestingly, recent patch-clamp studies have demonstrated that the RMD neurons display bistable potentials that depend on extrinsic activation of membrane conductance in the RMD neurons (Mellem et al., 2008). The expression of LGC-55 in RMD neurons suggests that tyraminergic inhibitory synaptic input may be important for the generation of RMD bistability.

LGC-55 expression in the AVB forward locomotion command neurons is required for tyraminergic modulation of reversal behavior. The forward locomotion command neurons make presumptive inhibitory inputs onto the backward locomotion command neurons to coordinate the animal's locomotion

program. Our data indicate that tyraminergic activation of LGC-55 in the AVB shifts the balance of the bistable circuit that controls the direction of locomotion in favor of the backward locomotion program. Tyramine reinforces the backward locomotion program allowing the animal to make a long reversal before reinitiating forward locomotion (Figure II-14). Long reversals (3 or more body bends) are usually coupled to an omega turn, in which the head bends ventrally towards the tail (Croll, 1975b). Omega turns usually change the direction of locomotion to one directly opposite to the original trajectory (approximately 180˚). Short reversals of 1 or 2 body bends lead to a relatively small (40˚ to 70˚, respectively) change in direction of locomotion (Gray et al., 2005; Zhao et al., 2003). Therefore, the suppression of head oscillations coupled to long reversals may allow the animal to engage in a more efficient escape response.

The *C. elegans* neural escape circuit is reminiscent of the neural escape circuit in flies. In the *Drosophila* escape response the giant fiber (GF) neurons coordinate distinct motor programs: leg extension and wing depression, which are required for fast flight initiation (Hammond and O'Shea, 2007; Card and Dickinson, 2008). Fly GF interneurons make electrical synapses with the TTMn motorneurons, which control leg jump, and the PSI interneurons, which control wing depression (Tanouye and Wyman, 1980). Additional synaptic connectivity exists between PSI interneurons and the TTMn neurons that presumably contribute to a coordinated motor response (Phelan et al., 1996). Like the worm AVA neurons, the fly GF neurons control two distinct motor programs. Could

tyramine play a role in the coordination of these motor programs in the fly escape response? Interestingly, tyramine appears to inhibit flight initiation (Brembs et al., 2007) and flies that have an excess of tyramine or lack the tyramine G-protein coupled receptor, TyR^{homo} do not jump as far as the wild type in fly escape assays (Zumstein et al., 2004). These striking similarities between worms and flies, suggests that tyramine may act as a universal coordinator of motor programs in invertebrate escape responses.

Figure II-1

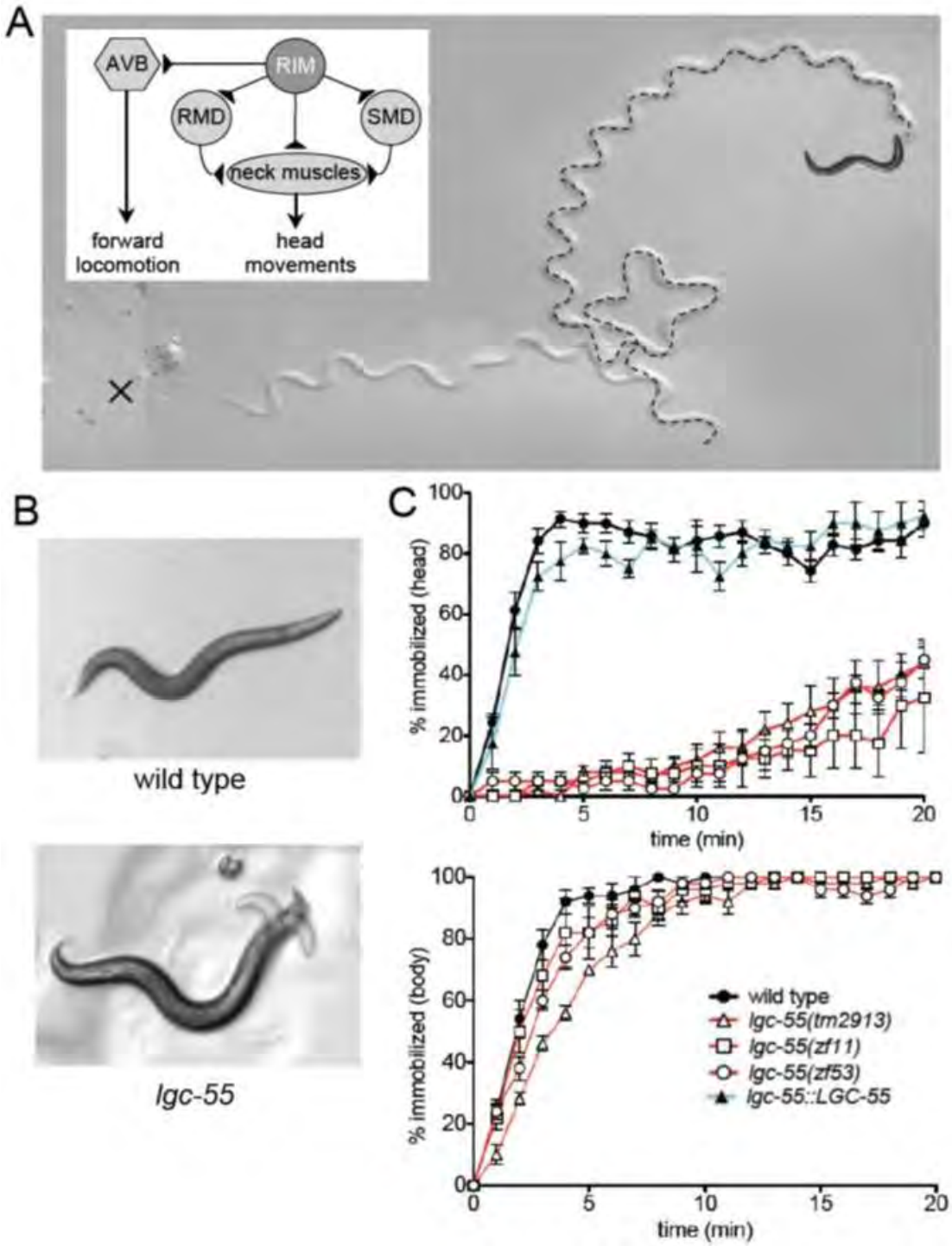
A
AVB
RIM
RMD
SMD
neck muscles
forward locomotion
head movements
B
wild type
lgc-55
C
% immobilized (head)
time (min)
% immobilized (body)
time (min)
wild type
lgc-55(tm2913)
lgc-55(zf11)
lgc-55(zf53)
lgc-55::LGC-55

Figure II-1. Exogenous Tyramine Induces Long Reversals and Suppresses Head Movements.

(A) Still image of locomotion pattern of wild-type animals on 30 mM tyramine prior to immobilization. The x marks the starting location and the dashed line marks the backward locomotory run (See Supplemental Movie S1). Inset: the main synaptic outputs of the tyraminergic RIM motorneurons include the AVB forward locomotion command neurons, the RMD and SMD motorneurons and neck muscles.

(B) Overlay of three still images of wild type and *lgc-55(zf11)* after five minutes on exogenous tyramine. Images were taken approximately 2 s apart. Wild-type animals completely immobilize. *lgc-55* mutants move their heads while their body remains immobilized.

(C) Quantification of head and body movements on 30 mM tyramine. Shown is the percentage of animals immobilized by tyramine each minute for 20 min. Each data point is the mean ± standard error of the mean (SEM) for at least four trials totaling 40 or more animals. *lgc-55* mutants continue to move their heads through the duration of the assay, while the body immobilizes similarly to wild-type animals.

Figure II-2

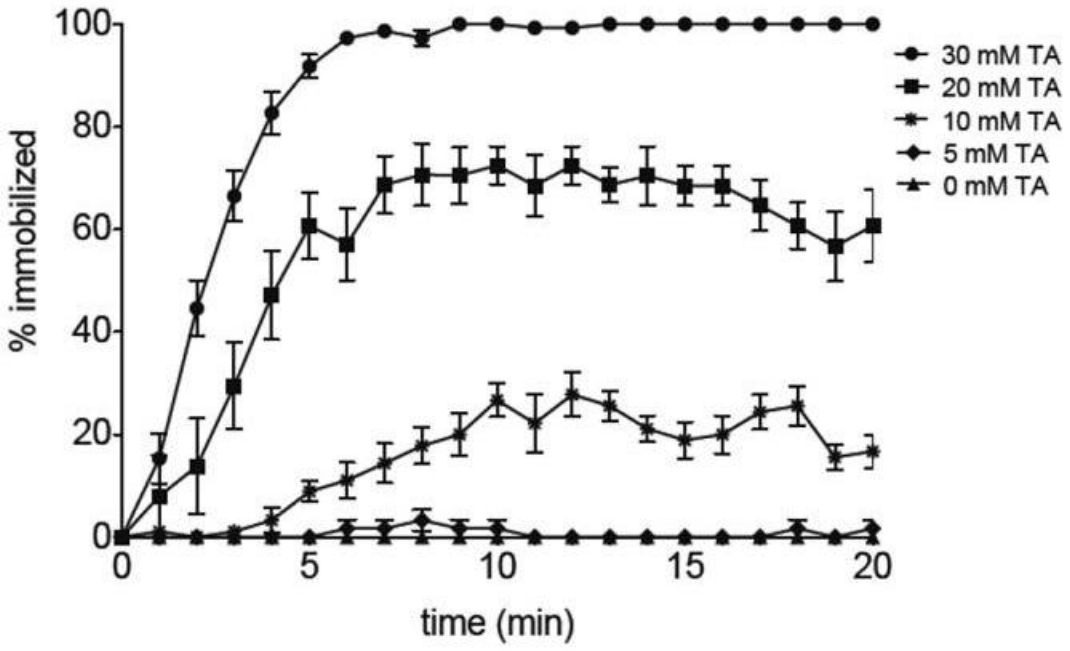

Wild-Type Animals Immobilize on Exogenous Tyramine.

Dose dependent immobilization of wild-type animals on exogenous tyramine. The percentage of immobilized animals, at varying concentrations of exogenous tyramine, are depicted over a 20 minute period. Each data point represent the average ± SEM for at least five trials totaling at least 50animal.

Figure II-3

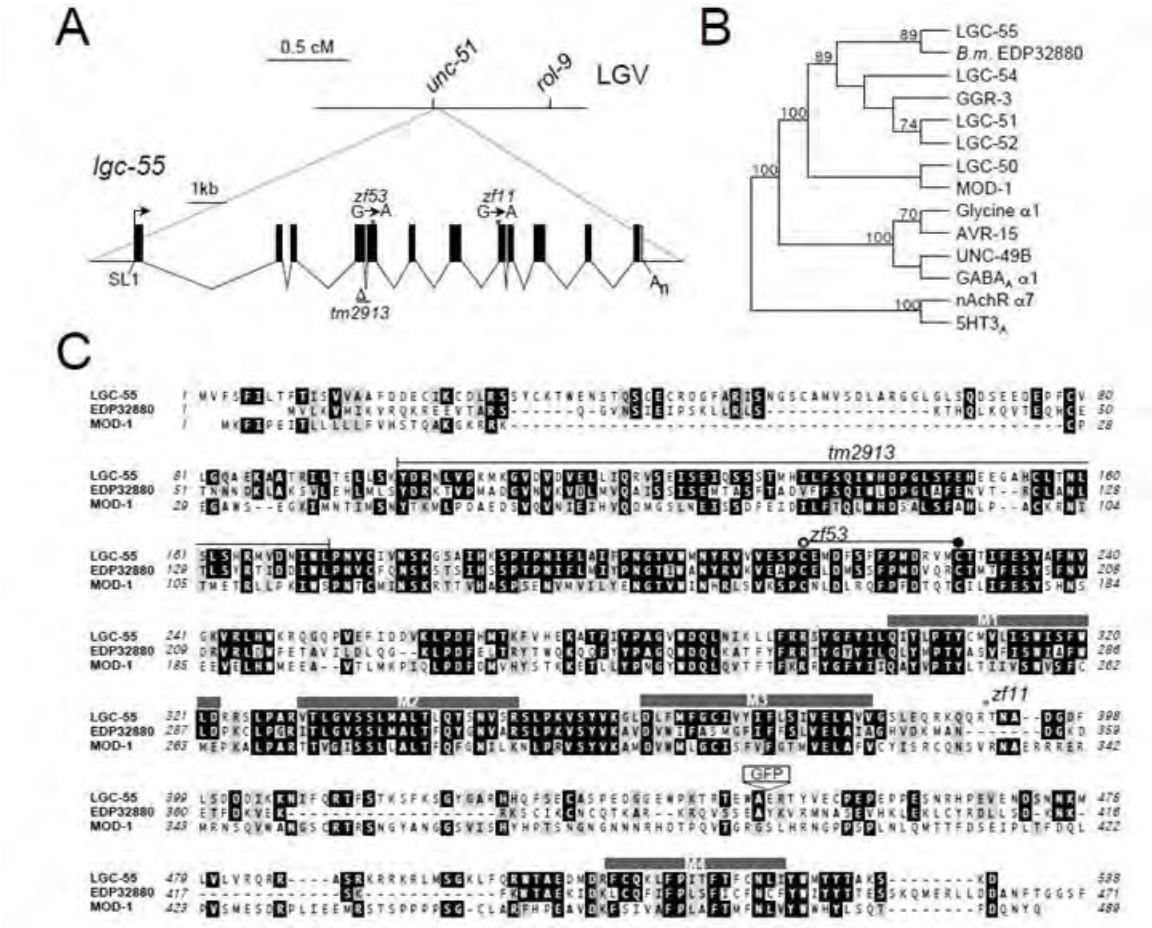

***lgc-55* encodes a ligand-gated ion channel subunit.**

(A) The *lgc-55* locus. Genetic map and gene structure of *lgc-55*: coding sequences are represented as black boxes; untranslated regions are represented as white boxes. The SL1 *trans*-spliced leader and the poly(A) tail are indicated. The position of the *lgc-55(zf11)*, *lgc-55(zf53)* and *lgc-55(tm2193)* alleles are indicated. The *lgc-55(tm2913)* has a 285 bp deletion that removes part of exon 4 and exon 5. The deleted region indicated by bars.

(B) Phylogenetic tree of LGC-55 and various ligand-gated ion channel subunits. Predicted *C. elegans* LGICs (Jones and Sattelle, 2008), including the 5HT receptor MOD-1, glutamate receptor AVR-15, GABA receptor UNC-49$_B$, the *Brugia malayi* predicted protein EDP32880, and human GABA$_A$□1, nAchR□7

and $5HT3_A$. A neighbor weighted tree of decarboxylase-conserved regions was determined and the bootstrap analysis and the Unweighted Pair Group Method with Arithmetic Mean (UPGMA) using MacVector software (Accelrys).

(C) Alignment of LGC-55 with MOD-1 and the closely related predicted protein from *Brugia malayi,* EDP32880. Identities are outlined in black and similarities are shaded. The four predicted transmembrane domains are indicated by black bars, and the Cys-loop is indicated by a line with two black with black circles. The LGC-55 *zf11* and *zf53* mutations are indicated by stars, the black line denotes the amino acids deleted in the *tm2913* allele. The position of the GFP insertion of the LGC-55::GFP translational fusion is indicated.

Figure II-4

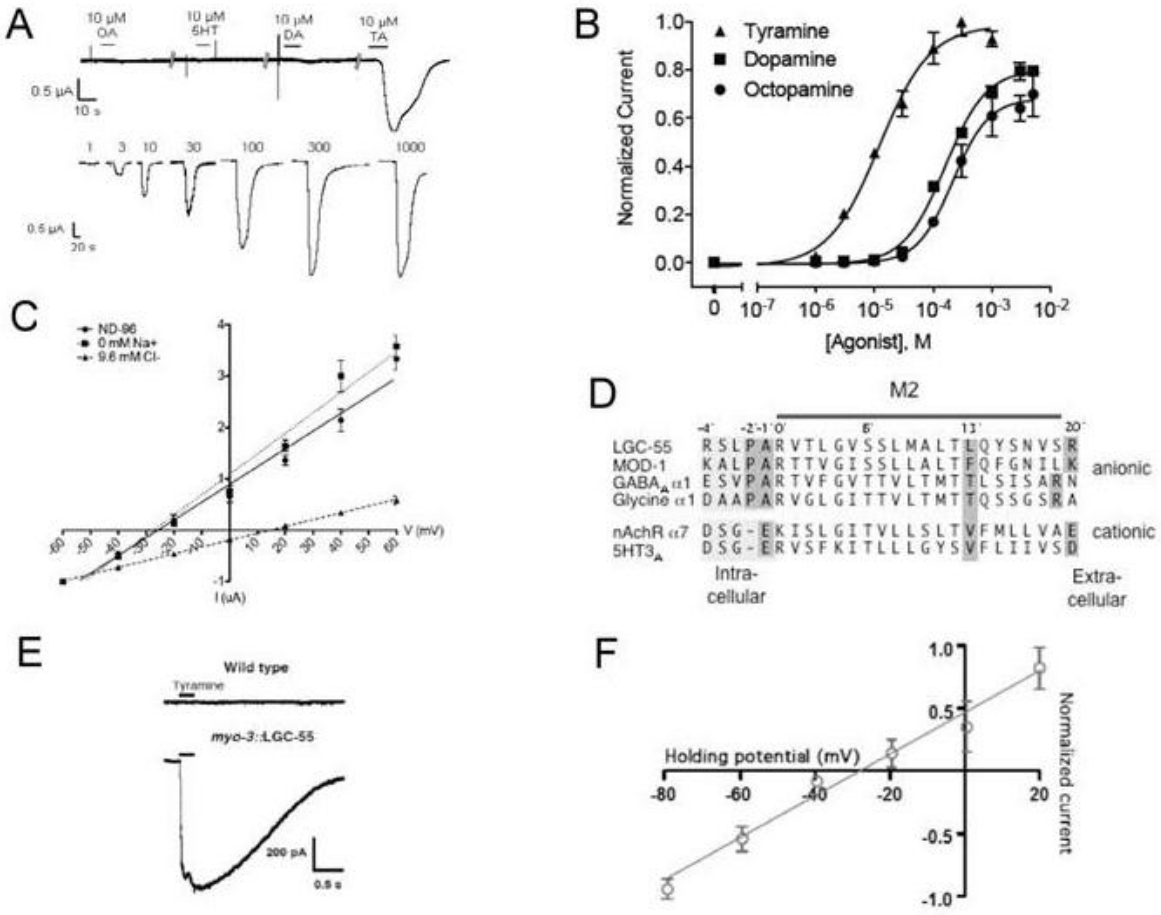

LGC-55 is a Tyramine Gated Chloride Channel.

(A) Representative traces from *Xenopus* oocytes injected with *lgc-55* cRNA showing responses to 10 µM octopamine (OA), serotonin (5HT), dopamine (DA), and tyramine (TA) as well 1-1000 µM TA in ND-96. Neurotransmitters were bath-applied for 10 s.

(B) LGC-55 TA, OA and DA dose response curves. EC_{50}TA = 12.1 ± 1.2 µM and Hill Coefficient = 1.0 ± 0.17, EC_{50}DA = 158.8 ± 1.1 µM, EC_{50}OA = 215.2 ± 1.1 µM. Each data point represents the mean current value normalized to the mean maximum current observed for tyramine, (I_{max} = 2.2 ± 0.17 µA). Error bars represent SEM.

(C) Ion selectivity of LGC-55 in *Xenopus* oocytes. TA-evoked (10 μM, 10 s) currents were recorded at the holding potentials shown. Filled circles, *I-V* curve determined in standard ND-96 (E_{rev} = -25.7 ± 0.9 mV, n=4). Filled squares: 0 mM Na^+ (E_{rev} = -27.2 ± 1.3 mV, n=4). Filled triangles: 9.6 mM Cl^- (E_{rev}= 15.0 ± 2.6 mV, n=4). Error bars represent SEM.

(D) Alignment of the M2 region of LGC-55 with other members of the Cys-loop ligand-gated ion channel family. Shaded regions indicate residues important for ion selectivity.

(E) Representative current responses to tyramine application (200 μM) recorded from *C. elegans* body wall muscle cells of wild-type (upper) or transgenic animals expressing *myo-3::*LGC-55 (lower). Black bars indicate duration of tyramine application (250 ms).

(F) Current-voltage relationship for LGC-55 receptors expressed in *C. elegans* body wall muscle cells under normal recording conditions. Current responses to tyramine were recorded at the holding potentials indicated.

Figure II-5

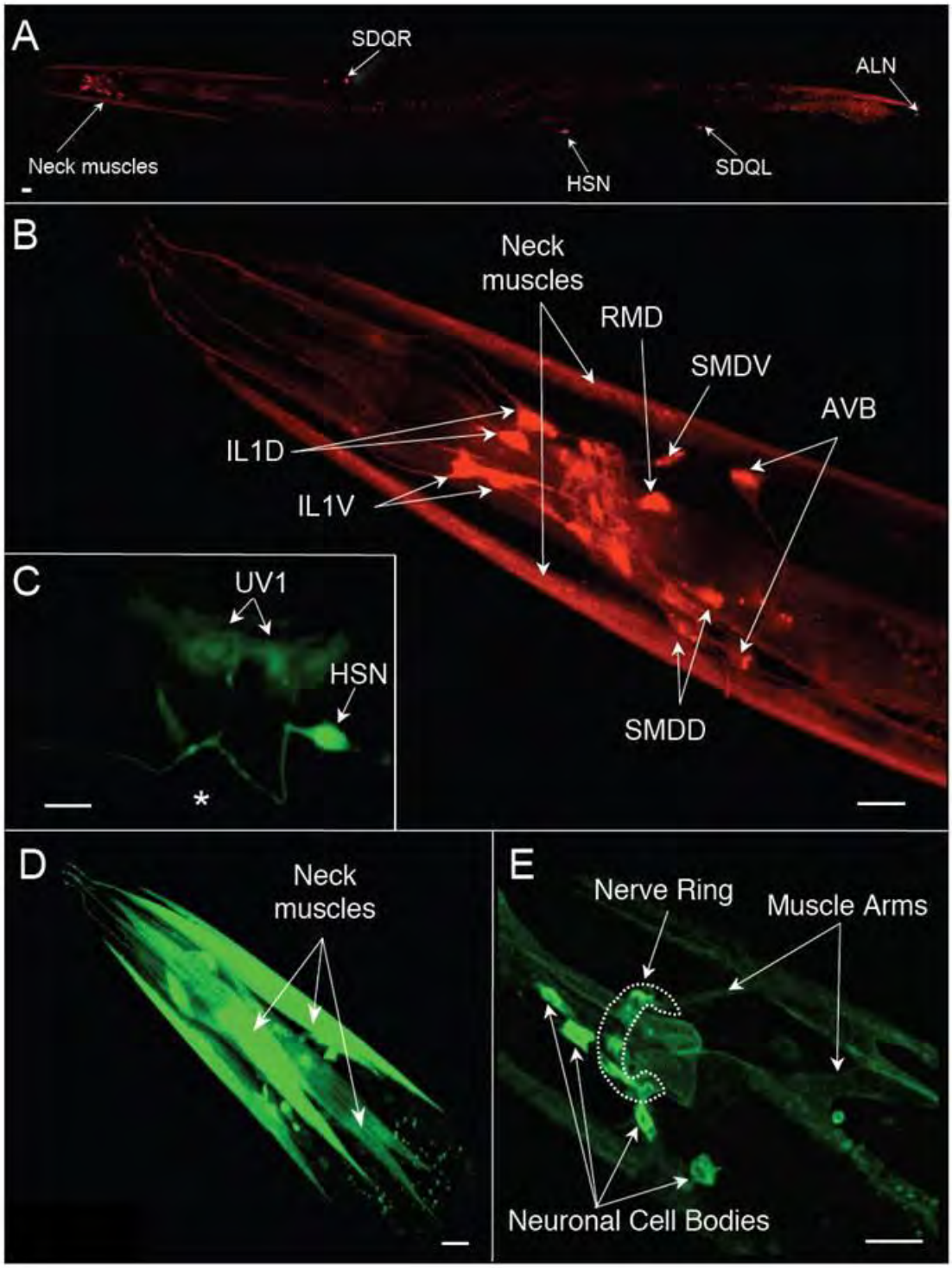
A
SDQR
ALN
Neck muscles
HSN
SDQL
B
Neck muscles
RMD
SMDV
AVB
IL1D
IL1V
SMDD
C
UV1
HSN
*
D
Neck muscles
E
Nerve Ring
Muscle Arms
Neuronal Cell Bodies

Figure II-5. Expression Pattern of *lgc-55*.

(A) Adult animal showing expression of a fluorescent *lgc-55*::mCherry transcriptional reporter in neck muscles, head neurons, SDQ, HSN and ALN neurons.

(B) Head region of an adult animal showing expression of *lgc-55*::mCherry (*zfIs4*) in head neurons, IL1, RMD, SMD, and AVB.

(C) Expression of *lgc-55*::GFP (*zfIs6*) in the HSN and uterine UV1 cells. The star indicates position of the vulva.

(D) Expression of *lgc-55*::GFP in the third row of neck muscle cells.

(E) Expression of LGC-55::GFP translational reporter showing subcellular localization to neuronal cell bodies, nerve ring and muscle arms. Position of the nerve ring is indicated by the dotted line. Scale bar, 10 μm. Anterior is to the left and ventral side is down in all images.

Figure II-6

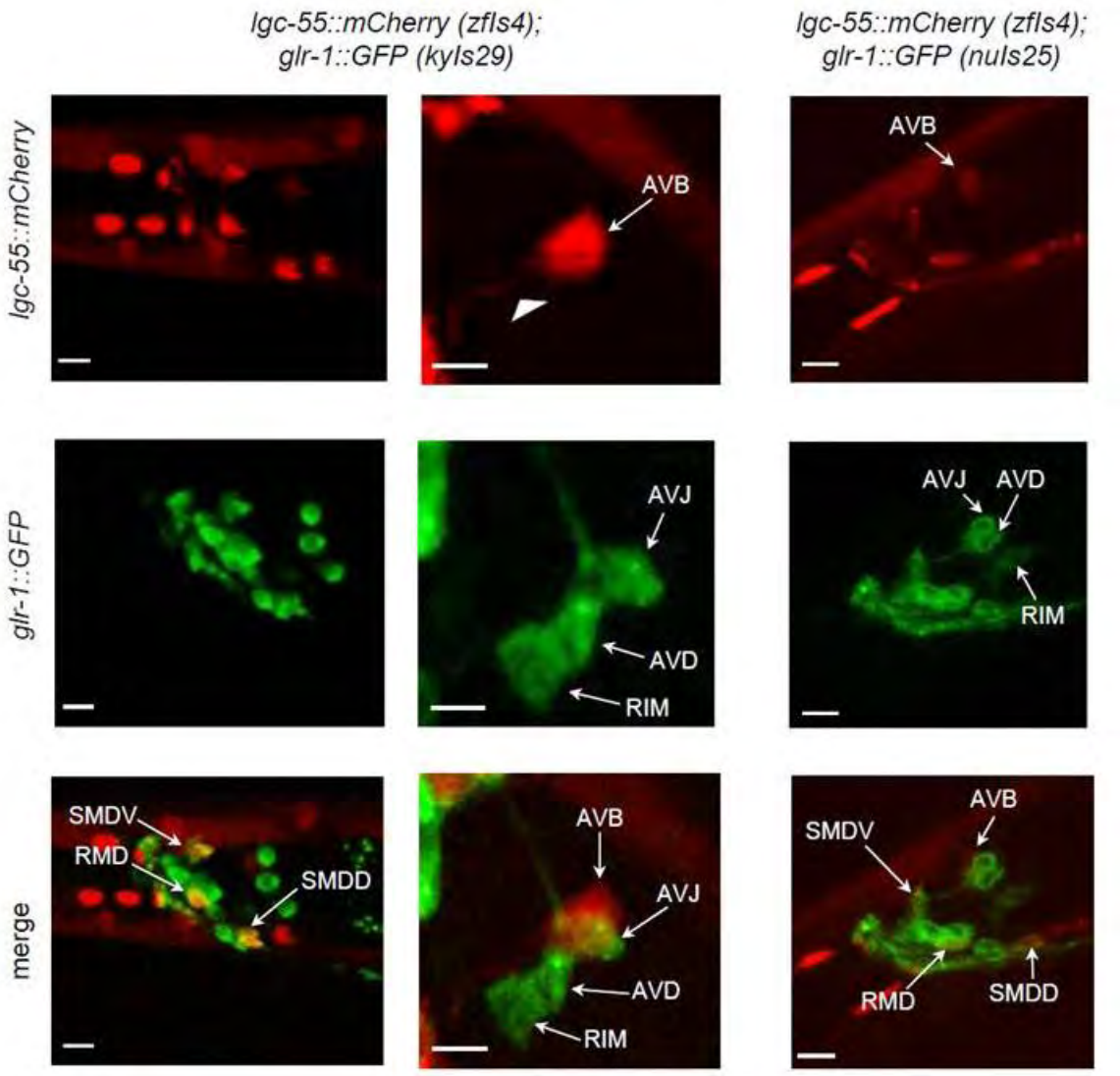

Coexpression of *lgc-55::mCherry* and *glr-1::GFP.*

Coexpression of *lgc-55::mCherry(zfIs4)* with *glr-1*::GFP*(kyIs29)* (Mariq et al., 1995) and *glr-1*::GFP(*nuIs25*) (Hart et al., 1995). Confocal images show coexpression of LGC-55 and GLR-1 in the RMD, SMDD, and SMDV. The AVB cell-body, similar to the cell labeled by *lgc-55*::mCherry, lies on the dorsal side of the animal just anterior to the posterior pharyngeal bulb and has a process that runs ventrally through the amphid commissure (indicated by arrow head) before turning anteriorly and entering the nerve ring (White, et al. 1986). It was previously reported that *glr-1* is expressed in AVJ, RIM, AVD and AVB (Hart et al., 1995, Mariqu et al., 1995). In the adult animal, we observe *glr-1*::GFP

expression (middle planels) in three cells just anterior to the posterior bulb. The dorsal most cell in this group is slightly ventral compared to the *lgc-55*::mCherry neuron and has a process that extends anteriorly into the nerve ring, similar to the cell body position and axon morphology of the AVJ. Based on cell body position, axon morphology, which includes a process that runs through the amphid commissure and coexpression with *sra-11*::GFP (See Figures II-7,8), we conclude *lgc-55* is expressed in the AVB. Anterior is to the left. Scale bar, 10 μm.

Figure II-7

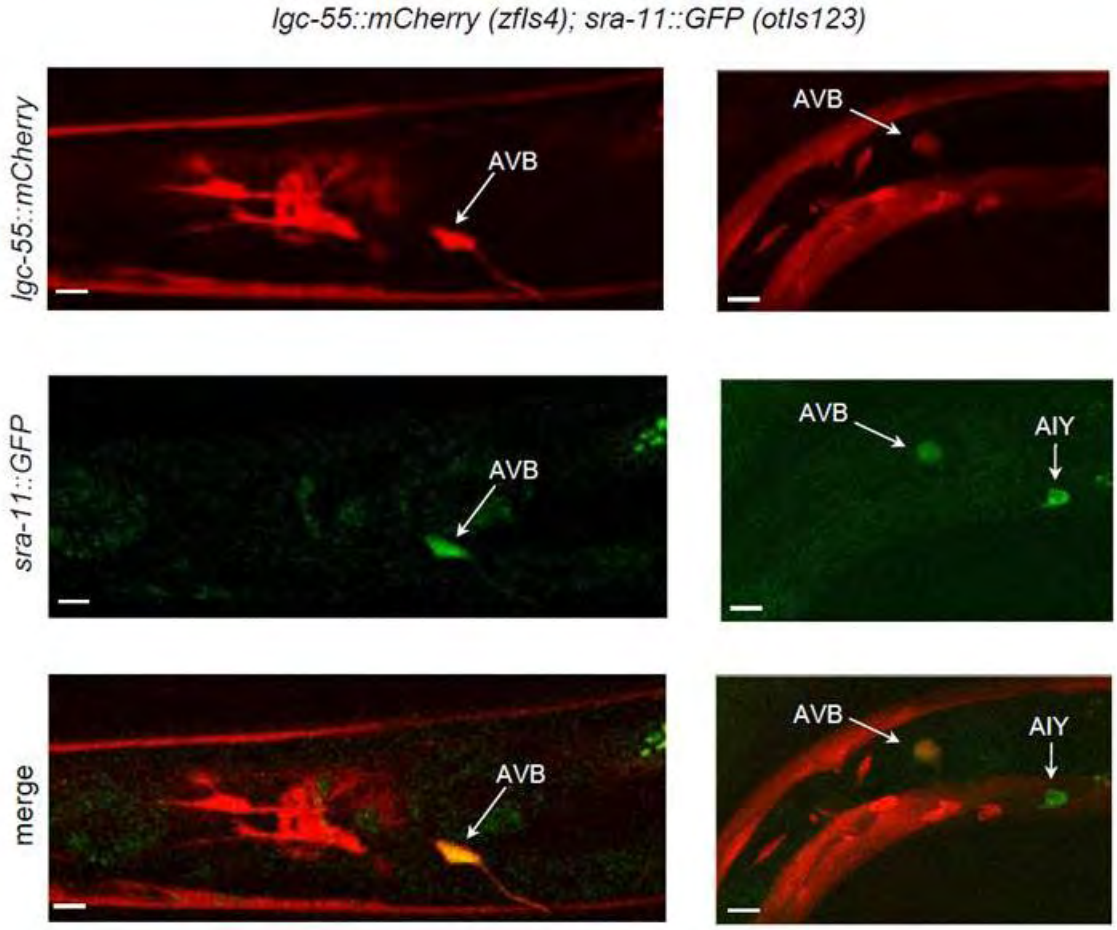

Coexpresion of *lgc-55*::mCherry and *sra-11*::GFP.

Coexpression of *lgc-55*::mCherry(zfIs4) with *sra-11*::GFP(*otIs123*) (Altun-Gutekin et al., 2001). Confocal images show LGC-55 expression in the AVB. Coexpressing cell is on the dorsal side of the animal just anterior to the posterior pharyngeal bulb and has a process that projects ventrally before turning anteriorly and entering the nerve ring in both sets of images. Anterior is to the left. Scale bar, 10 μm.

Figure II-8

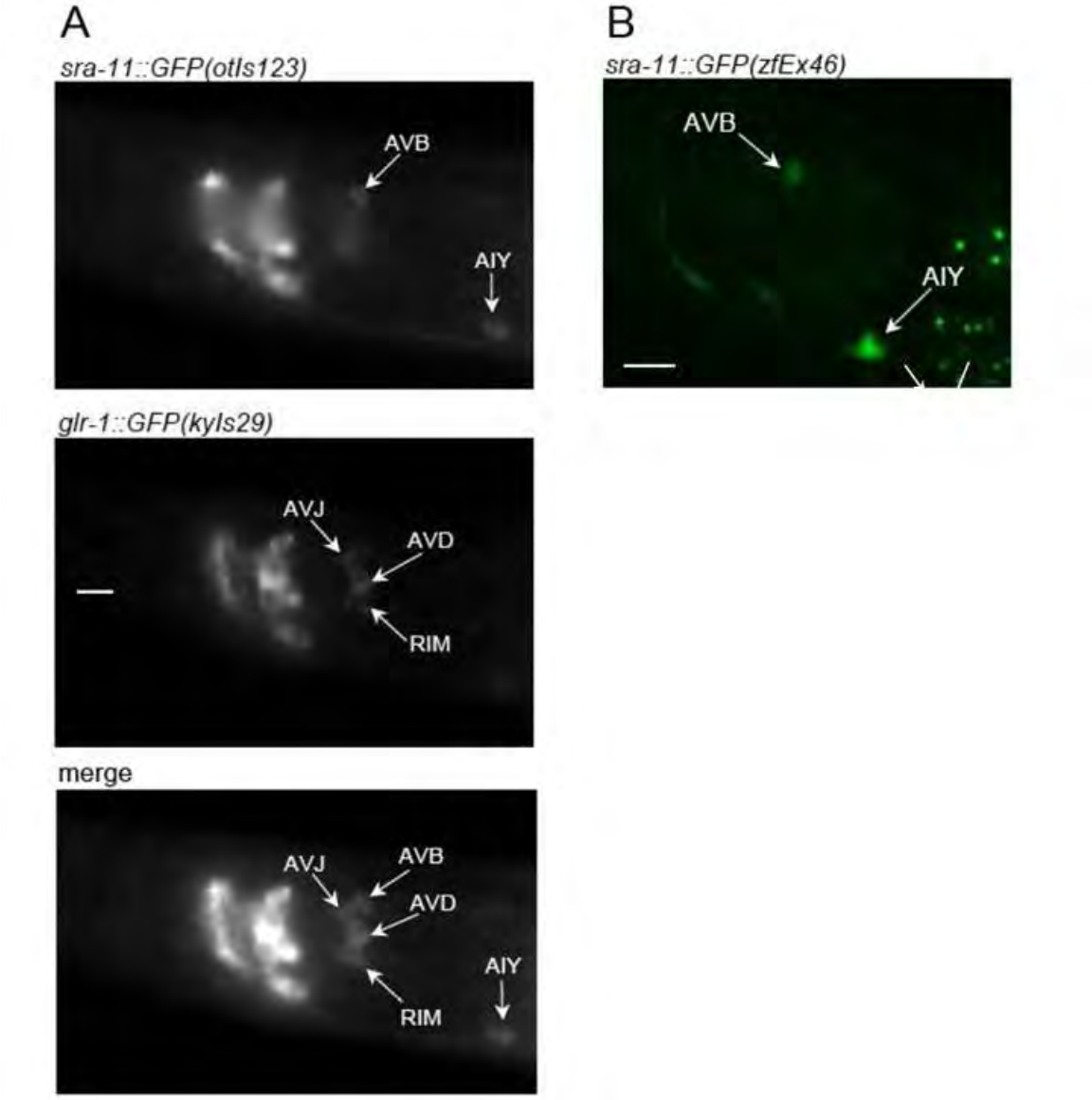

***sra-11*::GFP and *glr-1*::GFP Label Different Subsets of Neurons.**

(A) Fluorescence microscopy of animals expressing both *glr-1*::GFP(*kyIs29*) and *sra-11*::GFP(*otIs123*). Animals expressing both GFP markers were examined to determine the expression in the AVB. If *sra-11*::GFP and *glr-1*::GFP are both expressed in the AVB, three cells should be visible in animals expressing both transgenes. Here, four cells are visible suggesting that *sra-11*::GFP and *glr-1*::GFP label different subsets of neurons.

(B) Confocal image of *sra-11*::GFP(*zfEx46*). Promoter is the same as *sra-11*::LGC-55, and shows expression in the AVB and AIY similar to *sra-11*::GFP(*otIs123*).

Table II-1

Promoter	Expressing cells
myo-3	body-wall muscle
sra-11	**AVB**, AIA, AIY
glr-1	**RMD**, **SMD,** AIB, AVA, AVD, AVE, AVG, AVJ, DVC, PVC, PVQ, RIG, RIM, RIS, RME, URY
lim-4	**RMD**, RID, RIV, RME, SAA, SIA

Expression patterns of promoters used for cell specific rescue of *lgc-55*.

lim-4 (Sagasti et al., 1999); *glr-1* (Hart et al., 1995; Maricq et al., 1995); *sra-11* (Altun-Gultekin et al., 2001) and *myo-3* (Okkema et al., 1993). Note: In contrast to previous reports we could not detect expression of a *glr-1*::GFP reporter in the AVB neurons of adult transgenic animals; See Figure II-6-8. Cells overlapping with *lgc-55* expression are indicated in bold.

Figure II-9

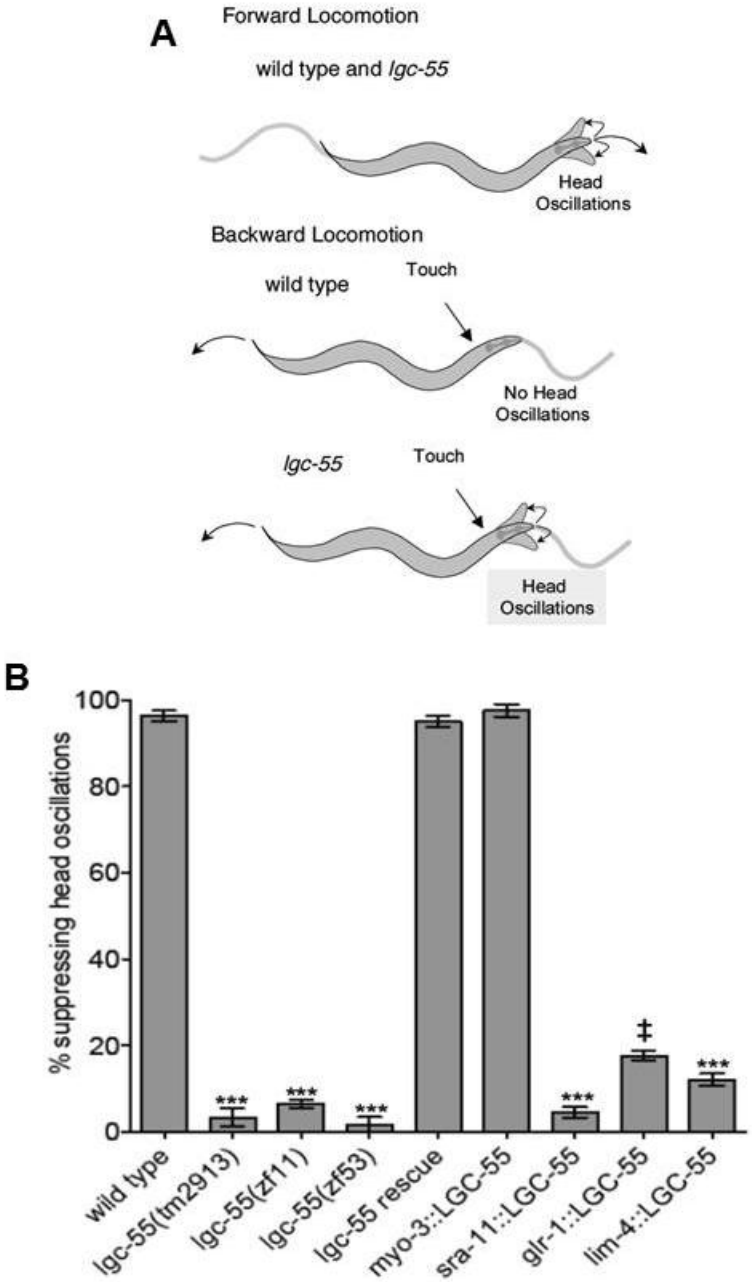

***lgc-55* Mutants Fail to Suppress Head Oscillations in Response to Anterior Touch.**

(A) Illustration of *C. elegans* head movements during locomotion. Wild-type animals and *lgc-55* mutants oscillate their heads during forward locomotion. Anterior touch of wild-type animals with an eyelash induces a reversal response

during which the head oscillations are suppressed. *lgc-55* mutants fail to suppress head oscillations during the reversal.

(B) Suppression of head oscillations in response to anterior touch was scored during the reversal response, wild-type (n=235), *lgc-55* mutants [*lgc-55(tm2913)*, n=205; *lgc-55(zf11)*, n=205, *lgc-55(zf53)*, n=170], *lgc-55* rescue [*lgc-55(tm2913); zfEx2,* (n=205)], *myo-3::*LGC-55 [*lgc-55(tm2913); zfEx31,* (n=100)], *sra-11::*LGC-55 [*lgc-55(tm2913); zfEx37*, (n=185)], *glr-1*::LGC-55 [*lgc-55(tm2913); zfEx42,* (n=130)], and *lim-4*::LGC-55 [*lgc-55(tm2913); zfEx44*, (n=115)] . Error bars represent SEM. Statistical difference from wild type; ***p<0.0001, two-tailed Student's t test. ‡ p<0.0001, two- tailed Student's t test. *glr-1*::LGC-55 transgenic animals do not completely suppress head oscillations and appear to have a kinked head during reversals in response to anterior touch. See text for details.

Figure II-10

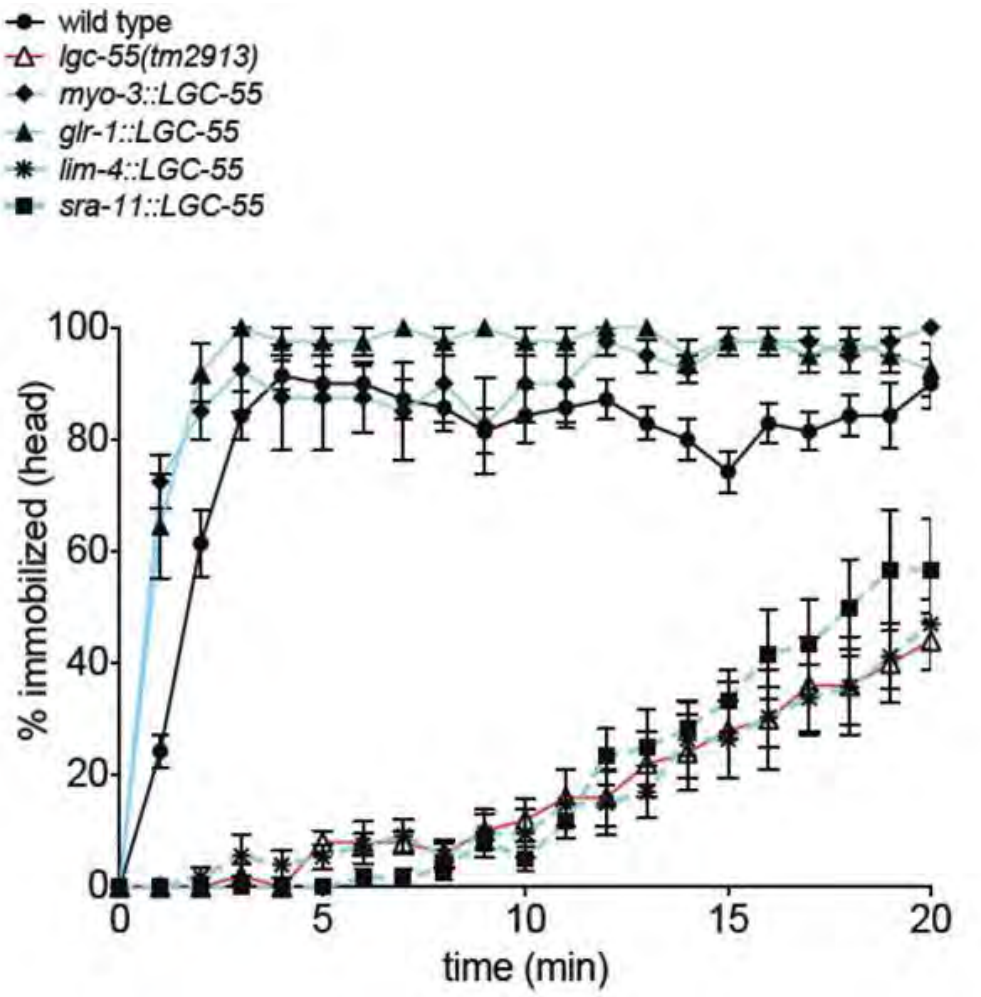

LGC-55 Expression in the RMD and SMD Neurons or Neck Muscles Restores Sensitivity to Exogenous Tyramine.

Quantification of head movements of tissue specific rescue lines on 30 mM tyramine. Expression of *lgc-55* in muscle (*myo-3*::LGC-55), RMD and SMD (*glr-1*::LGC-55) restores sensitivity to exogenous tyramine. Animals expressing *lgc-55* in AVB (*sra-11*::LGC-55) and RMD alone (*lim-4*::LGC-55) are resistant to exogenous tyramine.

Figure II-11

A

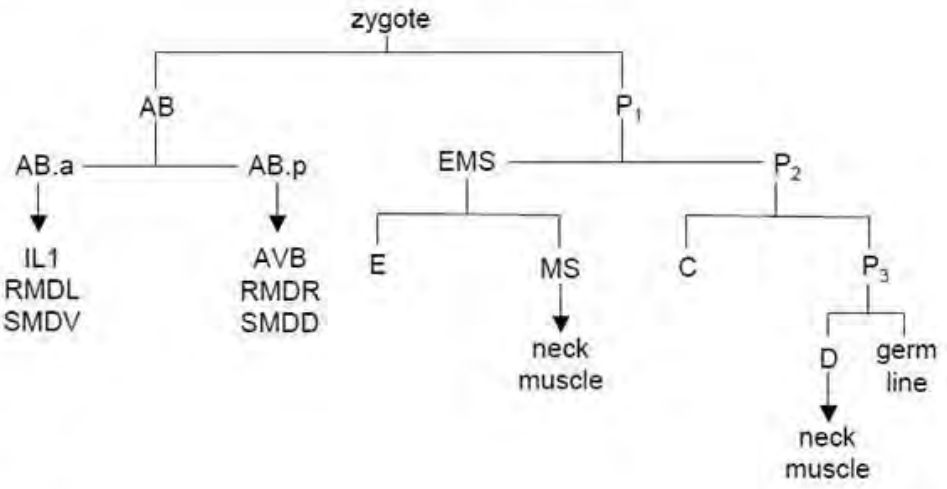

B

Expressing Cells	n	% supp. head oscillations	% head paralysis	longest backward run
All	11	100	100	26 +/- 3.5
None	13	0	0	1.8 +/- 0.3
Muscle	7	97 +/- 2.8	100	1.7 +/- 0.5
Neurons	6	17 +/- 3.3	67 +/- 21	14 +/- 5.1

***lgc-55* is Required in Neck Muscles to Suppress Head Oscillations.**

(A) Diagram of *C. elegans* early cell lineage. *lgc-55* expressing cells derived from AB and P1 are indicated.

(B) Mosaic Analysis. An *lgc-55* rescuing construct was injected into *lgc-55(tm2913)* mutant animals together with *lgc-55::*mCherry and *myo-3*::GFP as lineage markers. Animals lacking *lgc-55* function in either the AB or P1 lineages and non-mosaic controls were analyzed for suppression of head oscillations in response to anterior touch, head paralysis after 5 min. on exogenous tyramine (30 mM) and longest backward run (# backward body bends) on 30 mM tyramine. Data shown are the mean ± SEM.

Figure II-12

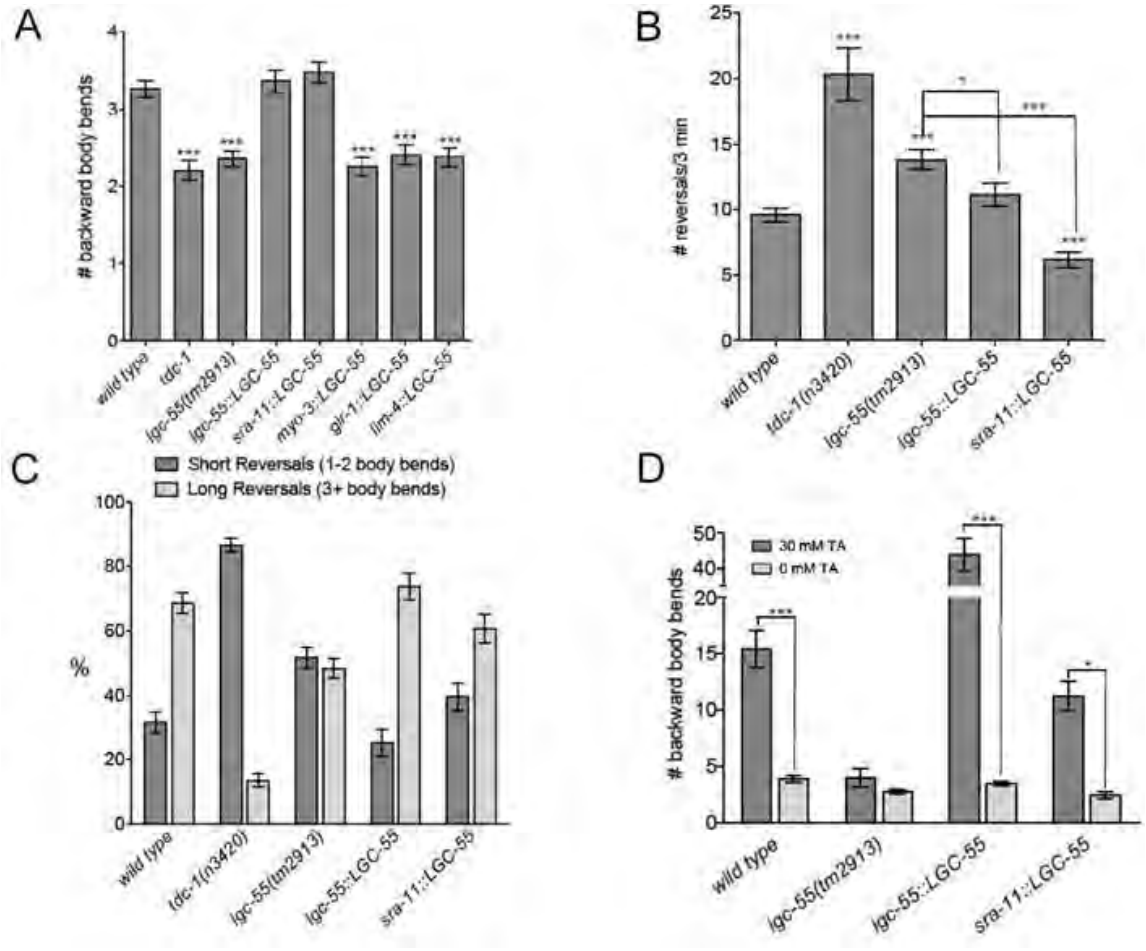

***lgc-55* Mutants Have defects in Reversal Behavior.**

(A) Average number of backward body bends in response to anterior touch of wild-type (n= 317), *tdc-1(n3420)* (n=139), *lgc-55(tm2913)* (n=257), *lgc-55* rescue [*lgc-55(tm2913); zfEx2,* (n=204)], *sra-11*::LGC-55 [*lgc-55(tm2913); zfEx37*, (n=190)], *myo-3*::LGC-55 [*lgc-55(tm2913); zfEx31*, (n=157)], *glr-1*::LGC-55 [*lgc-55(tm2913); zfEx42*, (n=133)], and *lim-4*::LGC-55 [*lgc-55(tm2913); zfEx44*, (n=108)] animals.

(B) Number of spontaneous reversals in 3 minutes of well-fed wild-type (n=55), *tdc-1(n3420)* (n=16), *lgc-55(tm2913)*, (n=40), *lgc-55* rescue [*lgc-55(tm2913); zfEx2,* (n=27)], and *sra-11*::LGC-55 [*lgc-55(tm2913); zfEx37*, (n=32)] animals on

plates without food. Statistical difference from wild type unless otherwise noted; ***p<0.0001, *p<0.01, two-tailed Student's t test.

(C) Distribution of short (1-2 body bends) and long (3+ body bends) spontaneous reversals made in 3 minutes. p<0.001, two-way ANOVA.

(D) Number of backward body bends made during the longest backward run before paralysis on 30 mM tyramine of wild-type (n=33), *lgc-55(tm2913)* (n=20), *lgc-55* rescue [*lgc-55(tm2913); zfEx2,* (n=20)], and *sra-11*::LGC-55 [*lgc-55(tm2913); zfEx37*, (n=29)] animals. 0 mM data represent the number of backward body bends during the longest backward run made in 3 min on agar plates without food for wild-type (n=28), *lgc-55(tm2913)* (n=20), *lgc-55* rescue [*lgc-55(tm2913); zfEx2* (n=20)], and *sra-11*::LGC-55 [*lgc-55(tm2913); zfEx37*, (n=12)] animals. p<0.0001, two-way ANOVA; ***p<0.001, *p<0.01, Bonferroni post-test. Error bars represent SEM.

Figure II-13

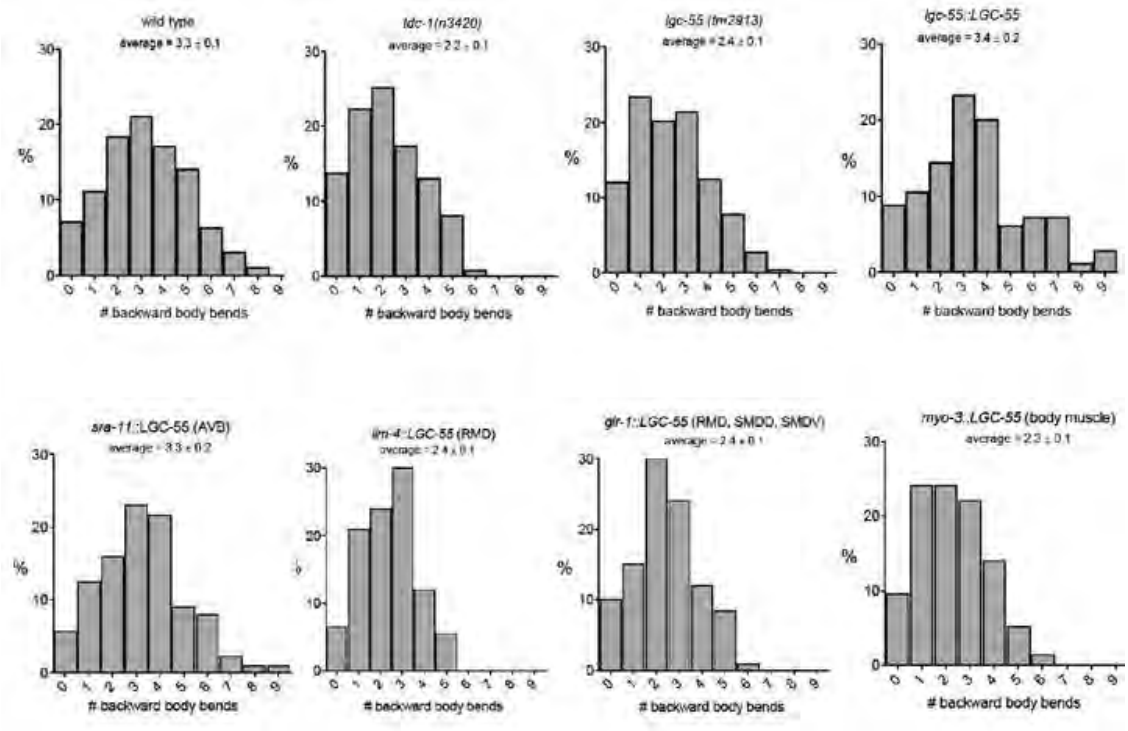

***lgc-55* Mutants Have Defects in Reversal Behavior.**

Distribution of number of backward body bends in response to anterior touch of wild type (n=317), *tdc-1(n3420)* (n=139), *lgc-55(tm2913)* (n=257), *lgc-55* rescue [lgc-55(*tm2913); zfEx2*, (n=204)], *sra-11*::LGC-55 [*lgc-55(tm2913); zfEx37,* (n=109)], *lim-4*::LGC-55 [*lgc-55(tm2913); zfEx44*, (n=108)], *glr-1*::LGC-55 [*lgc-55(tm2913); zfEx42*, (n=133)], *myo-3*::LGC-55 [*lgc-55(tm2913); zfEx31*, (n=157)] animals. See also Figure II-12A.

Figure II-14

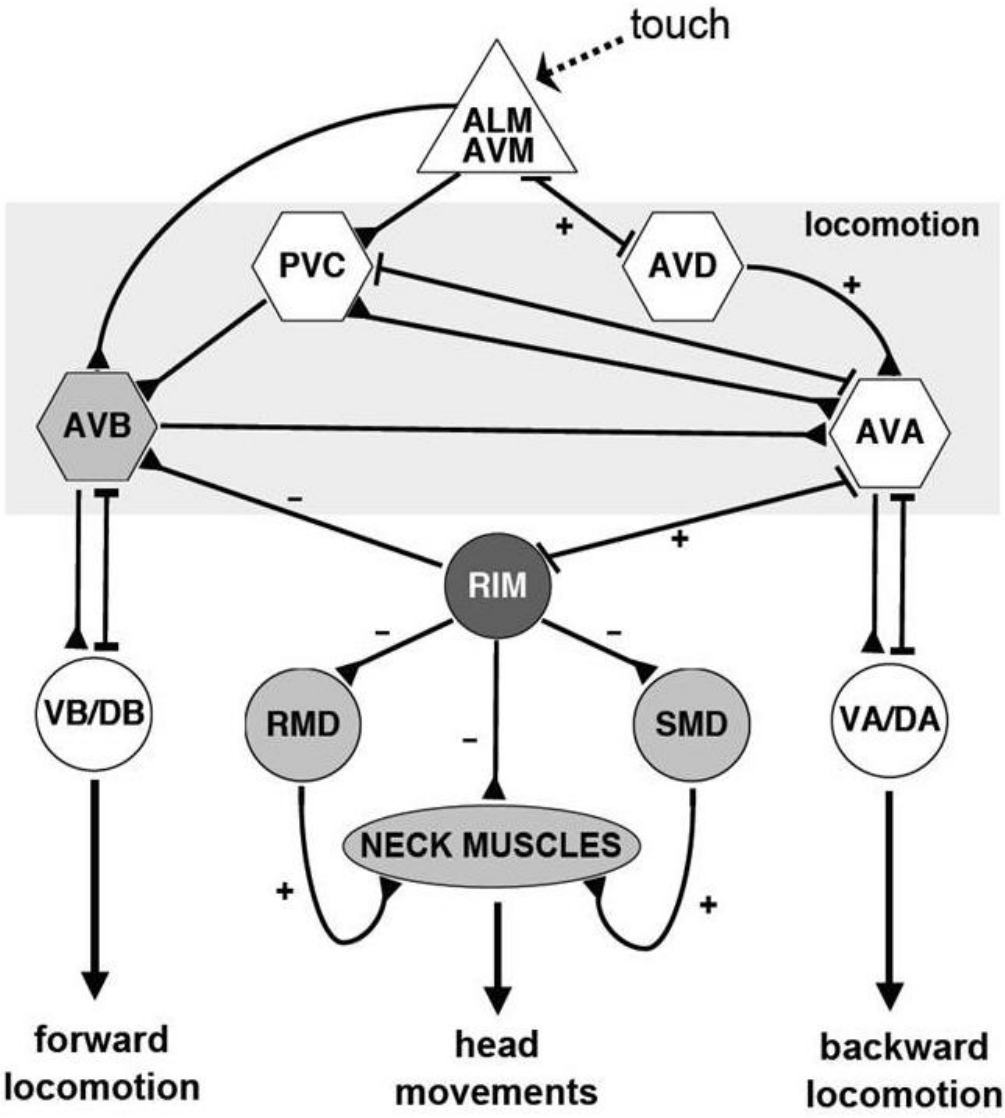

Model: Neural Circuit for Tyraminergic Coordination of *C. elegans* Escape Response.

Tyraminergic activation of LGC-55 hyperpolarizes neck muscles and the AVB command neurons inducing suppression of head oscillations and sustained backward locomotion in response to touch. Schematic representation of the neural circuit that controls locomotion and head movements. Synaptic connections (triangles) and gap junctions (bars) are as described by White et al. (1986). Sensory neurons shown as triangles, command neurons required for

locomotion are shown as hexagons, and motor neurons are depicted as circles. Neck muscles are represented as an oval. *lgc-55* expressing cells and neurons are light grey. The tyraminergic motor neuron (RIM) is dark grey. Hypothesized excitatory (+) connections of neurons in this circuit are based on the identification of neurotransmitters, laser ablation and genetic studies cited in this paper. Inhibitory (-) connections important for suppression of head oscillations in response to anterior touch and sustained backward locomotion are based on behavioral, electrophysiological, and expression data described in this paper. See text for details.

Movie II-1

Movie of a wild-type animal on plates containing 30 mM tyramine.

Filming began immediately after the animal was placed on the plate and ended shortly after paralysis. Movie was shot at 15 frames per second (fps) and sped up five times.

Movie II-2

Movie of a wild-type animal after 5 minutes on plates containing 30 mM tyramine.

Animals paralyze, but can still move in response to mechanical stimulation. Body movements are apparent, but the head and neck remain paralyzed. Movie was filmed at 15 fps.

Movie II-3

Movie of a *lgc-55* animal after 5 minutes on plates containing 30 mM tyramine.

lgc-55 mutant worms display sustained head movements, while body movements are inhibited. Movie was filmed at 15 fps.

Movie II-4

Movie of gentle anterior touch response of wild-type animals.

Wild-type animals suppress head oscillations in response to anterior touch.

Movie II-5

Movie of gentle anterior touch response of *lgc-55*(*tm2913*) mutant animals.

lgc-55 mutant animals fail to suppress head oscillations in response to anterior touch.

Movie II-6

Movie of gentle anterior touch response of transgenic animals expressing *glr-1*::LGC-55.

lgc-55(tm2913) mutant animals expressing a *glr-1*::LGC-55 transgene do not completely suppress head oscillations and have a kinked head during the reversal.

Movie II-7

Movie of gentle anterior touch response of transgenic animals expressing *myo-3*::LGC-55.

lgc-55(tm2913) mutant animals expressing a *myo-3::*LGC-55 transgene suppress head oscillations in response to anterior touch, similar to wild type.

CHAPTER III

Synaptic Engineering: An Ionic Switch of Behavior

The experimental work in this chapter has been written as a manuscript for publication at the time of this thesis preparation. Dr. Diego Rayes will also be credited with authorship on this manuscript for his work performing the electrophysiology experiments in Figure III-1 and Figure III-2 and his critical feedback on the manuscript.

Abstract

Unraveling the human connectome is considered by many to be an essential step in understanding how the brain controls behavior and how malfunction can lead to behavioral disorders. The neural connectivity map, however, does not provide information about the nature of synaptic connections. Whether a synapse within a neural network is excitatory or inhibitory should dramatically change the behavioral output produced by a neural circuit. In this paper we investigate if it is possible to change the behavioral output of a neural circuit by changing the electrical sign of the synapse and if this provides developmental constraints on the connectome. We address these questions in the nematode *C. elegans*, by selectively mutating the tyramine-gated chloride channel, LGC-55 to gate cations instead of anions. We show that the LGC-55 cation channel is appropriately trafficked and functional *in vivo*, leading to behavioral responses that are opposite those produced by activation of wild-type LGC-55. Our data suggest that changing the nature of a synapse within a neural circuit can reverse behavioral outputs and indicate that the neural network for escape behavior in *C. elegans* is established independent of the nature of synaptic activity or behavioral output.

Introduction

In recent years great efforts have been made to map all the neural connections within the human nervous system. Developing the human "connectome" has been considered a fundamental step in understanding complex behavior. The information one would glean from the connectome provides the basis for making the bridge between neurons and behavior. However, a neural network map carries no information about the activity of neurons and the types of synapses each neuron makes. This lack of information obscures the relationship between the connectome and behavioral output.

The clearest example that supports this idea is the neural connectivity map of the nematode *C. elegans*. The *C. elegans* hermaphrodite contains 302 neurons, which make 7,000 chemical synapses and 900 gap junctions (White, et al 1986; Hall and Russell, 1991; Varsheny, et al., 2011). The location of these neurons and their connectivity is fairly invariant animal to animal, which allowed for the reconstruction of the nervous system. How each of these neurons connect to one another has been completely mapped, making the *C. elegans* neural network the only currently known connectome. Even though the *C. elegans* neural connectivity map was described more than 25 years ago; we only really understand the few behaviors where we know the identities of the neurotransmitter and/or the nature of the postsynaptic receptor.

In order to fully understand the relevance of the connectome in predicting behavioral outputs, one of the questions that can be addressed is whether abnormal behavior is the result of aberrant wiring of neural circuits or if it is caused simply by deregulation in synaptic transmission within a given neural network. If the latter possibility is true, dramatic changes in behavior are expected to be observed if either the receptor or the nature of the synaptic connections involved is altered. Elegant sensory engineering experiments have demonstrated that animals can be reprogramed to avoid normally attractive molecules by expressing exogenous chemoreceptors on the sensory neurons. For example, in *C. elegans* endogenous expression of the chemoreceptor ODR-10 in the AWA neuron, leads to attraction to diacetyl. However, ectopically expressing ODR-10 in the AWB neuron, which is associated with aversive behaviors, leads to diacetyl avoidance (Troemel et al, 1997; Wes and Bargmann, 2001). In *Drosophila*, capsaicin-mediated activation of VR1 cationic channels expressed in Gr5a cells, which are involved in sugar sensing, and Gr66 cells, which are implicated in avoidance of bitter compounds, is sufficient to elicit taste attraction or avoidance respectively, when flies are presented with capsaicin (Marella, et al., 2006). Moreover, expression of the artificial opiate receptor RASSL in sweet sensing cells in mice leads to strong attraction to a synthetic opiate, whereas aversion to this compound is observed when RASSL is expressed in bitter sensing cells (Zhao, et al., 2003; Mueller et al., 2005). These studies strongly support the idea that the activation of sensory neurons is

hardwired to produce specific behavioral outputs. However, since these changes are limited to the edge of the neural network, no conclusion can be made about the effect of alterations in synaptic transmission at the interneuron and neuromuscular level.

Is it possible to alter behavior by changing synapses within the neural network? If we change the sign of one synapse within a connectome, would this be sufficient to completely reverse the behavioral outputs? Or are there developmental constraints and compensatory mechanisms that would alleviate the effects an alteration in synaptic activity would have on the behavioral output? Here, we address these questions using the neuronal circuit that mediates the *C. elegans* escape response.

C. elegans has a single pair of tyraminergic neurons in the head ganglia, the RIMs, which activate the homomeric tyramine-gated chloride channel, LGC-55. This receptor belongs to the cys-loop, ligand-gated ion channel family of receptors, similar to the nicotinic acetylchoine (nAcHR), γ-aminobutyric (GABA), glycine, and 5-HT3a ionotropic receptors. LGC-55 is the only ionotropic tyramine receptor expressed in both neurons and neck muscle cells that are directly postsynaptic to the RIM (Pirri, et al., 2009). Since, there is a single pair of neurons that release tyramine during the escape response and a single ionotropic postsynaptic receptor; we have a unique opportunity to determine if

changing the sign of a receptor can affect the behavioral output of a defined neural circuit.

Experimental Procedures

Cloning of LGC-55 L and LM2

Standard molecular biology techniques were used. ClustalW alignments were carried out using MacVector Software (Accelrys). An *lgc-55* rescue construct was made by cloning a *lgc-55* genomic fragment corresponding to nucleotide (nt) -2663 to +3895 relative to the translation start site into the EcoRV site in yk1072c7, as in Pirri, et al., 2009. To make the chimeric LGC-55 L receptor we performed DpnI site directed mutagenesis on the *lgc-55* rescuing construct using a primer that corresponded to the genomic sequence of the M1-M2 loop of the 5HT3a channel with 20 nt on either side homologous to the same region in LGC-55. LGC-55 LM2 was made using DpnI site directed mutagenesis with a primer that changed the codon in the LGC-55 cDNA at nts 1042 – 1044 relative to the translational start, corresponding to a R to D substitution at the 20' position of the M2 loop. For muscle specific expression of LGC-55 and LGC-55 LM2 the full length *lgc-55* or *lgc-55 LM2 cation* cDNA was cloned into pPD95.86 behind the *myo-3* promoter. *LGC-55::GFP* and *LGC-55 LM2::GFP* translational fusion constructs were made by cloning GFP into an engineered AscI restriction in the respective rescuing constructs in the sequence encoding the intracellular loop between TM3 and TM4. For AVB specific expression, nt -2663 to -121

relative to the translational start site of the *LGC-55::GFP* and *LGC-55 LM2::GFP* rescuing constructs were deleted using restriction digest.

All transgenic strains were obtained by microinjection of plasmid DNA into the germline. At least three independent transgenic lines were obtained and data are from a single representative line. All transgenic animals used in the experiments outlined in this paper are in an *lgc-55* null background, unless otherwise noted. Transgenic animals were made by co-injecting *lgc-55* rescuing, *lgc-55 L/LM2 cation*, *myo-3:*LGC-55, *myo-3::*LGC-55 L/LM2, *pAVB*::LGC-55::GFP, *pAVB::*LGC-55 LM2::GFP; *plgc-55*::LGC-55::GFP, or *plgc-55*::LGC-55 LM2::GFP at 20 ng/µl along with the *lin-15* rescuing plasmid pL15EK at 80 ng/µl into *lgc-55(tm2913); lin-15(n765ts)* animals.

Isolation and Culture of C. elegans Muscle Cells.

Embryonic cells were isolated and cultured as described by Christensen et al. (2002). Briefly, adult animals expressing the *myo-3::LGC-55 or LGC-55 LM2; myo-3::GFP* transgene were exposed to an alkaline hypochlorite solution (0.5 M NaOH and 1% NaOCl). Eggs released were treated with 1.5 U/ml chitinase (Sigma-Aldrich Co., St. Louis, MO) for 30 to 40 min at room temperature. The embryonic cells were isolated by gently pipetting and filtered through a sterile 5 µm Durapore syringe filter (Millipore Corporation, Billerica, MA) to remove undissociated embryos and newly hatched larvae. Filtered cells were plated on glass coverslips coated with peanut lectin. Cultures were maintained at RT in a

humidified incubator in L-15 medium (Hyclone, Logan, UT) containing 10% fetal bovine serum. Complete differentiation to muscle cells was observed within 24 h. Electrophysiology experiments were performed 2 to 8 days after cell isolation. Muscle cells from transgenic animals were identified by GFP expression.

Electrophysiology

Whole-cell patch clamp recordings were performed using a HEKA EPC-9 patch clamp amplifier. Recording pipettes with a resistance of 3-7 MΩ were used. The intracellular solution contained 115 mM K-gluconate, 25 mM KCl, 0.5 mM $CaCl_2$, 50 mM HEPES, 5 mM Mg-ATP, 0.5 mM Na-GTP, 0.5 mM cGMP, 0.5 mM cAMP, and 1 mM BAPTA (PH 7.4). For ionic selectivity experiments extracellular solutions with different concentrations of Na^+ and Cl^- were used: ES1 (standard solution, 150 mM NaCl, 5mM KCl, 1mM $CaCl_2$, 4 mM $MgCl_2$, 15 mM HEPES, 10 mM glucose, pH 7.2 with NaOH), ES2 (as ES1 except 15 mM NaCl, 135 mM NMDG-Cl) ES3 (as ES1, except 30 mM NaCl, 120 mM Na-gluconate). For K^+ and Ca^{++} permeability studies, the solutions used were: ES4 (as ES2 except 140 mM KCl) and ES5 (as ES2 except 25 mM $CaCl_2$, 85 mM NMDG-Cl).

Current voltage relationships were constructed by measuring the current peak after 250 ms perfusion of extracellular solution containing 0.5 mM tyramine at holding potentials ranging from -60 to +60 mV in 20 mV steps. Data analysis was performed using Igor Pro software (Wavemetrics Inc, Lake Oswego, Oregon). Mean currents were fitted by a single exponential function: $I_{(t)} = I_o \exp(-$

$t/\tau_d) + I_\infty$ were I_o is the current at the peak, I_∞ is the current at the end of the recording and τ_d the current decay time constant. Data were normalized to I_{max} and the mean peak value in each condition was obtained after averaging 3 different traces (obtained not consecutively, but in different voltage protocols in the same experiment). If the difference in current peak values were more than 80 % for a given condition, the whole experiment were discarded.

Reversal potential values are shown as mean ± standard error of 4-5 independent experiments for each extracellular solution. Curve fitting and statistical analysis was performed using Sigma Plot 11.0 (Systat Software Inc.)

Behavioral Assays

All behavioral analysis was performed with young adult animals (18-24 hr. post-L4) at room temperature (20º-23ºC); different genotypes were scored in parallel, with the researcher blinded to the genotype. Quantification of tyramine resistance and tyramine induced reversals were performed as in Pirri, et al. 2009. To quantify body length on exogenous tyramine, animals were placed on agar plates supplemented with 30 mM tyramine. Still frames were taken at 5 minutes after exposure to tyramine and animals were measured using ImageJ software. To quantify neck length on exogenous tyramine, animals were placed on 30 mM tyramine plates. Still frames were taken at 5 minutes after exposure to exogenous tyramine. The neck was defined as the length from the anterior most

point of the buccal cavity to posterior of the pharyngeal bulb (illustrated in Fig. 3b). Neck lengths were measured using ImageJ software.

To quantify neck lengths in response to touch animals were filmed for 10 seconds before and after touch posterior to the pharyngeal bulb with an eyelash using an Imaging Source DMK21F04 firewire camera and AstroII DC software. Still frames were grabbed from the video just prior and just after touch. Neck lengths were measured from these still frames using ImageJ software. Animals used in this set of experiments were in the *unc-3(e151)* background. *unc-3(e151)* animals have a defect in ventral cord specification that affects locomotion but not head and neck movements. We used these animals in these assays and in our optogenetic experiments to prevent locomotion so as to maintain the animal in the field of view at a magnification that would allow for accurate neck measurement.

Optogenetic head contraction assays were performed with transgenic animals containing either wild type LGC-55 or LGC-55 LM2 and *tdc-1*::ChR2 in an *unc-3 (e151)* mutant background. For these experiments, healthy L4 animals were transferred to assay plates that were seeded with either OP50 *E.coli* that was supplemented with *all-trans* retinal to a final concentration of 660 µM or plain OP50. Animals were fed retinal or non-retinal containing food overnight. To quantify neck lengths in response to optogenetic activation of the RIM, animals were filmed for 10 seconds before and after a 2 second blue light pulse. Still

frames were grabbed from the video just prior to and during the blue light exposure. Neck lengths were measured from the still frames as described above.

Results

Mutation of the LGC-55 M1-M2 intracellular linker results in cation selectivity.

Ligand-gated ion channels (LGICs) are the fundamental signaling component for fast chemical neurotransmission. These channels can either be excitatory or inhibitory, and this is determined by whether the channel is selective for cations or anions. The cys-loop LGIC family of receptors is a class of pentameric channels. Each individual subunit contains an extracellular N-terminal domain that harbors the ligand binding domain and four transmembrane spanning domains (M1-M4). The location of charge selectivity determinants is common to both anion and cation-selective channels, and mainly involves residues within the intracellular loop between M1 and M2 (Galzi et al., 1992, Keramidas et al., 2000). *In vitro* studies have largely shown that a PAR motif in this loop is critical for anion selectivity and its substitution by equivalent residues from excitatory channels is enough to convert the receptor selectivity from anionic to cationic (Glazi, et al. 1992, Keramidas et al., 2000, Gunthorpe and Lummis, 2001, Menard et al. 2005) (Figure III-1A,B).

To change the ion selectivity of LGC-55, we engineered a chimeric receptor which replaced the residues of the anionic M1- M2 loop (RRSLPA) with

those that are conserved in structurally related cationic channels (PDSG-E) (Figure III-1B). LGC-55 L, contains the M1-M2 loop of the cationic 5HT3a channel, while LGC-55 LM2 also includes an R to D substitution at the 20' position of the M2 segment (Figure III-1B). Given that this position has been reported as a main determinant of channel conductance (Imoto et al, 1998; Langosch et al, 1994), the introduction of a negatively charged amino acid is expected to increase the cation conductance of the chimeric receptor.

In order to determine the ionic selectivity of the LGC-55 receptor containing the M1-M2 intracellular loop of 5HT3aR, we recorded tyramine-elicited whole cell currents in cultured muscle cells obtained from two different *C.elegans* strains that ectopically expressed either the wild-type or the LM2 version of LGC-55 in body wall muscles (*myo-3*::LG-55 or LG-55 LM2; *myo-3*::GFP, see methods). We constructed the corresponding I-V relationships in the presence of different extracellular solutions: ES1 (Standard solution: 150 mM Na^+, 165 mM Cl^-), ES2 (low Na^+: 15 mM Na^+, 165 mM Cl^-) and ES3 (low Cl^-: 150 mM Na^+, 30 mM Cl^-). Given that similar mutations in other LGIC receptors have been reported to also alter the agonist EC50 (Keramidas et al., 2000; Gunthorpe and Lummis, 2001; Wotring et al., 2003), we perfused the patches with a high concentration of tyramine (0.5 mM) where saturation is expected to be achieved.

The reversal potential (Erev) of the wild type LGC-55 in standard solution (ES1) was -26.8 ± 3.1 mV (n=4) which is consistent with our reported data using

body-wall muscle recordings *in vivo*, and to the predicted Erev for an anion-selective channel in our conditions (Francis and Maricq, 2006; Pirri et al, 2009). As expected, no significant differences were observed in the Erev values for the wild-type receptor in the ES2 solution when compared to the standard conditions (Erev= -24.3 ± 1.6 mV, n=4). On the other hand, a 5.5-fold reduction of extracellular chloride concentration (ES3) lead to a ~20 mV rightward shift of the reversal potential (Erev= -1.9 ± 2.3 mV, n=4). Taken together, these observations agree with our previous report confirming that the tyramine receptor LGC-55 is predominantly permeant to anions (Pirri et al., 2009, Figure III-1C).

Equivalent experiments performed on cultured muscle cells that expressed LGC-55 LM2 showed that the reversal potential in standard solution was 2.4 ± 1.2 mV (n=5), near the GHK-predicted value for a cation-selective channel. Reduction of the extracellular chloride concentrations did not lead to significant changes in this value (Erev in ES3: 1.7 ± 0.9mV, n=4), whereas a ~ 24mV shift to more negative potentials is observed when we decrease the extracellular sodium concentration (Erev in ES2; -21.9 ± 2.6 mV, n=5). These findings indicate that the current passing through the chimeric LGC-55 LM2 channel is mainly carried by Na^+ and that the Cl^--dependent component of that current is negligible. We can therefore conclude that the replacement of the M1-M2 linker by that of the cationic 5HT3a receptor converts the selectivity of the LGC-55 channel from anionic to cationic (Figure III-1C).

To further study the ionic selectivity of the LGC-55 LM2 receptor, we varied the K^+ and Ca^{2+} concentrations of the extracellular solutions and performed whole cell experiments as described above (Figure III-2). An increase in the external K^+ concentration (from 5 mM to 140 mM in an external solution containing 15 mM Na^+, ES4) significantly displaced the reversal potential towards more positive membrane potentials (Δrev~ 23.8 mV), indicating that the channel is also highly permeant to K^+ (Figure III-2). On the other hand, a 25-fold increase in the external Ca^{2+} concentration (ES5) did not change the reversal potential suggesting negligible calcium permeability. These observations are consistent with previous reports showing that similar mutations in the M1-M2 linker of GlyR dramatically increase the permeability of monovalent cations but not of calcium (Keramidas et al., 2000).

Chimeric LGC-55 cation channels are functional *in vivo.*

To determine if the chimeric LGC-55 receptors are functional *in* vivo, transgenic animals that expressed either the wild-type or cationic LGC-55 channels in all muscle cells were exposed to exogenous tyramine. Over-expression of LGC-55 anion in all muscle cells caused muscle relaxation and overall lengthening of the animal (*myo-3::LGC-55 anion (zfEx31),* 8.6% increase in length, n=53) during exposure to exogenous tyramine. We observed that *lgc*-55 mutant animals were slightly contracted on tyramine. This is likely due to the activation of the tyraminergic GPCR, SER-2, which inhibits GABA release onto

body wall muscles (Donnelly, et al., 2013), leading to a slight contraction of the animal's ventral musculature (*lgc-55(tm2913)*, 5.3% decrease in length, n=25). In contrast, transgenic animals that expressed the LGC-55 L or LGC-55 LM2 cation channel in all muscle cells were extremely hypercontracted and shortened in response to exogenous tyramine (*myo-3::LGC-55 L (zfEx367)*, 16.6% decrease in length, n=59; *myo-3::LGC-55 LM2 (zfEx41)*, 20.1% decrease in length, n=55). This indicates that the chimeric LGC-55 cation channels are functional *in vivo* (Figure III-1D,E).

Changes in neuronal activity cause synaptic plasticity in LGC-55 cation mutants.

Our ectopic expression of the chimeric LGC-55 channels suggests they can be trafficked to the muscle cell surface and respond to tyramine *in vivo*. Since, LGC-55 is not normally expressed in all muscle cells, we wanted to determine if the cationic tyramine receptors can now be appropriately trafficked to the endogenous synapse, and how this might affect synaptic development. The tyraminergic RIM makes synaptic outputs onto the neck muscles and several neurons that express LGC-55. To visualize these tyraminergic synapses we expressed the synaptic vesicle marker, mCherry::RAB-3 in the RIM neurons and a rescuing LGC-55::GFP translational fusion under control of the *lgc-55* promoter in *lgc-55* mutant animals. Expression of mCherry::RAB-3 in the RIM neurons showed presynaptic varicosities along the ventral process and in the nerve ring

and LGC-55 receptors formed high density clusters opposite of these tyramine release sites (Figure III-3A). We compared this with the localization of synaptic vesicles and postsynaptic receptors in LGC-55 LM2 cation animals. Transgenic animals that expressed LGC-55 cation LM2::GFP under control of the *lgc-55* promoter and mCherry::RAB-3 in the RIM, have similar localization to synaptic specializations in the nerve ring and along the ventral process (Figure III-3A).

To further examine the localization of the chimeric receptor to the postsynapse, we visualized the synapses made by the RIM onto one of its postsynaptic partners, the forward locomotion command neurons, AVB. We expressed the translational fusion of LGC-55::GFP or LGC-55 LM2::GFP, under control of a promoter fragment that drives expression in a subset of LGC-55 positive cells, including the AVB. Electron micrograph reconstructions show the AVB neurons make several synaptic connections with the RIM in the segment of the ventral process that is most proximal to the cell body (White, et al. 1986, Figure III-3B). LGC-55 anion channels are localized to postsynaptic specializations opposing this presynaptic region in the RIM. Similarly, the LGC-55 LM2 cation channels are localized in the same region as the wild type, anion channel (Figure III-3D, Figure III-4). We measured the size of the pre- and postsynaptic density in wild-type animals and tyramine signaling mutants. Wild type animals show discrete regions of pre- (average width: 3.3 ± 0.3 μm, n=19) and postsynaptic density (average width: 5.0 ± 0.46 μm, n=19) (Figure III-3D,E). Mutants that lack tyramine (*tdc-1*) still form synapses in the correct region

however the presyanpse becomes larger (average width: 3.8 ± 0.3 μm, n=14) and the expression of LGC-55 in the postsynaptic region was increased and more diffuse (average width: 7.7 ± 0.7 μm, n=14) (Figure III-3C,D,E). In *lgc-55* null mutants, the presynaptic density becomes even larger than in the tyramine deficient animals (average width: 5.4 ± 0.4 μm, n=17) (Figure III-3D,E). Similarly, the presynaptic density in LGC-55 LM2 animals is also larger (average width: 6.1 ± 0.4 μm, n=11), and in the postsynaptic density expression is lower and more diffuse (average width: 5.5 ± 0.4 μm, n=12) (Figure III-3C,D,E). These results suggest that while the chimeric channels can be properly localized at the neuromuscular junction and at synaptic connections between neurons, there is some plasticity after neural connections are made. Expression of the postsynaptic receptor or volume of release sites may be up or down regulated based on activity levels within the circuit. However, changing the receptor from inhibitory to excitatory has no effect on the gross development of the neural circuit controlling *C. elegans* escape behavior.

LGC-55 cation channels change the behavioral outputs of the neural circuit controlling *C. elegans* escape.

Can the ionic switch of the LGC-55 receptor elicit an opposite behavioral response? To analyze the functional consequences of converting LGC-55 to a cationic receptor, we tested the response of *lgc-55* mutant animals that expressed LGC-55 anion or LGC-55 cation under control of the native promoter

to exogenous tyramine. Wild-type animals on exogenous tyramine exhibit neck relaxation and long backward locomotory runs before paralysis (Pirri, et al., 2009, Figure III-5, Movie III-1). Previous reports from our group indicated that paralysis is due to hyperactivation of the tyraminergic GPCR, SER-2, which inhibits GABA release in the ventral nerve cord affecting locomotion (Donnelly, et al., 2013). However, it is the hyperactivation of the LGC-55 anion channel that leads to neck relaxation and long backward runs. LGC-55 is expressed in the second row of neck muscles that control radial head movements. In wild-type animals exogenous tyramine causes hyperpolarization of the neck muscles through the activation of LGC-55, and the neck becomes relaxed and lengthened (wild type (anion), 5.2% increase in length, n=68; LGC-55 rescue (anion Ex), 5.8% increase in length, n=75) (Figure III-5A,B). In this assay, head movements persisted in *lgc-55* mutants (data not shown), and there was no significant change in the overall length of the neck (*lgc-55(tm2913)*, 1% increase in neck length, n=65). In contrast, transgenic animals that expressed the chimeric LGC-55 cation receptor variants under control of the native promoter had a hypercontracted and shortened neck in the presence of exogenous tyramine (LGC-55 L (cation (L) Ex), 7.8% decrease in length, n=49; LGC-55 LM2 (cation (LM2) Ex), 14.6% decrease in length, n=49) (Figure III-5A,B). LGC-55 is also expressed in the forward locomotion command neurons, AVBs, which drive locomotion. In wild-type animals, hyperactivation of LGC-55 by exogenous tyramine causes hyperpolarization of the AVB neuron and leads to long backward runs (wild-type

(anion), -16 ± 2.7 body bends, n=40; LGC-55 rescue (anion Ex), -33.7 ± 2.9 body bends, n=29) (Pirri, et al., 2009, Figure III-5A,D, Movie III-1). *lgc-55* mutants paralyze without making a significant locomotory run in either direction (*lgc-55 (tm2913),* backward: -6.6 ± 0.9 body bends, n=34; forward: 9.2 ± 0.9 body bends, n=29). However, LGC-55 cation animals exhibit dramatic long forward runs (LGC-55 L (cation (L) Ex), 48.3 ± 8.4 body bends, n=17; LGC-55 LM2 (cation (LM2) Ex), 81.7 ± 9.5 body bends, n= 24) which continued for an extended period of time (Figure III-5A,C,D, Movie III-2). We observed that animals expressing the LGC-55 anion channel become immobilized more quickly than those expressing the LGC-55 cation channel. This suggests that the fast inhibition of locomotion on exogenous tyramine is, in part, attributed to the inhibition of the forward locomotion command neuron, AVB, and not solely due to activation of SER-2 (Figure III-5C).

While the exogenous tyramine assays indicate that the LGC-55 cation receptor is functional in cells that normally express LGC-55, can it function in the endogenous tyraminergic circuit? A caveat to an exogenous drug assay is that they are only useful to evaluate gross receptor expression and functionality without giving much information regarding the behavior of the receptor in response to synaptic release of neurotransmitter. To test if the LGC-55 cation channel is acting at the synapse within the escape circuit, like its wild type counterpart, we tested the behavioral response of these animals to a touch stimulus.

Touch activates mechanosensory neurons that activate the backward locomotion command neurons leading to a reversal. Activation of the backward locomotion program simultaneously activates tyramine release from the RIM (Figure III-6A). Tyramine release then activates LGC-55 anion channels in the neck muscles causing suppression of exploratory head movements during the reversal and a slight lengthening of the neck (Figure III-6B, Figure III-7, Movie III-3, Pirri, et all., 2009). *lgc-55* null mutant animals, continue the exploratory head movements during the reversal and there is no significant change in neck length. However, in transgenic animals that expressed the LGC-55 cation channel, touch induced a contraction of the neck muscle, resulting in a shortened neck (wild-type (anion), 3.3% increase in length, n=39; *lgc-55(tm2913)*, 0.6% increase in length, n=21; LGC-55 L (cation (L) Ex), 7.2% decrease in length, n=32; LGC-55 LM2 (cation (LM2) Ex), 9.0% decrease in length, n=26) (Figure III-6B, Figure III-7, Movie III-4).

Additionally, LGC-55 plays a role in suppressing forward locomotion during the touch response so the animal can make a long reversal. Touch induced activation of the LGC-55 anion channel causes a hyperpolarization of the AVB, and leads to an extended reversal so the animal can escape the stimulus. In response to touch, wild type animals reversed for an average of 3 backward body bends (n=100) (Movie III-3), while *lgc-55* mutants failed to execute a long reversal (*lgc-55(tm2913),* 2.45 ± 0.15 body bends, n=100) (Figure III-6A,C, Figure III-8, Pirri et al., 2009). Transgenic animals that expressed the

LGC-55 cation channel variants also failed to reverse in response to touch, often not moving away from the point of stimulus (LGC-55 L, 1.57 ± 0.1 body bends, n=100; LGC-55 LM2, 1.22 ± 0.1 body bends, n=100) (Figure III-6C, Figure III-8, Movie III-4). In addition to response to touch, it has been previously reported that tyramine plays a role in spontaneous reversal rate and length. Mutants deficient in tyramine signaling, *tdc-1* and *lgc-55,* have an increase in spontaneous reversal rate and make shorter reversals (Alkema, et al., 2005; Pirri, et al., 2009). We also examined spontaneous reversals in our cation mutants and found that animals expressing LGC-55 L or LGC-55 LM2 have a dramatic increase in the number of spontaneous reversals (Figure III-9A) and in most cases failed to make a full body bend during the reversal (Figure III-9B). These data suggest that in the LGC-55 cation mutants, the simultaneous activation of the forward (AVB) and backward (AVA) locomotion command neurons contributes to the inability for the animals to move a significant distance in either direction (Figure III-6C, Figure III-8,9).

To determine if the behavioral response to touch is dependent on the tyramine release from the RIM, we specifically activated the RIM by expressing the light-gated cation channel, ChannelRhodopsin 2 (ChR2) in these neurons. This allows us to determine if the touch induced release of other signaling molecules, like neuropeptides or other transmitters, can affect the escape response. Upon exposure to blue light, wild type animals that expressed ChR2 in the RIM relaxed their necks (Figure III-6D, Figure III-10, Movie III-5) (wild-type

(anion), 3.7% increase in length, n=28). In contrast, LGC-55 cation animals, which also expressed ChR2 in the RIM, had hypercontracted necks in response to blue light exposure (Figure III-6D, Figure III-10, Movie III-6) (LGC-55 LM2 (cation LM2 Ex), 12.1% decrease in length, n=20). This response was abolished in *tdc-1* mutants that do not produce tyramine (*tdc-1(n3420);* LGC-55 LM2, 0.5% decrease in length, n=16) (Figure III-6D, Figure III-10). These data support the notion that tyramine is released from the RIM and activates the tyramine gated chloride channel, LGC-55 in the postsynapse. Furthermore, these results indicate that the chimeric LGC-55 cation channels are properly expressed and functional at the synapse within the neural circuit that modulates the *C. elegans* escape behavior.

Discussion

While many studies have suggested that activity is important to sculpt and maintain neural connections in the brain (Mennerick and Zourmski, 2000; Hua and Smith, 2004; Yamamoto and López-Bendito, 2012), our results suggest that the electrical nature of neural activity may not impact neural circuit development. Here we show that neck muscles and AVB neurons, which are predicted to be inhibited by tyramine, have no developmental or functional restrictions to the expression of the cationic version of LGC-55. Normally these cells that are postsynaptic to the tyraminergic neuron express an anionic version of LGC-55. By engineering a chimeric LGC-55 cation receptor and expressing it in the native

circuit, we have shown, for the first time, that it is possible to alter behavioral outputs by changing the nature of the synapse within a neural network. Mechanical stimulus or optogenetic activation of endogenous tyramine release triggers animals expressing the LGC-55 cation variants to hypercontract neck muscles. Furthermore, LGC-55 cation animals fail to reverse in response to touch, suggesting there is activation instead of inhibition of the forward locomotion command neuron, AVB. Our data suggests that the initial wiring of this neural circuit is established independently of the nature of synaptic transmission and that the type of neuronal activity, whether excitatory or inhibitory, seems to be irrelevant for the formation and stability of synaptic contacts in the neural circuitry that controls *C. elegans* escape behavior.

These observations are consistent with several reports showing that the nature of synaptic connections may be unimportant for the gross morphology and topology of the brain. It has been largely reported that the postsynaptic response elicited after the activation of a given receptor is dependent on the developmental stage of the nervous system and the neuron type. For example, the GABAAR, traditionally classified as inhibitory, generates excitatory responses in most embryonic neurons, and in some mature neuronal types in mammals (Ben Ari., 2002; Owens and Kriegstein 2002; Gulledge and Stuart, 2003; Chavas and Marty, 2003). These studies further support the idea that the sign of the synapse may not be critical for development of a neural circuit, since this type of variability

in the postsynaptic response would require very specific, complex and dynamic mechanisms for the development each type of synapse in the nervous system.

The expression of the chimeric LGC-55 cation channel may cause some plasticity in levels of receptor expression. We found that despite a complete change in the electrical nature of the synapse, the synaptic contacts between the tyraminergic RIM and its postsynaptic partners develop normally, however levels of receptor expression are decreased. Furthermore, null mutant animals that lack the biosynthetic enzyme for tyramine, TDC-1, or the LGC-55 receptor also develop normal synaptic contacts, suggesting that activity may not be important for the formation of this neural circuit. In *C. elegans,* release of the inhibitory neurotransmitter, GABA, is not required for clustering of GABA receptors at the neural muscular junction (NMJ), nor is it required for the formation of the presynaptic sites (Gally and Bessereau, 2003). Similarly, mice that do not synthesize acetylcholine form neuromuscular synapses form clusters of acetylcholine receptors similar to wild type animals (Misgeld, T., et. al., 2002) and the brain histology and cytoarchitecture of newborn GAD knockout mice, which are deficient in GABA production, do not show evident abnormalities (Ji et al., 1999). Moreover, blockage of neuronal activity with tetrodotoxin in the developing mammalian brain does not cause any gross morphological defects (Shatz, C., et al.,1988). Together these data indicate that neural circuits might first develop and then later expression of receptors dictates the nature of the connection. Also

raise the possibility that the resulting activity then shapes the final architecture of the mature neural circuit.

Our manipulation of synapses within the connectome suggests that function may not be emergent property of network connectivity. The flow of information may be predicted by the neural connectivity map, but behavioral output cannot be determined without knowledge of the signaling molecules that interpret that flow of information. While understanding how the nervous system is connected is an important step to unravel how the brain functions, it is only a foundation on which we can begin to understand how neural activity sculpts behavior. A detailed description of the type of molecules within the network, the contribution of extrasynaptic receptors, and description of the properties of the neurons involved, is also needed in order to accurately predict behavioral outputs from neuronal networks. Furthermore, study of how neural circuits develop, function and remain stable in relation to intrinsic or extrinsic activity will be critical to the understanding of how the nervous system controls behavior.

Figure III-1

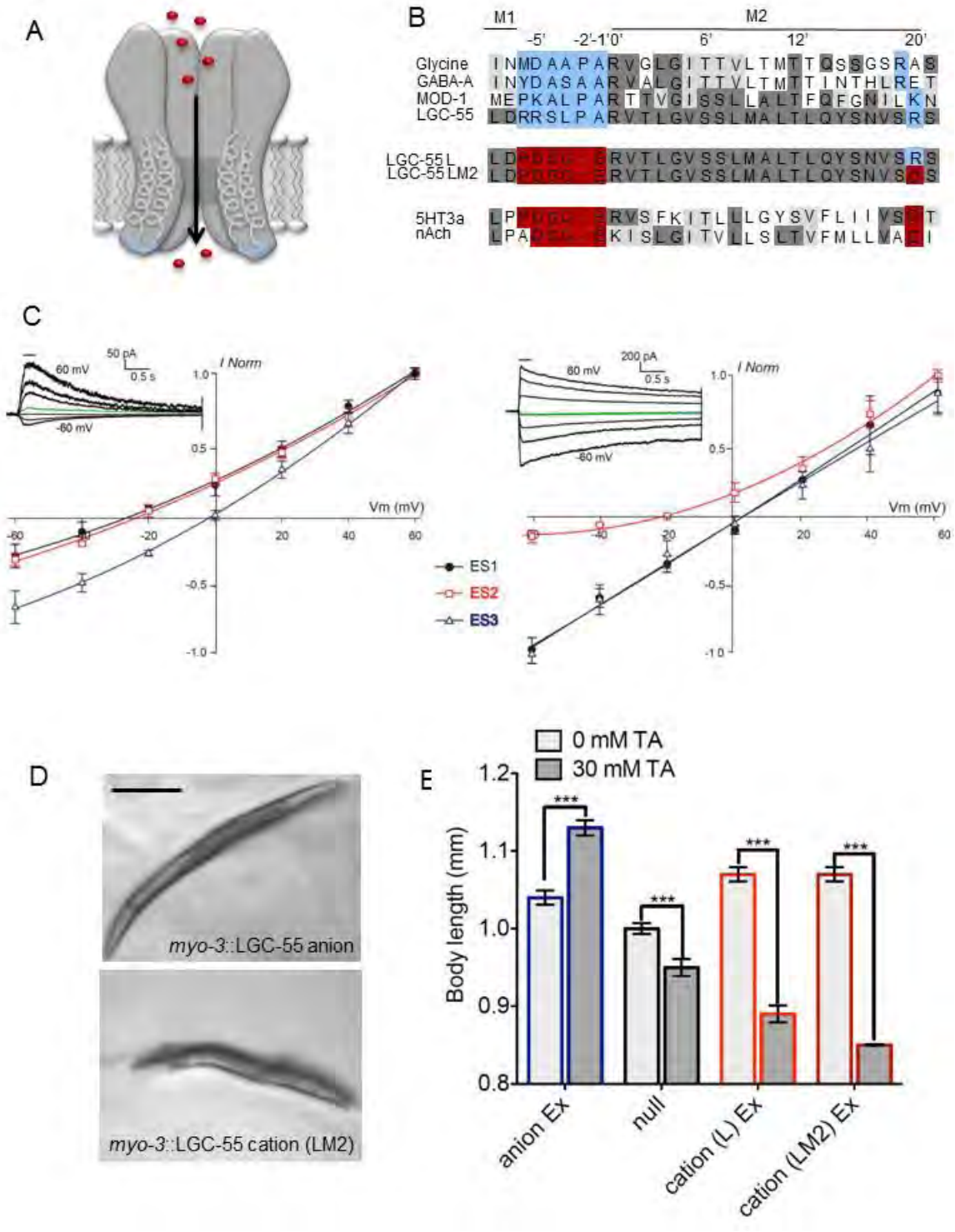
A
B
M1
M2
-5'
-2'
-1'
0'
6'
12'
20'
Glycine
GABA-A
MOD-1
LGC-55
LGC-55 L
LGC-55 LM2
5HT3a
nAch
C
60 mV
50 pA
0.5 s
-60 mV
I Norm
Vm (mV)
ES1
ES2
ES3
200 pA
D
myo-3::LGC-55 anion
myo-3::LGC-55 cation (LM2)
E
0 mM TA
30 mM TA
Body length (mm)
anion Ex
null
cation (L) Ex
cation (LM2) Ex
***

Figure III-1. LGC-55 cation channel mutants gate sodium and are functional *in vivo*.

(A) Cys-loop ligand gated ion channels are pentameric channels, each subunit containing four transmembrane domains. Depicted is a schematic representation of an LGIC with transmembrane domains 1 and 2 (M1, M2) in dark gray. In light blue is the intracellular loop that links M1 and M2, which is responsible for the ion selectivity of the channel, in this case chloride (red circles).

(B) Alignment of M1 loop region of LGC-55 with structurally related cys-loop ligand gated ion channels. Identities are shaded in dark gray, while similarities are light gray. The blue boxes indicate residues that play a role in selectivity of anions, while red boxes indicate those for cation selectivity. LGC-55 cation L and LM2, contain the M1 loop of the cationic 5HT3a receptor. LGC-55 cation LM2 also contains an additional mutation at the 20' residue, which is predicted to enhance cation selectivity (see text for details).

(C) Ion selectivity of LGC-55 anion (left) and LGC-55 cation LM2 (right) in cultured *C. elegans* muscle cells. TA evoked (0.5 mM, 250 ms) currents were recorded at the holding potentials shown. Black circles: ES1 (standard solution: 150 mM Na+, 165 mM Cl-), LGC-55 anion: Erev= -26.8 ± 3.1mV (n=4), LGC-55 cation LM2: Erev= 2.4 ± 1.2 mV (n=5); red squares: ES2 (low Na+: 15 mM Na+, 165 mM Cl-), LGC-55 anion: = -24.3 ± 1.6 mV (n=4), LGC-55 cation LM2: -21.9 ± 2.6 mV (n=5); blue triangles: ES3 (low Cl-: 150 mM Na+, 30 mM Cl-), LGC-55 anion: -1.9 ± 2.3 mV (n=4) LGC-55 cation LM2: 1.7 ± 0.9mV (n=5). Insets, representative macrocurrents of LGC-55 anion (top) and LGC-55 cation LM2 (below) elicited after perfusion of 0.5 mM tyramine at membrane holding potentials ranging from -60 to +60 mV in 20 mV steps.

(D) Still images of transgenic animals expressing LGC-55 anion (top) or cation LM2 (bottom) ectopically in all muscle cells, on exogenous tyramine. LGC-55 anion animals have relaxed body wall muscles, while LGC-55 cation LM2 animals are hypercontracted. Scale bar = 0.25 mm.

(E) Quantification of body length on exogenous tyramine. Animals expressing LGC-55 anion in all muscle cells are elongated in the presence of tyramine, due to a relaxation of the body wall muscles. Animals expressing the LGC-55 cation channel variants in all muscle cells are shortened, due to a hypercontraction of the body wall muscle. Error bars represent the standard error of the mean (SEM). Statistical significance as indicated *** $p<0.0001$.

Figure III-2

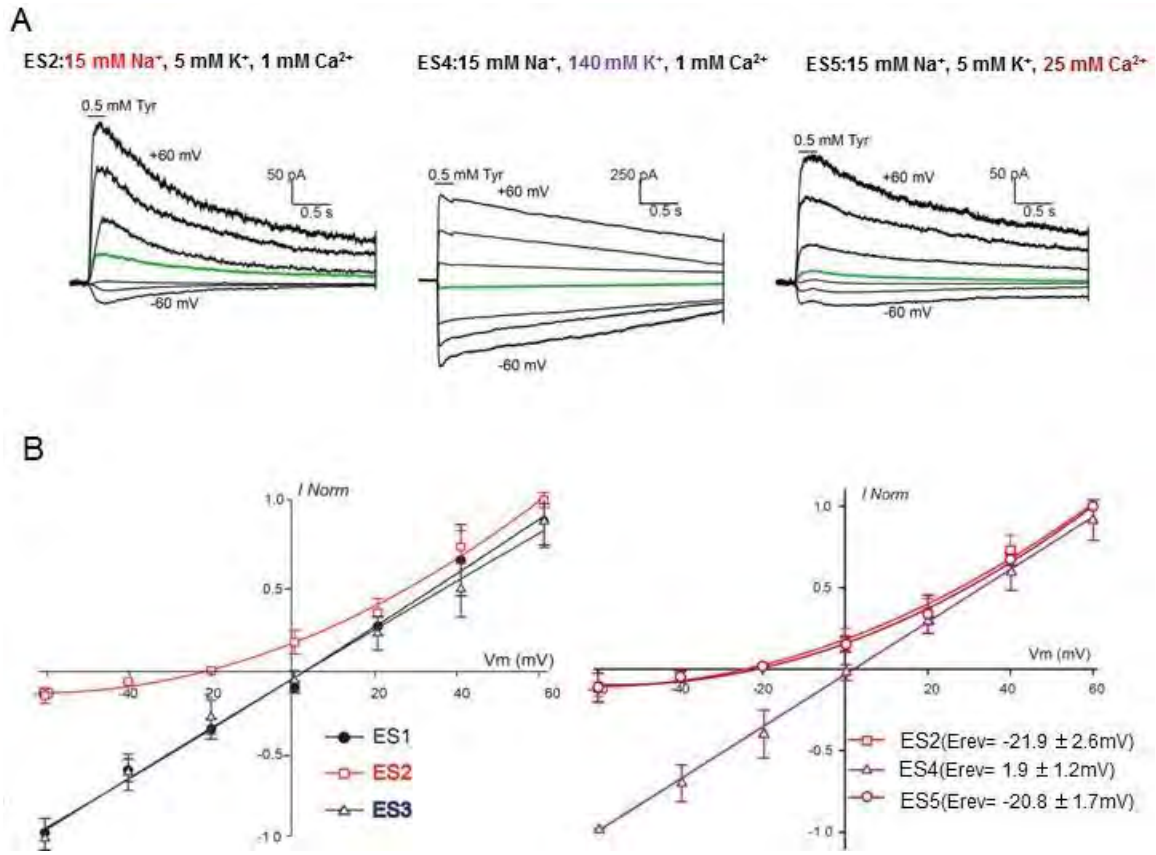

LGC-55 cation channels gate Na^+ and K^+, but not Ca^{2+}.

(A) Representative macrocurrents of LGC-55 cation LM2 elicited after perfusion of 0.5 mM tyramine at membrane holding potentials ranging from -60 to +60 mV in 20 mV steps in the indicated extracellular solutions.

(B) Ion selectivity of LGC-55 cation LM2 in cultured *C. elegans* muscle cells. TA evoked (0.5 mM, 250 ms) currents were recorded at the holding potentials shown. Black circles: ES1 (standard solution: 150 mM Na+, 165 mM Cl-), Erev= 2.4 ± 1.2 mV (n=5); red squares: ES2 (low Na+: 15 mM Na+, 165 mM Cl-), Erev= -21.9 ± 2.6 mV (n=5); blue triangles: ES3 (low Cl-: 150 mM Na+, 30 mM Cl-), Erev= 1.7 ± 0.9mV (n=5); purple triangles: ES4 (high K+: 140 mM K+, 1 mM Ca+, 15 mM Na+), Erev=1.9 ± 1.2mV (n=5); maroon circles: ES5 (high Ca++: 5 mM K+, 25 mM Ca+, 15 mM Na+), Erev= -20.8 ± 1.2mV (n=5).

Figure III-3

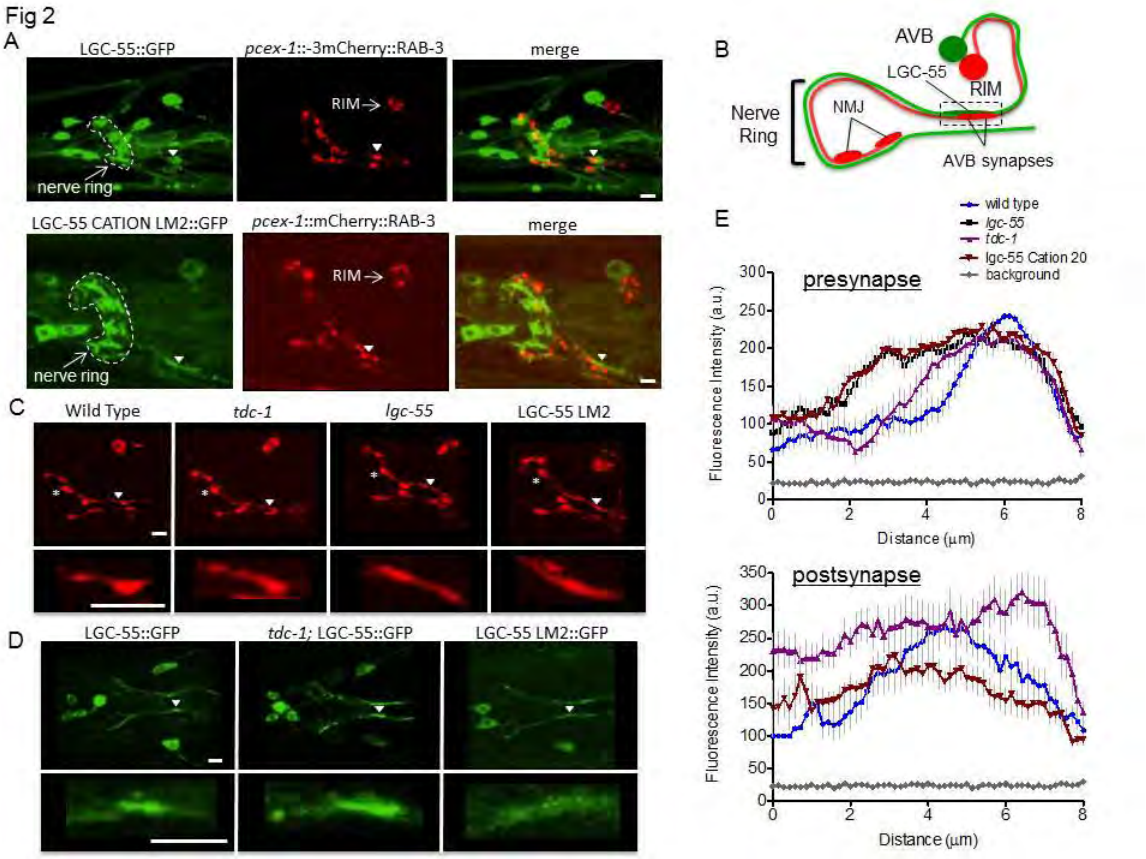

Neural activity is important for the refinement of synaptic connections within the *C. elegans* escape response neural circuit.

(A) Representative images of animals coexpressing the synaptic vesicle marker mCherry::RAB-3 in the RIM neurons (left) and a translational LGC-55::GFP or LGC-55 LM2::GFP reporter (center). Merge (right) identifies synaptic contacts between the RIM and LGC-55 expressing neurons. Anterior is the left, nerve ring indicated by dashed line, arrows indicate RIM-AVB synapse. Scale bars, 3 μm.

(B) Schematic diagram of the morphology of the RIM in the nerve ring (left) and the location of the major synaptic varicosities with outputs onto the AVB command interneuron as described in White, et al. (1986). The area measured for quantification of synaptic density is indicated by the dashed box.

(C) Head region of adult transgenic animals of indicated genotypes expressing the mCherry::RAB-3 presynaptic vesicle marker in the RIM. Region of presynaptic connectivity with the AVB measured in (E) is indicated with by the

white arrow and magnified below. Star indicates neuromuscular junction between the RIM and neck muscle in the nerve ring. Scale bars, 5 μm.

(D) Head region of an adult transgenic animals showing expression of the LGC-55::GFP or LGC-55 CATION (LM2)::GFP translational reporter in the AVB. The regions of postsynaptic density corresponding with synapses between the RIM and AVB that were measured in (E) are indicated by the white arrow and magnified below (See also Figure III-4). Anterior is to the left and the position of the nerve ring is indicated by a star. Scale bars, 5 μm.

(E). Top: Fluorescence intensity over the area containing the AVB synapses. Shown is the average fluorescence intensity in the presyanpse measured in regular intervals over 8 μm in transgenic animals expressing mCherry::RAB-3 in the RIM of wild type (n=19), *lgc-55* (n=17), *tdc-1*(n=14) and LGC-55 LM2 (n=11), animals. Measurements were taken from the anterior region of the AVB synaptic density to area just posterior. Fluorescence is more diffuse in *tdc-1* and *lgc-55* mutants, suggesting a change in synaptic vesicle localization. Botttom: Average fluorescence intensity in the postsynapse was measured in regular intervals over 8 μm in animals coexpressing mCherry::RAB-3 in the RIM and LGC-55::GFP (n=19) or LGC-55 LM2::GFP (n=12) in *lgc-55* or *tdc-1* (n=14) mutants. Measurements of the LGC-55::GFP density were taken from the region of colocalization with the AVB synapse (see Supplemental Fig.2). In *tdc-1* mutants LGC-55 expression is increased and the postsynaptic density is more diffuse. In LGC-55 LM2 animals, expression is lower and also slightly more diffuse. This suggests that activity may regulate postsynaptic receptor expression.

Figure III-4

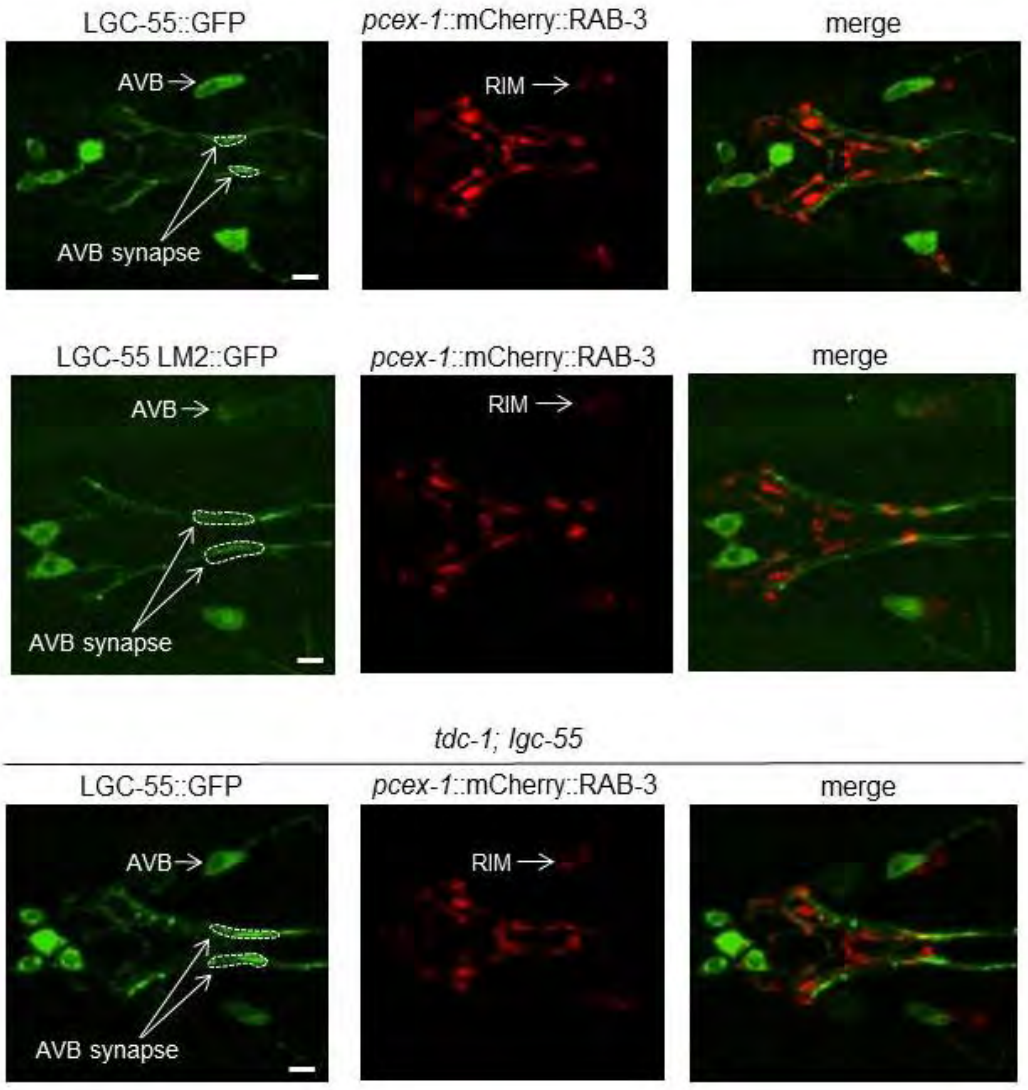

LGC-55 cation channels localize to postsynaptic specializations in the nerve ring.

Representative images of animals coexpressing a translational LGC-55::GFP or LGC-55 LM2::GFP reporter (left) under control of a minimal promoter that drives expression in a subset of neurons including the AVB (indicated) and the synaptic vesicle marker mCherry::RAB-3 in the RIM neurons (center). Head is to the left, AVB synapses indicated by dashed line. Scale bar, 5 μm. See Fig. III-3.

Figure III-5

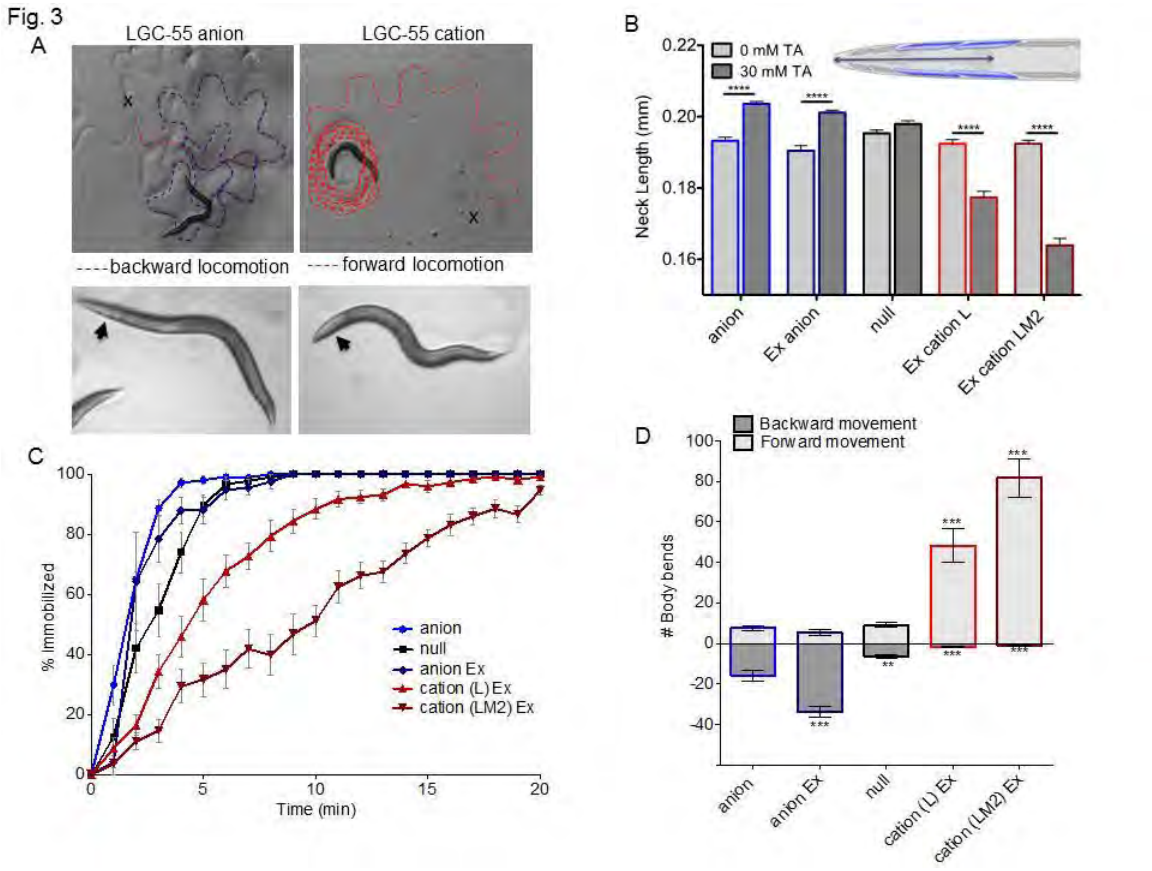

Exogenous tyramine induces long forward runs and neck contractions in LGC-55 cation animals.

(A) Top: Still images of the locomotion pattern of LGC-55 anion and LGC-55 cation (LM2) animals prior to immobilization on 30 mM tyramine. The x marks the starting location and the dashed red line indicates the forward locomotion, while the dashed blue line indicates backward locomotion. LGC-55 anion animals make long backward runs, while LGC-55 cation animals make long forward runs. Bottom: Still images of LGC-55 anion and LGC-55 cation animals after five minutes on exogenous tyramine, arrow denotes neck region. LGC-55 anion animals exhibit a relaxation of the head muscles causing an elongation of the neck, while the presence of the LGC-55 cation mutation causes contraction of the head muscles and a shortening of the neck.

(B) LGC-55 cation animals hypercontract their neck on exogenous tyramine. Shown is the quantification of neck lengths on exogenous tyramine. The length of the neck was measured from the posterior of the pharynx to the tip of the nose

after 5 minutes on 30 mM tyramine (dark grey bars) or 0 mM tyramine (light grey bars). Error bars represent the standard error of the mean (SEM). Statistical difference as indicated; *** $p<0.0001$, two tailed Student's t test.

(C) LGC-55 cation animals immobilize more slowly on exogenous tyramine. Shown is the percentage of animals immobilized by tyramine each minute for 20 minutes. Each data point is the mean +/- SEM for at least four trials totalling 40 or more animals.

(D) LGC-55 cation animals make long forward runs on exogenous tyramine. Shown is the number of backward (dark grey bars) and forward (light grey bars) body bends made before paralysis on 30 mM tyramine. Error bars represent SEM. Statistical difference from anion, ** $p<0.001$, ***$p<0.0001$, two tailed Student's t test.

Figure III-6

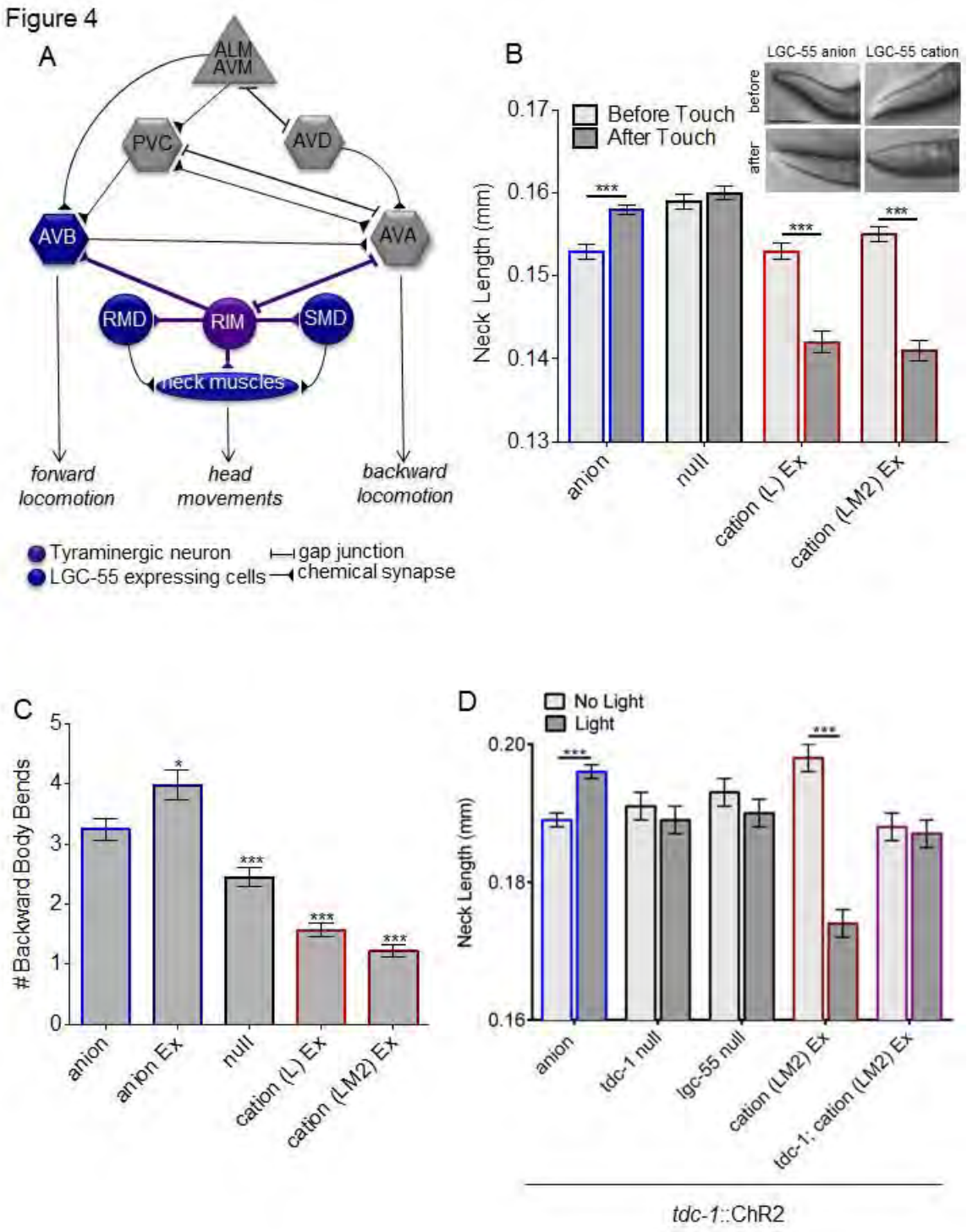
Figure 4
A
ALM
AVM
PVC
AVD
AVB
AVA
RMD
RIM
SMD
neck muscles
forward locomotion
head movements
backward locomotion
Tyraminergic neuron
LGC-55 expressing cells
gap junction
chemical synapse
B
LGC-55 anion
LGC-55 cation
before
after
Before Touch
After Touch
Neck Length (mm)
0.17
0.16
0.15
0.14
0.13
***
anion
null
cation (L) Ex
cation (LM2) Ex
C
Backward Body Bends
5
4
3
2
1
0
*
anion
anion Ex
null
cation (L) Ex
cation (LM2) Ex
D
No Light
Light
Neck Length (mm)
0.20
0.18
0.16
anion
tdc-1 null
lgc-55 null
cation (LM2) Ex
tdc-1; cation (LM2) Ex
tdc-1::ChR2

Figure III-6. LGC-55 cation acts synaptically to induce neck contraction and activation of forward locomotion.

A) Schematic representation of the neural circuit for tyraminergic coordination of head movements and locomotion in response to touch. Gentle touch activates release of tyramine from the RIM (purple) onto cells expressing LGC-55 (blue). Tyraminergic activation of LGC-55 hyperpolarizes neck muscles and the forward locomotion command neuron, AVB, to suppress head movements and promote backward locomotion. Synaptic connections indicated as triangles and gap junctions as bars, are as described by White, et al. (1986). Sensory neurons are triangles, command neurons required for locomotion as hexagons, motor neurons as circles and muscles as an oval.

B) Touch induces neck contraction in LGC-55 cation animals. Shown is the length of the neck from posterior of the pharynx to the tip of the nose before (light gray bars) and after (dark gray bars) anterior touch. Error bars represent SEM. Statistical difference as indicated, ** $p<0.001$, ***$p<0.0001$, two tailed Student's t test. Inset: still images of the animal's head before (top) and after (bottom) mechanical stimulus. Scale bar, 0.1mm.

C) LGC-55 cation animals fail execute a long reversal in response to touch. Shown is the average number of backward body bends in response to anterior touch. Error bars represent SEM. Statistical difference from anion, * $p<0.01$, ***$p<0.0001$, two tailed Student's t test.

D) Tyramine release from the RIM activates the LGC-55 cation channel. Shown is the length of the neck (as measured in b) before (light gray bars) and after (dark grey bars) exposure to blue light in retinal fed animals expressing the light activated cation channel, ChR2 in the RIM. Blue light causes activation of the RIM and release of tyramine. Tyraminergic activation of LGC-55 anion causes a relaxation of the neck muscles, while activation of LGC-55 cation LM2 causes a hypercontraction of the neck muscles. There is no response in animals that are not fed retinal (see Figure III-10). Error bars represent SEM. Statistical difference as indicated, ** $p<0.001$, ***$p<0.0001$, two tailed Student's t test.

Figure III-7

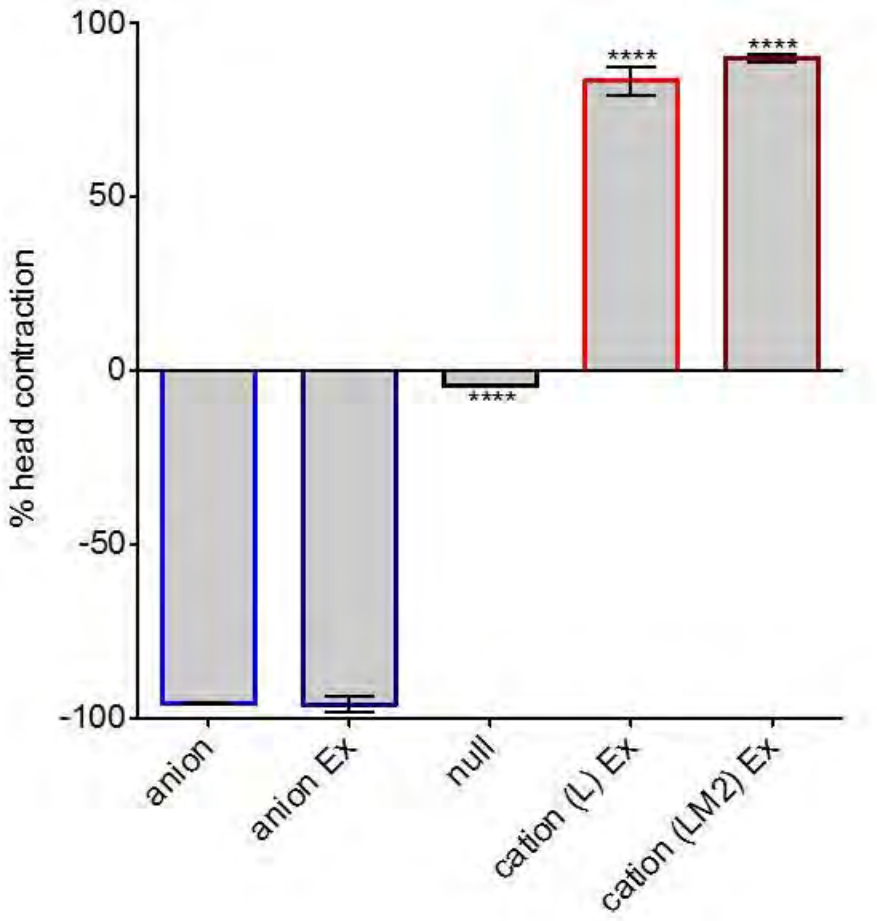

LGC-55 cation channels contract their heads in response to touch.

Shown is the percentage of animals which contract their necks in response to touch. Positive response indicates contraction while negative response indicates relaxation. *lgc-55* mutants neither contract or relax their necks, while transgenic animals expressing either LGC-55 anion or LGC-55 cation channels contract their necks in response to touch. See text for details. ****$p \leq 0.0001$.

Figure III-8

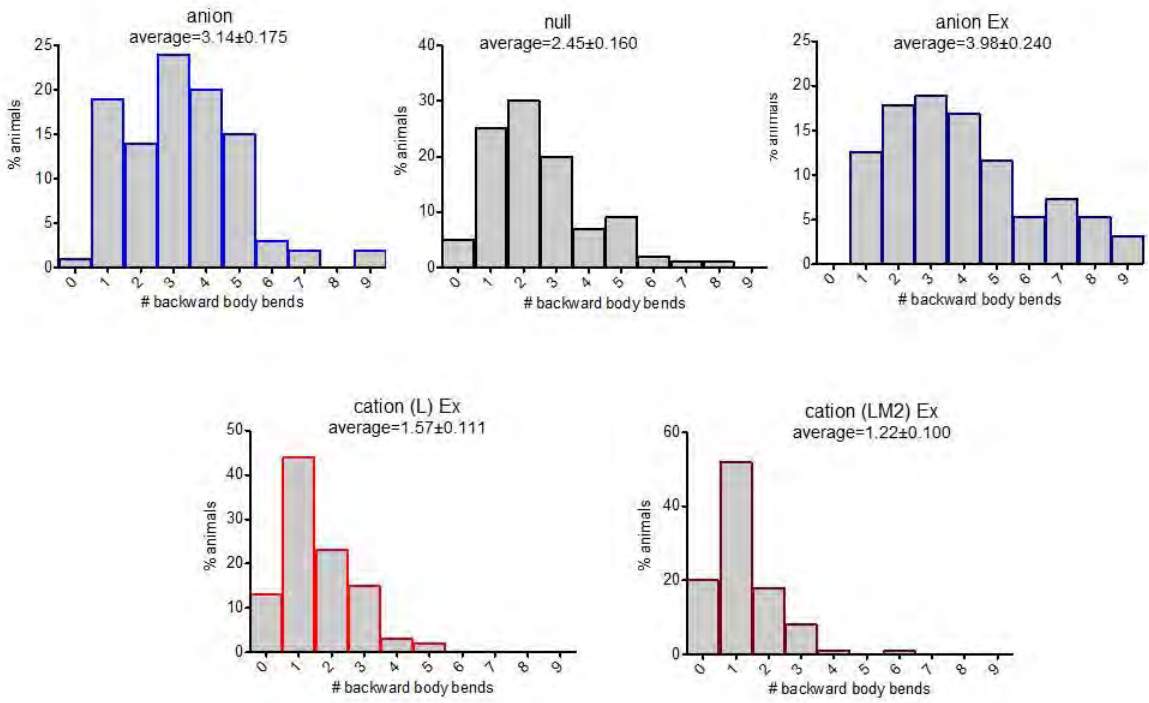

LGC-55 cation animals make short reversals in response to touch.

Shown is the distribution of number of backward body bends in response to touch, average and SEM are indicated (wild type, n=100; *lgc-55 rescue*, n=100; *lgc-55(tm2913)*, n=95; *lgc-55(tm2913);* LGC-55 cation (L), n=100; *lgc-55(tm2913);* LGC-55 cation (LM2), n=100).

Figure III-9

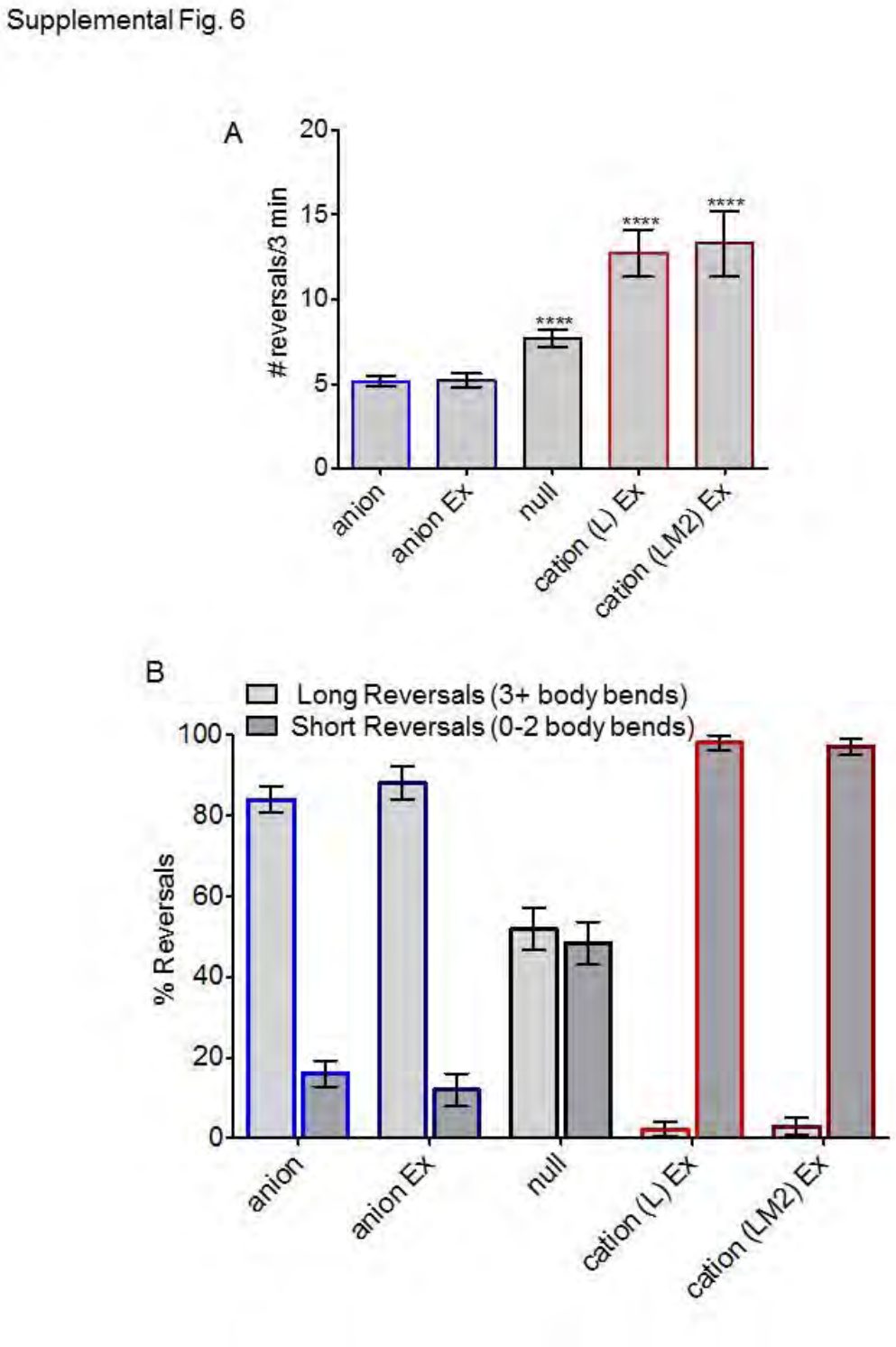
Supplemental Fig. 6
A
reversals/3 min
20
15
10
5
0
****
****
****
anion
anion Ex
null
cation (L) Ex
cation (LM2) Ex
B
Long Reversals (3+ body bends)
Short Reversals (0-2 body bends)
% Reversals
100
80
60
40
20
0
anion
anion Ex
null
cation (L) Ex
cation (LM2) Ex

Figure III-9. LGC-55 cation animals have defects in spontaneous reversal behavior.

(A) Number of reversals made in 3 minutes of wild type, 5.2 ± 0.3 body bends, n=30; LGC-55 rescue, 5.2 ± 0.4 body bends, n=18; *lgc-55(tm2913)*, 7.86± 0.5 body bends, n=25; LGC-55 L, 12.7 ± 1.4 body bends, n=27; LGC-55 LM2, 13.3 ± 1.9 body bends, n=10. LGC-55 cation animals exhibit hyper reversal behavior.

(B) Distribution of short (1-2 body bends) and long (3+ body bends) spontaneous reversals made in 3 min of wild-type (n=30), LGC-55 rescue (n=18), *lgc-55(tm2913)* (n=25), LGC-55 L (n=27), LGC-55 LM2 (n=10). LGC-55 is expressed in the forward locomotion command neuron, AVB. In wild-type animals, spontaneous release of tyramine activates LGC-55 anion causing a hyperpolarization of the AVB leading to a long reversal. In LGC-55 cation animals, spontaneous release of tyramine causes an activation of the AVB, leading to a shortened reversal length, and an increase in the number of shortened reversals made in 3 minutes.

Figure III-10

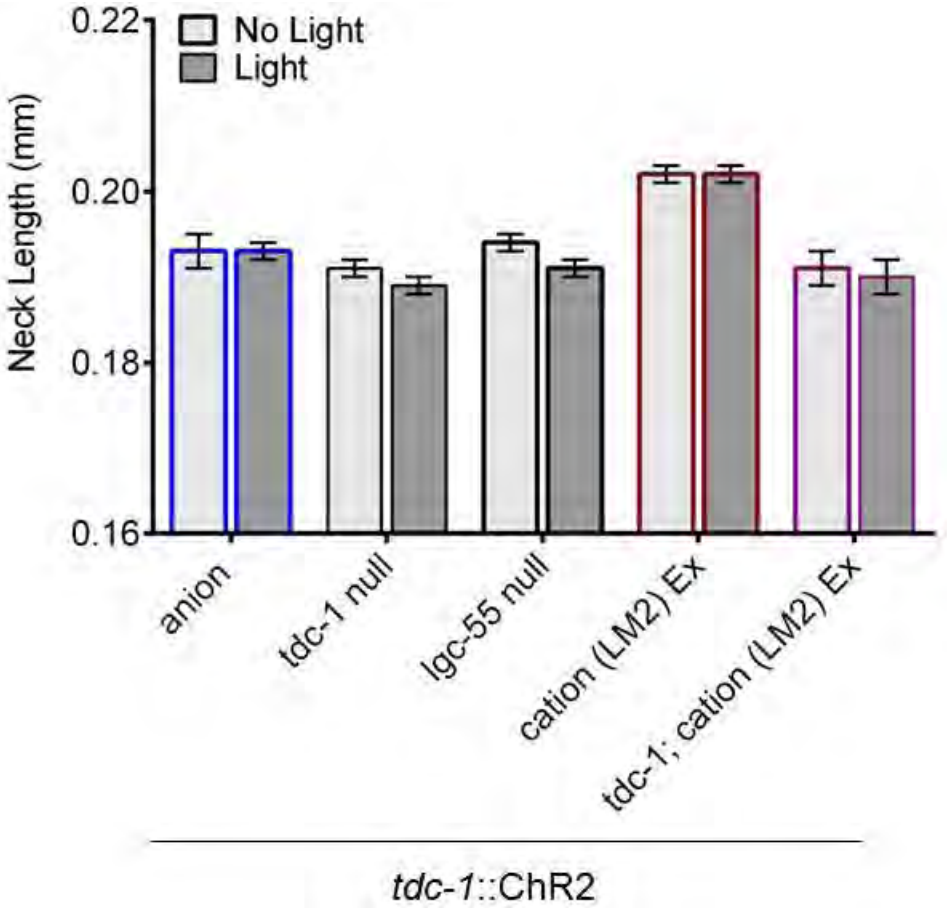

Tyramine release is dependent upon activation of the RIM.

Shown is the average neck length before (wild type, 0.193 ± 0.002µm (n=17); *tdc-1,* 0.191 ± 0.001µm (n=21); *lgc-55,* 0.194 ± 0.001µm (n=17); LGC-55 LM2, 0.202 ± 0.001µm (n=25); *tdc-1;* LGC-55 LM2, 0.191 ± 0.002µm (n=10)) and after (wild type, 0.193 ± 0.001µm (n=17); *tdc-1,* 0.189 ± 0.001µm (n=21); *lgc-55,* 0.191 ± 0.001µm (n=17); LGC-55 LM2, 0.202 ± 0.001µm (n=25); *tdc-1;* LGC-55 LM2, 0.191 ± 0.002µm (n=10)) blue light exposure of animals that were not fed retinal. There is no significant head contraction or relaxation response to blue light, indicating that tyramine is released only when the RIM is activated and any behavioural response to illumination with blue light does not cause significant tyramine release.

Movie III-1

Movie of a wild-type animal on a plate containing 30 mM tyramine.

Filming began immediately after the animal was placed on the plate and ended shortly after paralysis. Movie was shot at 15 frames per second (fps) and sped up five times. Wild-type animals exhibit an elongated, straightened neck and execute a long backward run before immobilization.

Movie III-2

Movie of LGC-55 LM2 on a plate containing 30 mM tyramine.

Filming began immediately after the animal was placed on the plate and ended shortly after paralysis. Movie was shot at 15 frames per second (fps) and sped up five times. Animals expressing the chimeric cation channel under control of the native promoter exhibit a hyper-contracted neck and execute long forward runs before paralysis, behaviors opposite to that of wild type.

Movie III-3

Movie of gentle anterior touch response of wild-type animals.

Wild-type animals suppress head oscillations in response to anterior touch and execute a long reversal.

Movie III-4

Movie of gentle anterior touch response of LGC-55 LM2 animals.

Animals expressing the LGC-55 LM2 cation channel under control of the endogenous promoter hypercontract their neck and fail to execute a long reversal in response to anterior touch.

Movie III-5

Movie of wild-type animals expressing *ptdc-1*::ChR2 in response to blue light.

Wild-type animals suppress head oscillations and lengthen there neck in response to stimulation of tyramine release by activation of ChR2 in the RIM.

Movie III-6

Movie of LGC-55 LM2 animals expressing *ptdc-1*::ChR2 in response to blue light.

LGC-55 LM2 cation animals suppress hypercontract their neck in response to stimulation of tyramine release by activation of ChR2 in the RIM.

CHAPTER IV

Characterization of a Novel Gain of Function Voltage-Gated Calcium Channel

The experimental work written in this chapter represents a currently unpublished project done in conjunction with Yung-Chi Huang. At the time of this thesis preparation, the work represented here is my contributing half to what we expect to be a co-authored paper. In this chapter, Yung-Chi Huang preformed the thrashing assays in Figure IV-5, worked closely with me on the suppressor screen and identification of mutants, and made the *H.s.* CACNA1A gf construct for HEK 293 cell expression. Credit is also given to Dr. Diego Rayes performing the whole-cell electrophysiology. Additionally, credit is given to Dr. Yasunori Saheki and Dr. Corneila Bargmann for the generation of the UNC-2 and UNC-2 GF rescuing constructs. Two undergraduate students, Samuel Raj and Dhruv Sarin, assisted with the suppressor screen discussed in this chapter and I thank them for their efforts.

Abstract

The release of neurotransmitter is critical to propagating signals that generate behavioral outputs. In a genetic screen for mutants that are resistant to the paralytic effects of exogenous tyramine, we isolated a mutant, *zf35*, which displays a hyperactive locomotory and egg laying phenotype. We identified *zf35* as an allele of *unc-2,* the pore forming α_1 subunit of a voltage-gated calcium channel essential for synaptic vesicle exocytosis. *zf35* phenotypes are directly opposite to those of *unc-2* loss-of-function mutants, which are sluggish and have a decrease in endogenous synaptic activity. This indicates that the *zf35* lesion represents a gain-of-function-mutation. Electrophysiological studies show the *zf35* mutation causes an increase in channel conductance and shifts in the activation potential of the channel, which may lead to an increase in neurotransmitter release. This mutation provided us with a unique opportunity to identify new genes that interact with *unc-2* at the synapse. We performed a pilot suppressor screen for mutations that suppress the hyperactive phenotypes of *unc-2(zf35)*. We isolated 23 mutants, many of which are new alleles of genes known to be essential for expression and processing of calcium channels.

Introduction

Voltage-gated calcium channels (VGCCs) play a critical role in nervous system function. In addition to participating in the regulation of gene expression, neuronal migration and stimulus-contraction coupling, voltage-gated calcium channels act as the bridge between neural activity and neurotransmitter release. They accomplish this by responding to changes in membrane potential by opening and allowing the necessary influx of Ca^{2+} to trigger vesicular fusion events. Additionally, calcium influx through VGCCs can activate signaling cascades that lead to transcription, muscle contraction and growth (reviewed in Catterall, 2000).

VGCCs are multi-subunit complexes composed of four to five components, α_1, $\alpha_2\delta$, β, and γ subunits. The α_1 subunit forms the voltage sensor and the central pore, while the other subunits have been shown to modulate channel activity and expression (Caterall, 2000; Singer, et al, 1991). In mammals, there are five types of calcium channels encoded by 10 α_1 subunit genes, L- (Ca_V1), N-, P/Q-, R- (Ca_V2), and T- (Ca_V3) type, and are organized according to their distinct pharmacological properties. The Ca_V2 or N-, P/Q- and R-types are the predominant VGCCs in presynaptic nerve terminals where channel opening and Ca^{2+} influx triggers the fusion of synaptic vesicles with the cell membrane (Catterall, 2000).

Although there has been much research done on the pharmacological and electrophysiological properties of these channels, how their activity, expression,

and localization are precisely regulated is largely unknown. Furthermore, deregulation of Ca_v2 channel function can cause severe neurological disorders including ataxia, epilepsy, migraine and autism-spectrum disorders (reviewed in Gargus, 2009; Splawski, et al., 2004; Hans, et al., 1999; Serra, et al., 2008; Barrett, et al., 2005). Determining how Ca_v2 channel activity and expression are regulated will not only provide insights into normal calcium signaling mechanisms within neural networks, but it will also contribute to our understanding of the pathology of these channelopathies.

In contrast to the mammalian nervous system, the nematode *Caenorhabditis elegans* has only three α_1 subunit genes, *egl-19*, *cca-1* and *unc-2* which are homologous to the mammalian L- (Ca_V1), T- (Ca_V3) and N/P/Q (Ca_V2) type, respectively (Lee, et al., 1997; Steger, et al., 2005; Shtonda and Avery, 2005; Schafer and Kenyon, 1995). Additionally, *C. elegans* encodes $\alpha_2\delta$ (*unc-36*) and β (*ccb-1*) subunit homologues (Schafer and Kenyon, 1995; Schafer, et al., 1996; Laine et al, 2011). It has been shown that *unc-2* regulates acetylcholine, GABA and biogenic amine signaling, that control behaviors including, locomotion, defecation and egg-laying (Schafer and Kenyon, 1995; Mathews, et al., 2003). These studies show that *unc-2* acts to orchestrate the calcium flux necessary for neurotransmission, suggesting a functional correlation to the mammalian Ca_V2-type channels. The similarity in function and composition to the mammalian VGCCs combined with the advantages of a

limited genome and simple nervous system, makes *C. elegans* is an excellent model in which to study Ca_V2 regulation and function *in vivo*.

We have identified a novel gain-of-function allele of the *unc-2* gene, *zf35.* Here we describe a comprehensive characterization of *unc-2(zf35)* and show that the *zf35* lesion produces changes to channel properties by increasing channel conductance and shifting the voltage of activation to more negative potentials. Furthermore, we developed a suppressor screen to uncover new molecules involved in processing, expression and subunit composition of Ca_V2 channels. Our suppressor screen identified new alleles of *calf-1, unc-10, unc-13, unc-36* and *unc-31,* which have all been previously implicated in calcium channel localization and function (Saheki and Bargmann, 2009; Kaeser, et al., 2011; Schafer, 1996; Frøkjær-Jensen et al., 2006). Continued characterization of mutants isolated from our screen may identify new genes involved in the proper assembly and trafficking of functional calcium channels.

Experimental Procedures

Genetic Screen, Mapping and Cloning of UNC-2 GF

All strains were cultured at 22˚C on NGM agar plates with the *E. coli* strain OP50 as a food source. The wild-type strain was Bristol N2. All strains were obtained from the *C. elegans* Genetics Center (CGC) unless otherwise noted. The genetic screen which isolated *zf35* was carried out as in Chapter II, briefly; wild-type animals were mutagenized with 50 mM EMS (Brenner, 1974). Young adult F2 progeny of approximately 14,000 mutagenized F1 animals were washed

twice with water and transferred to 40 mM tyramine plates. After 10 to 20 minutes animals that displayed sustained head or body movements were picked to single plates. Primary isolates were retested on 30 mM tyramine. Twelve mutants were isolated; *zf35* was partially resistant to the paralytic effects of tyramine for both head and body movements.

We mapped *unc-2(zf35)* to LG X using the SNP mapping procedure as previously described (Wicks, et al., 2001; Davis, et al., 2005). Further three-factor mapping placed *unc-2(zf35)* to the left of *lon-2* close to *dpy-3.* Full length UNC-2 WT and GF rescuing clones were obtained from Y. Saheki and C. Bargmann. Briefly, the UNC-2 cDNA containing a synthetic intron at nt position 1142-1192 relative to the translational start and was cloned behind the *tag-168* pan neuronal promoter using restriction sites AscI and XhoI to generate the *ptag-168*::UNC-2WT construct. *ptag-168* drives expression in all neurons. The UNC-2 GF construct was generated using site directed mutagenesis to engineer the *zf35* mutation in *ptag-168*::UNC-2.

All transgenic strains were obtained by microinjection of plasmid DNA into the germline. At least three independent transgenic lines were obtained and data are from a single representative line. Transgenic animals for rescue experiments were made by co-injecting *ptag*-168::UNC-2WT or *ptag-168::*UNC-2GF plasmids at 20 ng/µl along with the *lin-15* rescuing plasmid pL15EK at 80 ng/µl into the loss of function animals, *unc-2(e51); lin-15(n765ts)* or *lin15(n765ts)*.

Behavioral Assays

All behavioral analysis was performed with young adult animals (24 hours post L4) at room temperature (22-24°C), unless otherwise noted; different genotypes were scored in parallel, with the researcher blinded to the genotype. To quantify resistance to aldicarb or levamisole, young adult animals were transferred to NGM supplemented with 1 mM aldicarb or 100 µM levamisole and the percentage of paralyzed animals was scored every 15 minutes for a 120-minute period. Paralysis was defined as the failure of an animal to respond to a harsh stimulus to the middle of the body. 100% of wild-type animals were paralyzed on 1 mM aldicarb or 100 µM levamisole at 120 minutes. Aldicarb plates were prepared by adding aldicarb (Chemservice) dissolved in 100% isopropanol to a concentration of 1mM to standard NGM. Similarly, levamisole plates were prepared by adding levamisole (Sigma) dissolved in water to a concentration of 100 µM to standard NGM. Plates were freshly seeded with OP50 the night before the assay to prevent animals from crawling off the plates during the assay.

Spontaneous reversal frequency was scored on seeded NGM agar. Animals were transferred from their culture plate to a freshly seeded plate and allowed to recover for 1 minute. After the recovery period the animals were scored for 3 minutes. The reversal frequency was determined as described in Tsalik and Hobert (2003). Animals that crawled to the edge of the plate during

the assay were discarded. Thrashing rate was quantified by counting the number of body-bends animals made in liquid in 30 seconds. Animals were transferred singly to wells of a 96-well plate filled with 50 µL of M9 buffer and the thrashes were counted for 30 seconds after a 30 second equilibration period.

Egg laying assays were performed as in Koelle and Horvitz, 1996. Briefly, quantification of brood size was performed by placing a single L4 to a NGM plate seeded with OP50 and the total number of offspring was counted after 5 days at room temperature. This was repeated with at least 5 animals for each genotype. The number of eggs in the uterus was counted 36 hours after L4 by dissolving worms but not fertilized eggs in a 20% sodium hypochlorite solution. The stage of eggs laid was quantified by allowing adult animals, 36 hours after L4, to lay eggs on food for one hour. The eggs were then examined and classified in developmental stages according to the number of cells present.

Electrophysiology of UNC-2

A stable HEK293 cell line expressing the calcium channel auxiliary subunits β_{1c} and $\alpha_2\delta$ (generous gift from Dr. Tsien, Department of Molecular and Cellular Physiology, Stanford University School of Medicine)(Piedras-Renteria et al., 2001) was used to transiently transfect 5 µg of wild-type or mutant human $\alpha_{1A}/Ca_v1.2$ subunit using the calcium phosphate method. A plasmid encoding green fluorescent protein (pGreen lantern) was also included for recordings to allow identification of transfected cells under fluorescence optics. The cells were

kept in DMEM supplemented with 10% fetal bovine serum and 1000 U/ml penicillin–streptomycin.

Whole-cell inward currents were recorded 24–36 hr after transfection with a HEKA EPC-9 patch clamp amplifier. Recordings were filtered at 2 kHz and acquired using Patchmaster software, version 10.1 (HEKA). The extracellular recording solution contained 5mM $BaCl_2$, 1mM $MgCl_2$, 10mM HEPES, 40mM TEACl, 10 mM glucose, and 87.5 mM CsCl, pH 7.4. Typically the pipettes exhibited resistances ranging from 2 to 4 MΩ and were filled with internal solution containing (in mM): 105 CsCl, 25 TEACl, 1 $CaCl_2$, 11 EGTA, and 10 HEPES, pH 7.2.

Cell capacitance (16.7 ± 6.7 pF; n = 24) and series resistance (9.7 ± 4.6 MΩ before compensation; n = 24) were measured from the current transient after a voltage pulse from -80 to -90 mV. Series resistance was typically compensated by 80–90%. Cells with large currents in which errors in voltage control might appear were discarded. I-V curves were generated by measuring the peak currents obtained after stepping the membrane potential from a holding potential of -120 mV to voltages between -55 and 40 mV in 5mV increments for 200 msec. *I-V* curves were fitted with Equation 1:

$$I = G(G - Erev) (1+\exp (V_{0.5} - V)/ka)^{-1}$$

where G is membrane conductance, E_{rev} is the reversal potential, $V_{0.5}$ is the midpoint, and k_a the slope of the voltage dependence. Current densities were obtained by dividing the current peak amplitude to the cell capacitance for each experiment.

To measure steady-state inactivation profiles, conditioning prepulses (10 sec) from -90 to 20mV in 10mVsteps were applied, and the membrane was then stepped to the peak of the I–V curve. Currents were normalized to the maximal value obtained at the test pulse and plotted as a function of the prepulse potential. Data were fitted with Boltzmann equations:

$$I/Imax = \{1 + \exp[(V-V_{0.5})/k_{in}]^{-1}\}.$$

All experiments were performed at room temperature. Data analysis was performed using the IgorPro software (WaveMetrics Inc., Lake Oswego, OR); figures, fitting and statistical analysis was done using the SigmaPlot software (version 11.0; Systat Software Inc.). Data are presented as mean ± SD. Significant differences were determined using Student's t test with the significance value set at *p>0.01.*

UNC-2GF suppressor screens

Two suppressor screens were performed. First, UNC-2GF animals were mutagenized in 50 mM EMS as described (Brenner, 1974). Young adult F2 progeny of approximately 8,000 mutagenized F1 animals were washed twice with

water and transferred to 1 mM aldicarb plates. Animals resistant to paralysis by aldicarb in 60 minutes were recovered. Primary isolates were retested on 1 mM aldicarb, and those that were resistant to aldicarb were kept for further analysis and outcrossing. 4 mutants were isolated (see Table IV-1). *zf87, zf88, zf89* and *zf90* were highly resistant to 1 mM aldicarb. We identified *zf88, zf89,* and *zf90* using SNP mapping procedure as previously described (Wicks, et al., 2001; Davis, et al., 2005), complementation tests, and sequence analysis.

We performed a second suppressor screen, similarly to Miller, et al., 1996. Briefly, UNC-2GF animals were mutagenized in 50 mM EMS as described (Brenner, 1974). Approximately 10,000 mutagenized F1 animals were washed twice with water and bleached to release their fertilized eggs. F2 mutant eggs were plated on seeded NGM plates containing 0.25 mM aldicarb, and examined after 7, 14, and 21 days. Aldicarb at this concentration causes larval arrest in UNC-2GF animals, resistant animals that reached adulthood by the specified time points were recovered. Primary isolates were retested for their resistance to paralysis on 1 mM aldicarb. 16 mutants were isolated and alleles were identified by complementation testing and sequence analysis (Table IV-1).

Results

zf35 is an allele of *C. elegans* the voltage-gated calcium channel, UNC-2.

To identify genes involved in tyramine signaling, in Chapter II we performed a genetic screen for mutants that are resistant to the paralytic effects of exogenous tyramine. We placed approximately 10,000 F2 progeny of

mutagenized wild-type hermaphrodites on plates containing 30 mM tyramine and selected mutants that displayed sustained body movement. One mutant isolated, *zf35*, was partially resistant to the paralytic effects of exogenous tyramine (Figure IV-1). Additionally, *zf35* mutants are smaller than wild type (data not shown), and display a severe hyper-reversal phenotype (Figure IV-5A,B, Movie IV-1,2). Despite the difference in size and defects in locomotion, *zf35* mutants were viable with normal brood sizes.

We mapped the *zf35* mutation using single nucleotide polymorphisms and three-factor mapping to the left of chromosome X, close to *dpy-3* (Figure IV-2A). This genomic region contains a gene, *unc-2*, which encodes the α-subunit of the *C. elegans* P/Q type ($Ca_V2.1$) voltage-gated calcium channel. Sequence analysis of *zf35* revealed a single base transition in the coding sequence of *unc-2*. The predicted UNC-2 protein contains four homologous domains (TM I-IV), each containing six transmembrane segments (S1-6), and intracellular N- and C-termini (Caterall, 2000). The *zf35* allele is a mutation in the highly conserved intracellular linker between TM III-S6 and TM IV-S1 that converts a glycine residue to an arginine (G1132R) (Figure IV-2B,C). The intracellular linkers between TM domains have been implicated in association with the voltage sensing domains of the channel (S4), accessory subunits, and signaling molecules that regulate channel activity (Caterall, 2000), suggesting that the *zf35* mutation may cause a change in the electrophysiological properties of the channel.

The UNC-2 G1132R mutation causes a shift in activation voltage and an increase in Ca^{2+} influx.

In order to investigate the functional consequences of the missense mutation G1132R in UNC-2 we introduced the corresponding mutation in the human homologue of the α_1A voltage-gated calcium channel subunit, CACNA1A, and expressed the wild-type or the mutant α_1A subunit in a stable HEK 293T cell line expressing the auxiliary calcium channel subunits β_1C and $\alpha_2\delta$. Representative whole-cell Ba^{2+} currents for the wild-type and the G1132R mutant versions are shown in Figure IV-3A. The maximal current densities were significantly larger for the G1132R mutation when compared to the wild-type: 80.6 ± 5.7 (n=11) versus 47.5 ± 4.3 (n=13) ($p>0.05$; Figure IV-3B).

The G1132R mutation caused the current-voltage relationship to shift ~10 mV to more negative potentials in comparison to the wild-type. In 5 mM Ba^{2+}, currents through the wild-type channels were first activated at approximately -20 mV and peaked at approximately 10 mV. In contrast, the G1132R mutant channel was activated and peaked after depolarizations of -30 and 0 mV, respectively (Figure IV-3B). The $V_{0.5act\ value}$, or the membrane potential where half of the maximal activation is achieved, was -3.9 ± 0.2 and -12.6 ± 0.6 mV for the wild-type and mutant channel respectively, and the slope of the activation curves is only slightly affected in the mutant (K_aWT= 3.7 ± 0.2 mV; K_a G1132R=4.5 ± 0.3).

The extent of inactivation was measured as the relationship between the residual current at the end of a 200ms test pulse and the current peak, and is not

altered in the mutant as shown in Figure IV-3C. However, comparison of the steady-state inactivation properties demonstrated a slight displacement to more depolarized membrane potentials in the G1132R mutant (Figure IV-3D). The membrane potential at which half of the current was inactivated in the mutant was about 7-8 mV more positive when compared to the wild-type ($V_{0.5inact}$= -55.0 ± 1.0 and -47.3 ± 1.0 for the wild-type and mutant, respectively) (Figure IV-3D).

Take together these data indicate that the G1132R mutation in the human α_1A subunit of voltage gated neuronal $Ca_v2.1$ Ca^{2+} channels produces a significant shift of the activation to lower voltages and an important increase of the whole cell Ba^{2+} influx in HEK 293T cells. The increase in activity caused by the G1132R mutation suggests a gain of channel function which may lead to an increase the rate of neurotransmitter release. Similar changes were observed in studies examining the properties of known gain of function mutations in human $Ca_v2.1$, such as S218L and R192Q (Figure IV-2B), which have been associated with Familial Hemiplegic Migraine (FHM) (Hans et al., 1999; Tottene et al., 2005).

The UNC-2 G1132R mutation causes an increase in neurotransmission.

To test if the UNC-2 G1132R mutation causes a change in neurotransmission, we used a pharmacological assay, where we exposed animals to the antihelminthic drug, aldicarb. Aldicarb is an acetylcholinesterase inhibitor, which stops the breakdown of acetylcholine causing a buildup of acetylcholine at the synapse. Acetylcholine is the major excitatory

neurotransmitter at the neuromuscular junction (NMJ) in *C. elegans*; therefore an increase in acetylcholine signaling due to failure to clear the neurotransmitter from the synapse induces paralysis and eventually death. It has been shown that animals that have an increase in neurotransmitter release become hypersensitive to aldicarb, while animals with a decrease in neurotransmitter release are resistant to the effects of the drug (Nonet et al., 1993; Miller et al., 1996; Mahoney, et al., 2006). *unc-2(zf35)* mutants are highly hypersensitive to 1mM aldicarb, paralyzing approximately 2-fold faster than wild-type animals (Figure IV-4). In contrast, the deletion allele of *unc-2, e55*, which most likely represents a null (Schafer and Kenyon, 1995; Mathews, et al., 2003, Figure IV-4), is more resistant to aldicarb than wild type. Animals that are heterozygous for the *zf35* mutation are also hypersensitive to aldicarb, although not to the same levels as the homozygous mutant, suggesting the *zf35* allele is semi-dominant (Figure IV-4).

Further behavioral analysis also showed hyperactivity in several behaviors. *unc-2(zf35*) animals have a dramatic increase in reversal and thrashing rates compared to wild type. These behaviors are opposite that of *unc-2(e55)* animals, which are mostly paralyzed (Mathews, et al., 2006; Figure IV-5A,B; Movie IV-3). Additionally, although *unc-2(zf35)* animals had a normal brood size (wild type, 288 ± 5; *unc-2(zf35)*, 253 ±14) they had a reduced number of eggs in their uterus and laid eggs at earlier stages than wild-type or *unc-2(e55)* animals, suggesting they are also hyperactive in egg laying behavior (Figure IV-

5C,D,E). Together with our pharmacological experiments, these data suggest that the *zf35* mutation causes an increase in neurotransmission that effects behavioral outputs.

To determine if the G1132R mutation is the cause of these behavioral phenotypes we made transgenic animals that expressed UNC-2G1132R in all neurons in either *unc-2(e55)* null mutants or wild-type animals. The transgenic animals expressing the UNC-2G1132R transgene exhibit hyper-reversal behavior and hypersensitivity to aldicarb, similar to *unc-2(zf35)* mutants. *unc-2(e55)* transgenic animals that express UNC-2 WT in all neurons were rescued for locomotion defects and resistance to aldicarb (Figure IV-6A, B). This indicates that the G1132R mutation confers the hyperactive phenotypes of *unc-2(zf35)* animals. The electrophysiological properties of the G1132R, and the behavioral hyperactivity of *unc-2(zf35)*, which is opposite to that of the null allele *unc-2(e55)*, suggests that *unc-2(zf35)* is a gain-of-function allele of the *C. elegans* voltage gated calcium channel. Additionally, our data indicate that expression of UNC-2G1132R in the nervous system at both the NMJ and inter-neuronal connections causes an increase in neural activity.

Suppressor Screen to Identify Novel Calcium Signaling Components.

To identify genes that are involved in processing, expression, and composition of voltage-gated calcium channels we performed a genetic screen for mutants that suppressed the hyperactive phenotypes of *unc-2(zf35)* animals. We obtained 50

mutants from this screen, which were resistant to the effects of aldicarb. We then tested these mutants on 100μm levamisole, an acetylcholine agonist. Since this drug activates postsynaptic receptors, a resistance to this drug in addition to resistance to aldicarb indicates a postsynaptic defect rather than a defect at the presyanpse. Of the 50 mutants we isolated that were resistant to aldicarb, 30 were also resistant to levamisole, suggesting that these isolated mutants were alleles of genes acting in the postsynapse. We focused our analysis on the 20 mutants, which were resistant to aldicarb only, allowing us to identify genes that were likely to have a genetic interaction with *unc-2* localization at the presyanpse.

Using single nucleotide polymorphisms, three factor mapping and sequence analysis, we identified the lesions in 17 of the 20 mutants we isolated (Table IV-1). We obtained 7 intragenic suppressors of *unc-2*, including several alleles which cause early transcription termination (Figure IV-2B, Table IV-1). This supports the notion that the *zf35* lesion causes is a gain of channel function. We also isolated three alleles of *unc-10/RIM,* one allele of *unc-13*, and one allele of *unc-31*, which are involved in synaptic vesicle docking and fusion (Gracheva, et al., 2008; Weimer, et al., 2006; Hammarlund, et al., 2007; Lin, et al., 2010). Additionally we identified four alleles of the $\alpha_2\delta$ subunit, *unc-36*, and one allele of the localization factor *calf-1*. Both of these genes have been previously implicated in regulating the localization of *unc-2* to the synapse (Saheki and Bargmann, 2009). This screening approach was highly successful in identifying

genes that interact with *unc-2* in the presyanpse. Furthermore, since we also have 3 currently unidentified mutants, which do not appear to be alleles of genes known to function in calcium channel function or trafficking, we might uncover novel molecular components or mechanisms for calcium channel processing and expression.

Discussion

Pre-synaptic Ca_v2 channels play a central role in neural network function as they translate neuronal activity into synaptic transmission within dynamic signaling networks. We have identified a novel gain of function allele of the *C. elegans* Ca_v2 gene, *unc-2(zf35).* Our electrophysiological analysis shows that the G1132R mutation in UNC-2caused by the *zf35* allele produces an increase in Ca2+ influx as well as shifts the activation voltage to more negative potentials, leading to more frequent and robust release of neurotransmitter. *unc-2(zf35)* animals are also hyperactive in thrashing, reversal and egg laying behaviors and the hypersensitivity of *unc-2(zf35)* mutants to aldicarb support the notion that this mutation causes an increase in neurotransmission. It is possible the increased conductance and lower voltage dependence causes a higher probability or an incoordination of synaptic release events. It has been shown that mutants in genes that regulate the frequency of synaptic release, such as components of the Go/Gq signaling cascade, also display hyperactive phenotypes similar to *unc-2(zf35)*, suggesting that the G1132R mutation likely causes an increase in neurotransmission (Mendel et al., 1995; Segalat, et al., 1995; Koelle and Horvitz,

1996; Lackner, et al., 1999; Miller, 1999; Miller 2000). Perturbations of Ca_v2 channel function may disrupt the timing and control of motor programs involved in locomotion and egg laying, resulting in an overall hyperactivity of these behaviors in *zf35* animals.

Mammalian studies indicate that the regulation of Ca_v2 channels is complex and is modulated by interactions with synaptic proteins, neuromodulatory pathways that activate G-protein signaling cascades, cross-talk with other intracellular signaling pathways (Catterall, 2000) and probably other factors yet to be characterized. To identify molecular components involved in Ca_v2 processing and expression, we performed a suppressor screen in which we isolated mutants that were resistant to aldicarb. We isolated 20 mutants, of which we identified components of the synaptic machinery (*unc-10, unc-13, unc-13)*. It has been shown that UNC-10, UNC-13 and UNC-31 play a role in localizing UNC-2 to the active zone. These studies have shown that direct interaction with the synaptic machinery is critical for calcium influx to appropriately trigger vesicular fusion (Saheki and Bargmann, 2009, Kaeser, et al., 2011). We also identified alleles of *claf-1* and *unc-36*. These genes have been shown to play a key role in trafficking of *unc-2* to the synapse (Saheki and Bargmann, 2009). In particular, *calf-1* is critical for the exit of *unc-2* from the endoplasmic reticulum. *unc-36* is the *C. elegans* $\alpha_2\delta$ subunit and has been shown to play a role in trafficking *unc-2* to the active zone, as well as modulating channel activity.

Our identification of a rare gf mutation in the gene coding for the UNC-2/Ca_v2 channel opens new avenues for the analysis of Ca_v2 function, modulation and localization *in vivo*. Our *unc-2/Ca_v2(gf)* suppressor screen indicates that the spectrum of isolated mutants is different from previous aldicarb-resistance screens (Nonet et al., 1993; Miller et al., 1996). Molecular characterization of the remaining mutants and perhaps further screening should define new genes required for Ca_v2 processing and expression. Many aspects of Ca_v2 function and modulation are still unknown and further study of our gain-of-function mutant may provide new insights into the pivotal role of Ca_v2 channels in the integration of circuit activity.

Figure IV-1

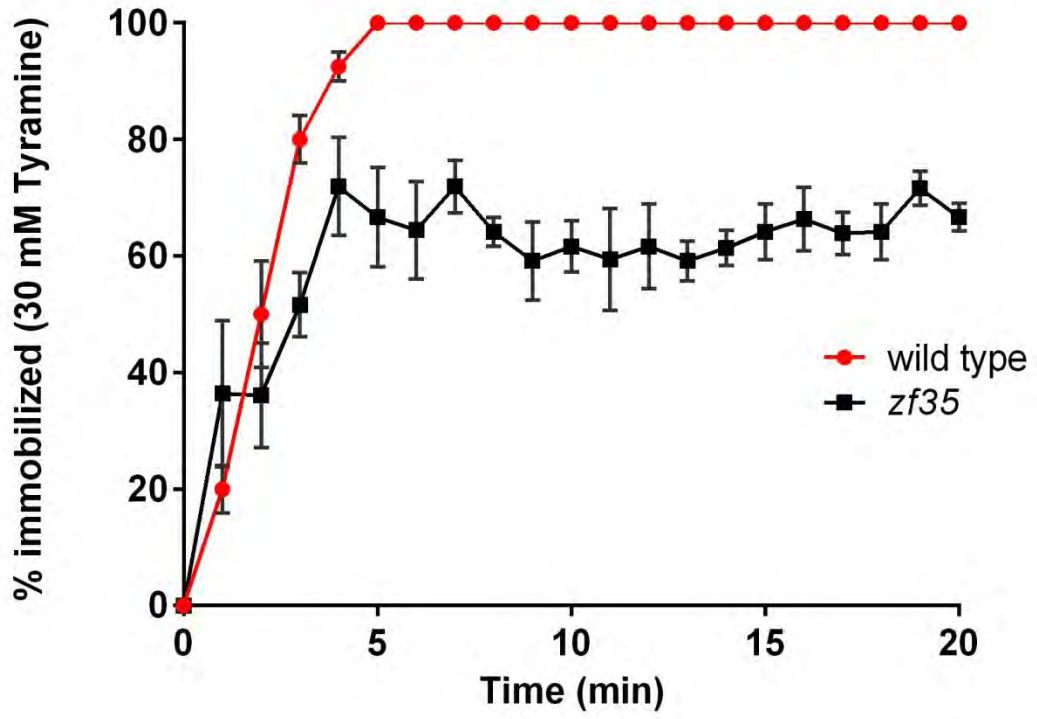

***zf35* mutants are partially resistant to the paralytic effects of exogenous tyramine.**

Show is the quantification of body movements on 30 mM tyramine. Each data point represents the mean ± SEM of the percentage of animals immobilized on exogenous tyramine every minute for 20 minutes for at least four trials totaling 40 animals. *zf35* mutants continue to move through the duration of the assay while 100% of wild type animals are immobilized after 5 minutes.

Figure IV-2

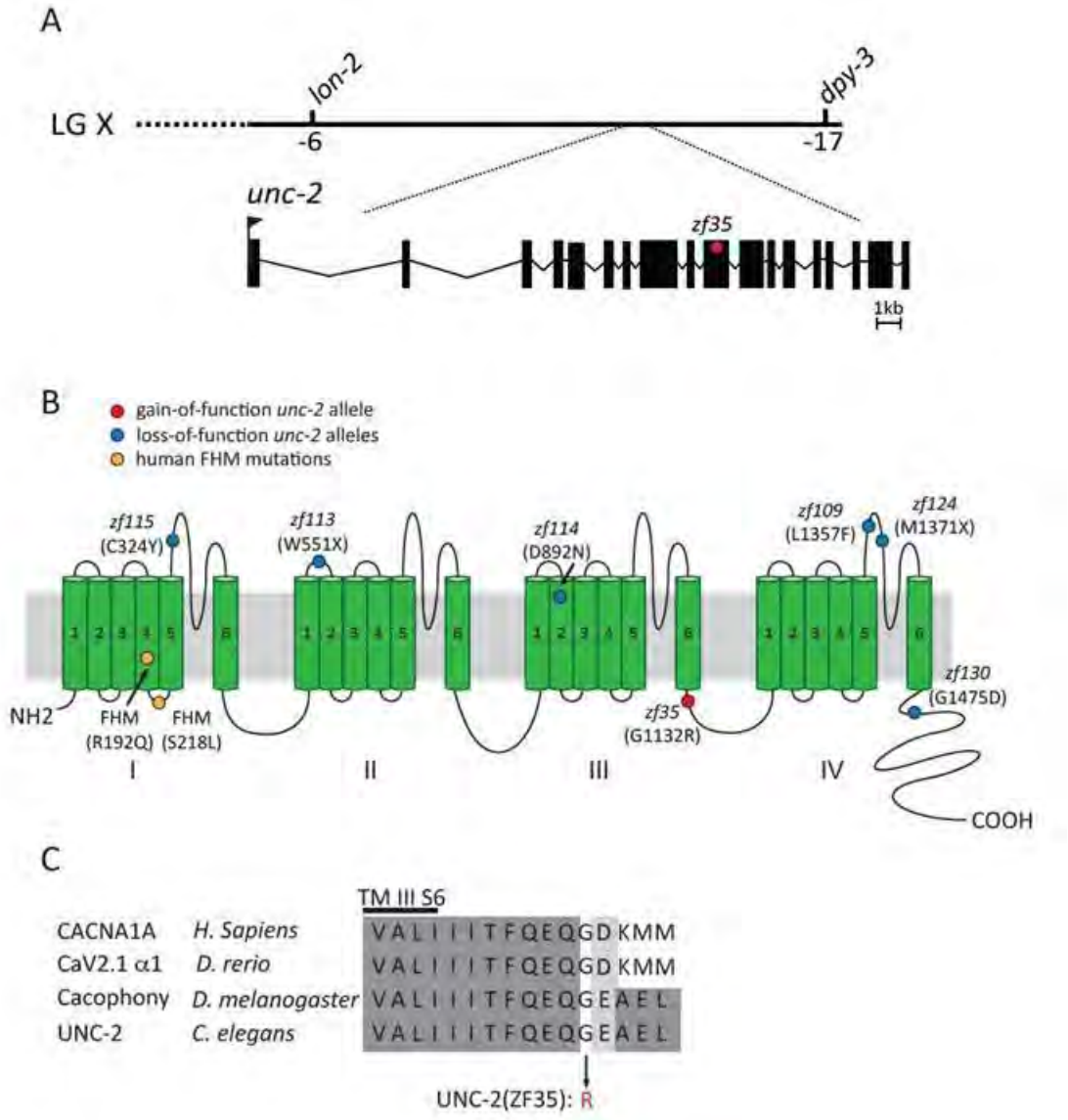

zf35* is an allele of *unc-2.

(A) The *unc-2* locus. Genetic map and gene structure of *unc-2*: coding sequences are represented as black boxes. Red circle indicates the position of the *unc-2(zf35)* allele. The *zf35* gain-of-function allele is a single nucleotide transition (GGA → AGA) resulting in a glycine to arginine (G → R) amino acid substitution at position 1132.

(B) Schematic diagram of the UNC-2 protein. UNC-2 consists of four homologous domains (TM I-IV), each consisting of six transmembrane, alpha-helix segments (1-6) as indicated by the green cylinders. The UNC-2 (G1132R) gain-of-function mutation is located in the third intracellular loop between TM III and IV, indicated by the red circle. Blue circles indicate positions of intragenic suppressors isolated in our genetic screen (see Table IV-2). Yellow circles indicate the location of known gain-of-function mutations implicated in Familial Hemiplegic Migraine (FHM) (Hans et al., 1999; Tottene et al., 2005).

(C) Alignment of *C. elegans* UNC-2 with $Ca_V2.1$ channels from human (CACNA1A), zebra fish ($Ca_V2.1$ 1α), and *Drosophilia (*Cacophony). Identities are shaded in dark grey, similarities in light grey. Location of the G1132R mutation is indicated, which is a the highly conserved region of the UNC-2 protein between TM III-S6 and TM IV-S1.

Figure IV-3

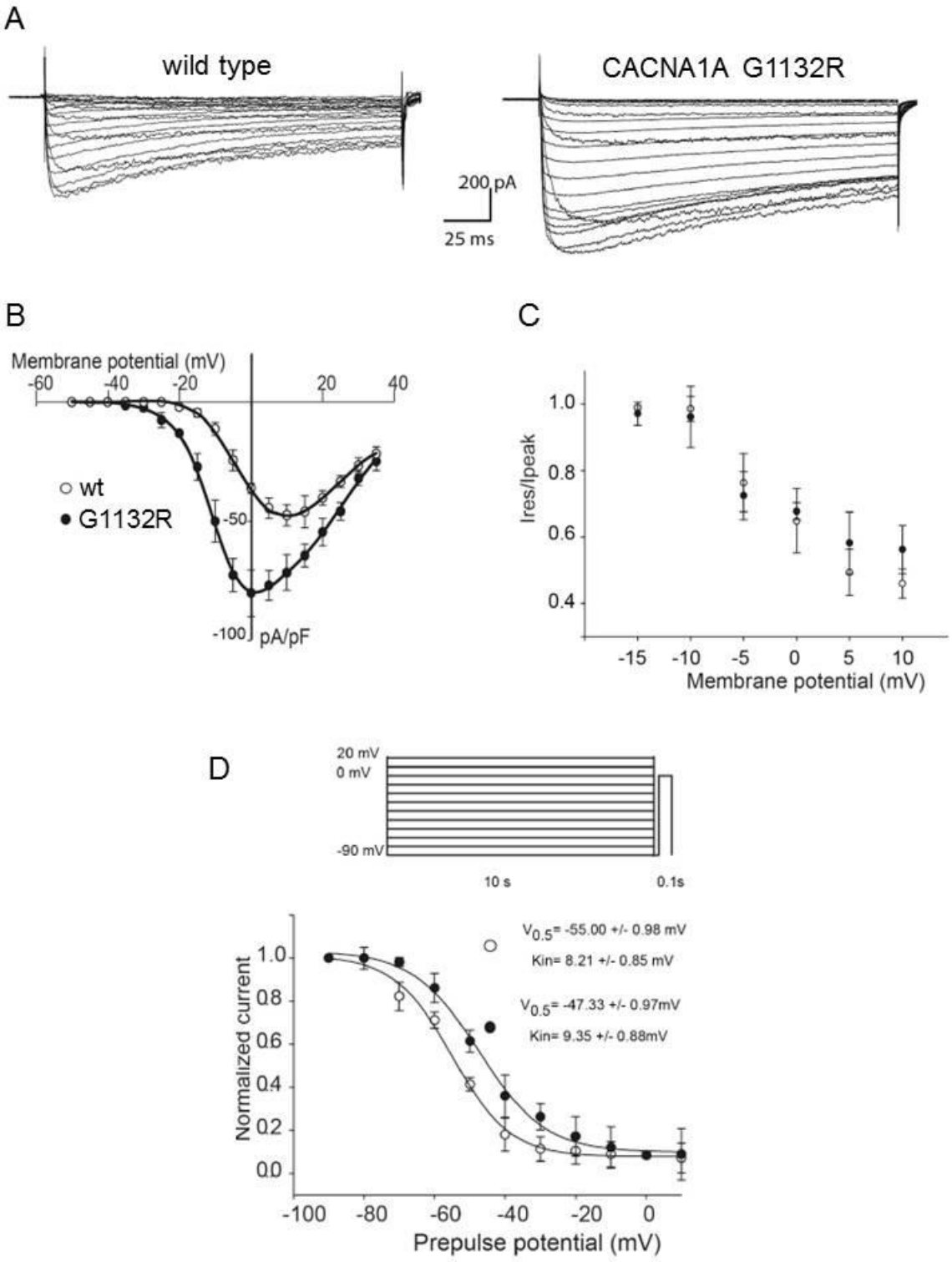
A
wild type
CACNA1A G1132R
200 pA
25 ms
B
Membrane potential (mV)
-60
-40
-20
20
40
wt
G1132R
-50
-100
pA/pF
C
Ires/Ipeak
1.0
0.8
0.6
0.4
-15
-10
-5
0
5
10
Membrane potential (mV)
D
20 mV
0 mV
-90 mV
10 s
0.1s
Normalized current
1.0
0.8
0.6
0.4
0.2
0.0
V0.5= -55.00 +/- 0.98 mV
Kin= 8.21 +/- 0.85 mV
V0.5= -47.33 +/- 0.97mV
Kin= 9.35 +/- 0.88mV
-100
-80
-60
-40
-20
0
Prepulse potential (mV)

Figure IV-3. The G1132R mutation causes functional changes in channel properties in α_1A subunit of the human P/Q type calcium channel, CACNA1A.

Shown are the whole-cell patch-clamp recordings with 5 mM Ba2+ as charge carrier from HEK293T cells transiently expressing either the wild type or G1132R mutant of the human $Ca_v2.1$ α_1A subunit, CACNA1A. The recordings were obtained from cells incubated at 37°Cfor 24-36 hours after transfection.

(A) Representative macrocurrents of wild-type (left) and mutant (right) CACNA1A elicited after stepping the membrane potential to voltages between -55 and 40 mV in 5mV increments from a holding potential of -120 mV for 200 ms.

(B) Voltage dependence of whole-cell current density for wild-type and mutant channels. The current density values were obtained by dividing current amplitudes and cell capacitance (wild-type, n=9; G1132R, n=11).

(C) Comparison of the extent of inactivation (measured as the relationship between the residual current at the end of the test pulse and the current peak) as a function of membrane potential. No significant differences were observed (wild-type, n=9; G1132R, n=11).

(E) Steady-State Inactivation curves. The G1132R mutation causes a slight positive shift in the midpoint voltage in the steady-state inactivation curves. No significant differences were observed in the slope factor of the steady-state inactivation. Currents were normalized to the maximal value obtained at the test pulse and plotted as a function of the prepulse potential. Data were fitted with the Boltzmann equation of the form: $I/I_{max}=\{1+\exp[(V-V_{0.5})/k\text{in}]\} - 1$.

Figure IV-4

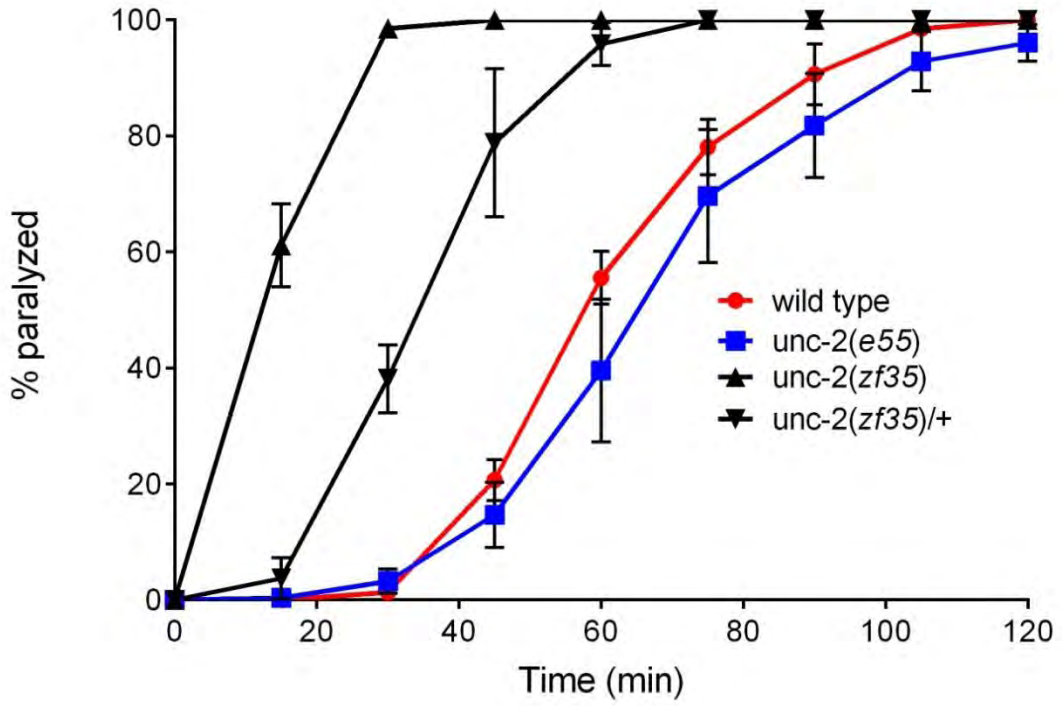

***unc-2(zf35)* animals are hypersensitive to 1 mM aldicarb.**

Show is the quantification of movement on 1 mM aldicarb. Each data point represents the mean ± SEM of the percentage of animals paralyzed by aldicarb every 15 minutes for at least five trials totaling 50 animals. Homozygous *zf35* mutants are hypersensitive to aldicarb. Heterozygous mutants are also hypersensitive aldicarb although not to the same extent as homozygotes, indicating that *zf35* is a semi-dominant allele of *unc-2*.

Figure IV-5

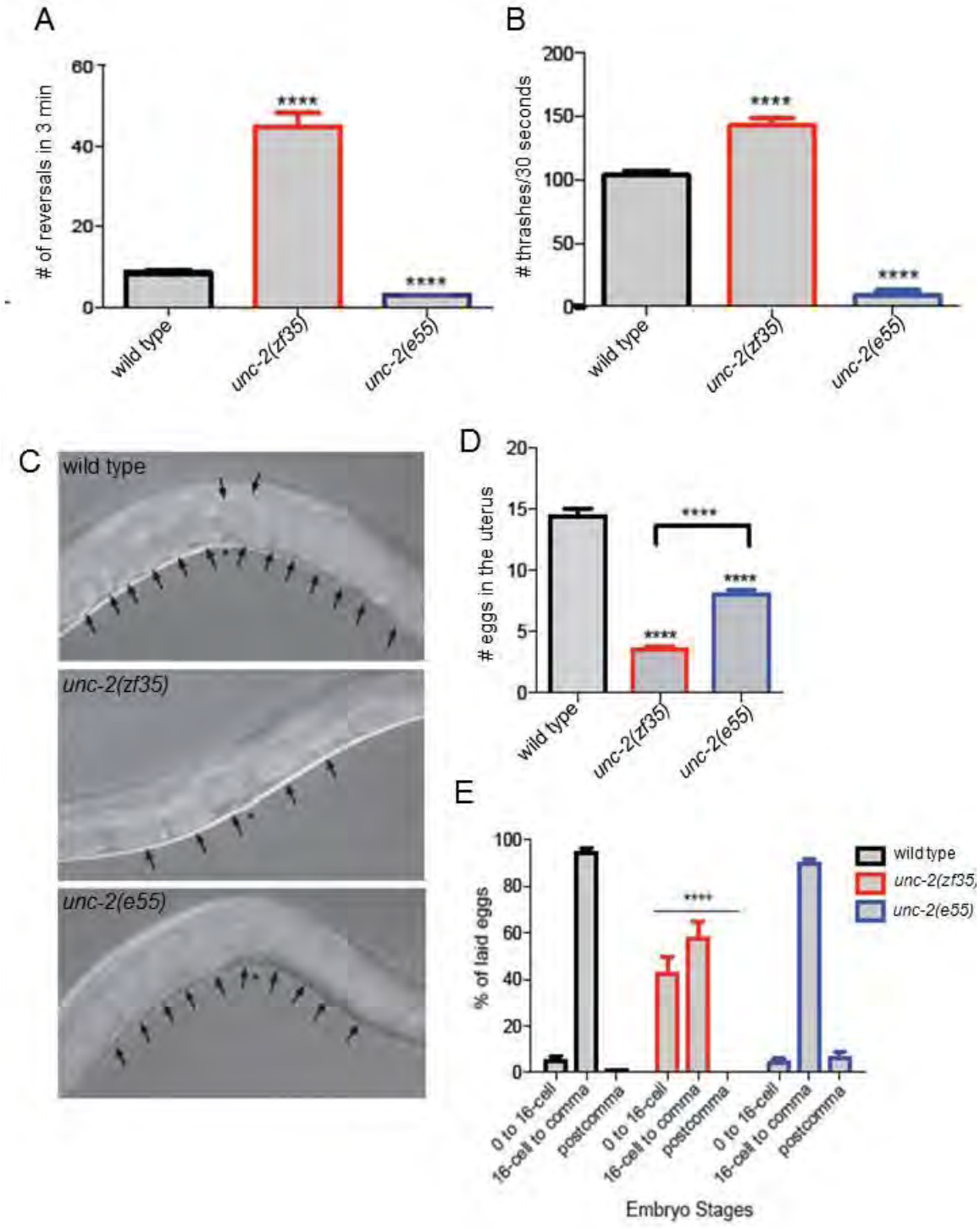
A
# of reversals in 3 min
60
40
20
0
****
****
wild type
unc-2(zf35)
unc-2(e55)
B
thrashes/30 seconds
200
150
100
50
0
****
****
wild type
unc-2(zf35)
unc-2(e55)
C
wild type
unc-2(zf35)
unc-2(e55)
D
eggs in the uterus
20
15
10
5
0
****
****
****
wild type
unc-2(zf35)
unc-2(e55)
E
% of laid eggs
100
80
60
40
20
0
****
wild type
unc-2(zf35)
unc-2(e55)
0 to 16-cell
16-cell to comma
postcomma
Embryo Stages

Figure IV-5. ***unc-2(zf35)*** **animals are hyperactive in locomotion and egg laying behaviors.**

(A) Quantification of number of reversals. Shown is the average number of reversals made by wild-type (6.87 ± 0.40 reversals, n=60), *unc-2(zf35)* (43.2 ± 1.9 reversals, n=65), and *unc-2(ze55)* (2.64 ± 0.23 reversals, n=44) in 3 minutes on food. Statistical difference from wild type; **** p<0.0001, two-tailed Student's T test.

(B) Quantification of the number of body bends during swimming behavior. Shown is the average number of body bends made by wild type (103.6 ± 0.40 thrashes, n=20), *unc-2(zf35)* (143.2 ± 1.9 thrashes, n=20), and *unc-2(ze55)* (8.2 ± 0.23 thrashes, n=20) in 30 seconds in liquid. Statistical difference from wild type; **** p<0.0001, two-tailed Student's T test.

(C) Representative images of unlaid eggs in adult wild-type, *unc-2(zf35)* and *unc-2(e55)* animals. Arrows indicate eggs; asterisk denotes position of the vulva.

(D) Quantification of the number of eggs in the uterus. Shown is the average number of eggs in the uterus of adult wild type (13.4 ± 0.72 eggs, n=59), *unc-2(zf35)* (3.01 ± 0.15 egg, n=64) and *unc-2(e55)* (7.71 ± 0.40 eggs, n=30) 40 hours post L4. *unc-2(zf35)* animals had fewer eggs in the uterus than wild type or *unc-2(e55)*. Statistical difference from wild type unless otherwise noted; **** p<0.0001, two-tailed Student's T test.

(E) Distributions of stages of freshly laid eggs in wild-type (n=100), *unc-2(zf35)* (n=100), and *unc-2(e55)* (n=100). *unc-2(zf35)* animals laid eggs at an earlier stage (0-16 cell) than wild-type or *unc-2(e55)* animals. The distribution of the stage of the laid eggs of the *unc-2(zf35)* mutants is statistically significantly different from those of wild type and *unc-2(e55)* mutants. ****p<0.0001**,** two-way ANOVA.

Figure IV-6

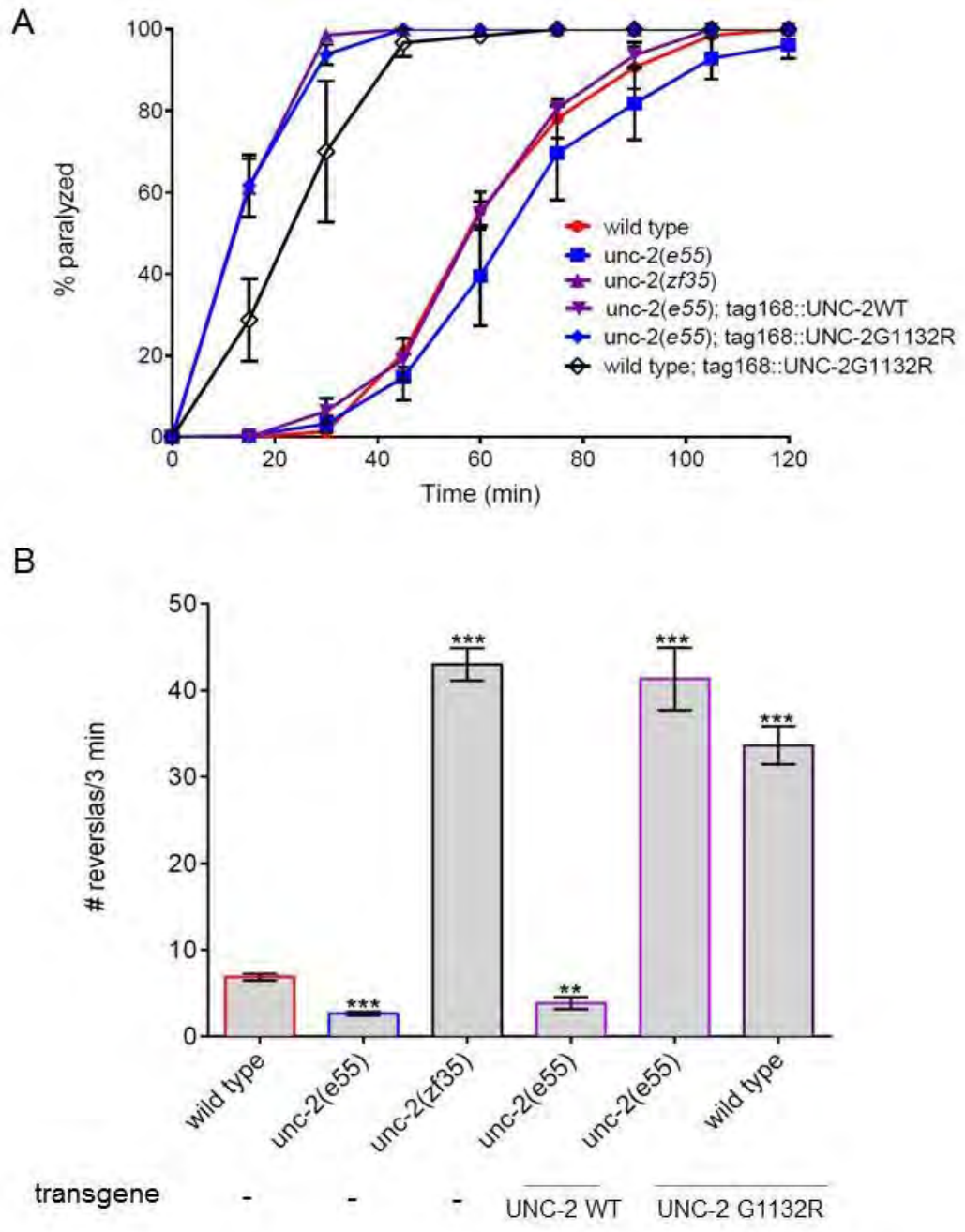
A
% paralyzed
Time (min)
wild type
unc-2(e55)
unc-2(zf35)
unc-2(e55); tag168::UNC-2WT
unc-2(e55); tag168::UNC-2G1132R
wild type; tag168::UNC-2G1132R
B
reverslas/3 min
wild type
unc-2(e55)
unc-2(zf35)
unc-2(e55)
unc-2(e55)
wild type
transgene
-
-
-
UNC-2 WT
UNC-2 G1132R

Figure IV-6. UNC-2G1132R confers increase in neurotransmission.

(A) Show is the quantification of movement on 1 mM aldicarb. Each data point represents the mean ± SEM of the percentage of animals paralyzed by aldicarb every 15 minutes for at least five trials totaling 50 animals. *unc-2(e55)* loss-of-function or wild-type animals expressing the *tag-168*::UNC-2G1132R transgene is expressed in all neurons, are hypersensitive to aldicarb. Resistance to aldicarb induced paralysis is rescued by expression of the *tag-168*::UNC-2WT transgene in *unc-2(e55)* loss-of-function animals.

(B) Quantification of number of reversals. Shown is the average number of reversals made by wild-type (6.87 ± 0.40 reversals, n=60), *unc-2(zf35)* (43.2 ± 1.9 reversals, n=65), *unc-2(ze55)* (2.64 ± 0.23 reversals, n=44), *unc-2(e55); ptag-168*::UNC-2WT (±), *unc-2(e55); ptag-168*::UNC-2G1132R (±), and *ptag-168*::UNC-2G1132R (±) in 3 minutes on food. Animals expressing the G1132R transgene have an increased reversal rate similar to *unc-2(zf35)* animals. Statistical difference from wild type; **** $p<0.0001$, two-tailed Student's T test.

Table IV-1

	Suppressor alleles
Intragenic (*unc-2*)	*zf109 (L1357F)*, *zf113* (W551X), *zf114* (D892N), *zf115* (C324Y), *zf122*, *zf124 (M1371X)*, *zf130 (G1475D)*
Auxiliary subunit (α2δ)	*unc-36: zf108, zf112, zf118, zf125*
Channel trafficking and localization	*calf-1(zf88), unc-10(zf87, zf90, zf129)*
Synaptic vesicle docking & fusion	*unc-13(zf110), unc-10(zf87, zf90, zf129)*
Dense core vesicle fusion	*unc-31(zf107)*
unknown	*zf89, zf121, zf132*

***unc-2(zf35)* suppressor screen identifies new alleles of genes associated with VGCC trafficking and function.**

Shown is a list of alleles identified in the *unc-2(zf35)* suppressor screen grouped according to function. We isolated 20 mutants that were resistant to the effects of aldicarb and sensitive to levamisole. Genetic and sequence analysis lead us to identify 17 of the 20 mutations, all of which occur in genes known to play a role in *unc-2* trafficking and function. Three alleles are still unidentified.

Movie IV-1

Movie of wild-type animals on food.

Filming began after a 3 minute equilibration period after the animals were transferred to a freshly seeded plate of food from the growth plate. Movie was shot at 15 frames per second. Wild-type animals move slowly on food and make few reversals.

Movie IV-2

Movie of *zf35* animals on food.

Filming began after a 3 minute equilibration period after the animals were transferred to a freshly seeded plate of food from the growth plate. Movie was shot at 15 frames per second. *zf35* animals have an increased speed on food and make many reversals.

Movie IV-3

Movie of *e55* animals on food.

Filming began after a 3 minute equilibration period after the animals were transferred to a freshly seeded plate of food from the growth plate. Movie was shot at 15 frames per second. *e55* animals have are slow, sluggish and appear mostly paralyzed.

Chapter V

Final Thoughts: Discussion and Future Directions

Signaling networks or neural circuits direct complex sequences of activity that culminate in what we recognize as coordinated behavior. A good example of a complex behavioral sequence is an escape response in which an animal evades a threatening stimulus. In many cases the response to a threat is modulated by biogenic amine signaling. We know that in the mammalian nervous system noradrenaline and adrenaline mediate the "fight or flight" response (Brede, et al., 2004) however, how these biogenic amines work to coordinate distinct neural programs or networks to produce a coordinated response is unknown. With trillions of neuronal connections in the mammalian brain, studies of neuronal control of these behaviors becomes challenging. My dissertation aimed to explore how the nervous system coordinates a complex behavior through biogenic amine signaling in an organism with a simpler nervous system, the nematode *C. elegans*.

In invertebrates the biogenic amines octopamine and tyramine are considered analogous to noradrenaline and adrenaline (Roeder, 2005), in that they may orchestrate neural activity to produce complex behaviors in response to stress. The role for tyramine was initially described in both mammalian and invertebrate systems as a precursor or a metabolic by product in the pathway to make other neurotransmitters (Roeder, 1999; Berry, 2004). Previous work in *C. elegans* identified a subset of tyraminergic cells in the *C. elegans* nervous system, the RIMs, and showed that these cells played an important role in escape behavior (Alkema, et al., 2005). Additionally, identification of GPCRs that

are activated by tyramine in *C. elegans* (Rex and Kouminecki, 2002; Rex, et al., 2005) suggested a role far beyond that of an intermediate molecule. However, how tyramine functioned in the nervous system remained unclear.

In a genetic screen for tyramine signaling components we identified alleles of a previously uncharacterized ion channel, LGC-55, which we determined was activated by tyramine in Chapter II. I also identified that activation of this channel was critical to coordinate the motor programs of the initial phases of the *C. elegans* escape response (Figure V-1, Figure II-14). Normally, forward locomotion is accompanied by exploratory head movements, where the animal's head oscillates from side to side. Gentle touch to the head of the animal elicits a backing response during which the exploratory head movements are suppressed. This long reversal is followed by a deep ventral bend which allows the animal to make a sharp turn (omega turn) to resume locomotion in the opposite direction (Figure V-1). I found that LGC-55 is expressed in the neck muscles and neurons that control head movements and the AVB forward locomotion command neurons, cells which are directly postsynaptic to the tyraminergic RIM. During the escape response, the activation of LGC-55 by tyramine is necessary to cause a relaxation of the neck muscles to suppress head movements. It is also critical for the prolonged inhibition of the forward locomotion command neurons, AVB, to facilitate a reversal long enough so the animal can make an omega turn, as typically these turns only occur after 3 or more body bends (Gray, et al., 2005). The work in Chapter II identifies tyramine

as a classical neurotransmitter; as we show the ability for tyramine to directly affect the excitability of postsynaptic cells through the activation of LGC-55. Furthermore, we were able to complete the neural circuit for the escape response, by identifying the role for the RIM in coordinating two distinct motor programs, locomotion and head movements (Figure II-14).

The identification of a tyramine gated ion channel supports a new role for biogenic amines at the synapse. A majority of the biogenic amine receptors identified in mammals and invertebrates are metabotropic and thus the assumption remains that monoamines function largely as neuromodulators. In *C. elegans,* ion channels that are gated by serotonin, dopamine and now tyramine have been identified (Ranganathan, et al., 2000; Ringstad, et al., 2009; Pirri, et al., 2009), supporting the notion that biogenic amines can function to directly activate or inhibit neural circuits. *C. elegans* has a large family of cys-loop LGICs, and many of the receptors in the family remain uncharacterized (Jones and Sattelle, 2008). It is therefore a possibility that all monoamines might function in fast neurotransmission in the worm. The *C. elegans* nervous system is quite small, only 302 neurons, and despite this they have a large repertoire of behaviors. A way to generate flexibility in behavioral output with such a limited nervous system would be to increase complexity on the neurochemical level, perhaps through expansion of the types of neurotransmitter receptors. Now a single neurochemical could both modulate and directly impact neural circuit activity through expression of different receptor types.

These findings beg the question of whether there are biogenic amine gated ion channels in other animals. In the vertebrate nervous system, serotonin is known to activate a cys-loop ligand-gated cation channel (5HT3a) (Derkach, et al., 1989; Maricq, et al., 1991), and histamine has been show to rapidly produce inhibitory synaptic signals in the hypothalamus that are not mediated by GPCRs (Hatton and Yang, 2001). This presents the possibility that the classic biogenic amines might have corresponding LGICs that function in the mammalian brain. However, there is no indication that a trace amine gated chloride channel, like LGC-55, exists in the mammalian genome (JKP and MJA unpublished observations). Therefore, a tyramine gated channel might be specific to the invertebrate nervous system.

Is tyraminergic signaling conserved in other nematodes? Most other species of soil nematodes suppress head movements in response to anterior touch, and have cells that express TDC-1 (see Appendix II). However, it is currently unknown whether they utilize tyramine to coordinate motor programs, like *C. elegans*. Work from our lab has shown that the coordination of head movements with backward locomotion through that activation of LGC-55 by tyramine is critical for the ability of *C. elegans* to escape its natural predator; the nematophageous fungi (Figure V-2; Maguire, et al., 2011). As fungi that consume nematodes as a nitrogen source are not discriminating in their taste for worms, it is reasonable to think that all soil nematodes employ a similar mechanism for evading capture.

Species of the Pleiorhabditis clade tend to be parasitic, and not reside in the soil. These nematodes do not suppress head oscillations in response to touch (See Appendix II), suggesting they may not utilize tyramine signaling as a part of their locomotory stress response. Identification of a tyramine-gated chloride channel in the parasitic nematodes, *Haemonchus contortus* and *Brugia malayi* (Rao, et al., 2010, Pirri, et al., 2009), as well as identification of tyraminergic cells in the Pleiorhabditis species (JA, SM and MJA unpublished observations, see Appendix II) indicates that parasitic nematodes might employ tyramine signaling for a different purpose. In *C. elegans* defects in tyramine signaling can also affect reproduction, causing a decrease in egg laying capability (Alkema, et al., 2005, MJA and JKP unpublished observations). Additionally, it has been shown that tyramine deficiencies can lead to infertility in the fly (Monastirioti, et al., 1996; Avila, et al., 2012). Given the possible role for tyramine in fertility, and the fact that there would be no cross reactivity with the vertebrate nervous system, tyramine-gated chloride channels may be excellent targets for anthelmintic drugs and other pesticides.

The discovery of the novel homomeric tyramine channel, LGC-55, put us in a unique position to address the question of how the electrical nature of a synapse might affect the development and output of a neural network. Much emphasis has been placed on determining all the neural connections in the human nervous system and developing this “connectome” is considered an essential step for understanding how the brain controls behavior. However, while

a connectome provides important information about the physical relationships between neurons, it harbors no information about the nature of synaptic connections and this lack of critical information therefore clouds the relationship between connectome and behavior.

In Chapter III I addressed whether changing the nature of a synapse could alter the behavioral output of a defined neural network, a feat that has not been attempted in any organism. I chose to use LGC-55 to address this question since it is a homomeric receptor with expression limited to cells that are directly postsynaptic to a single pair of tyraminergic neurons, the RIM. Additionally, activation of this receptor produces a defined behavioral output that can be easily monitored. I showed that changing the selectivity of LGC-55 from anions to cations can cause a behavioral switch. In the transgenic "LGC-55 cation" animals touch now induces behaviors that are virtually opposite from the wild type. Animals expressing the cationic version of LGC-55 hypercontract the neck and have stunted reversals, while the wild type relax the neck and make long reversals. This work shows that the output of a connectome can be changed simply through receptor expression within the circuitry and illustrates the limitations of a neural network map to predict behavior. Surprisingly, the identity of the receptor or in turn the behavioral output provides no constraints on the development of the of the *C. elegans* neural circuit for escape.

The data in Chapter III suggests there is some plasticity in levels of receptor expression; however despite a complete change in the nature of the synapse, the *C. elegans* nervous system seems to develop independently of synaptic activity. This might indicate that connectomes first develop and later expression of receptors dictates the nature of the connection, giving the nervous system certain degrees of freedom to produce excitatory or inhibitory synapses. This would allow an animal to generate diversity in behavioral outputs by having bivalent receptors that respond to the same neurotransmitter. There are several examples of this in *C. elegans,* acetylcholine, GABA and glutamate receptors have both an activating cation and an inhibitory anion channel version of the channel (Cully, et al., 1994; Maricq, et al., 1995; Dent, et al., 1997; Beg and Jorgensen, 2003; Jones and Sattelle, 2004; Schuske, et al., 2004; Putrenko, et al., 2005).

With the expanded complexity of the mammalian brain, things may not be so simple. While there is evidence that suggests similar phenomena in the mammalian brain, where activity is not necessary for gross development, neural circuit refinement may be impaired (Shatz, C., et al., 1988; Ji et al., 1999; Misgeld, T., et. al., 2002). However, there is little evidence to suggest that inhibitory or activating synapses develop differently. In fact, there are cases where classically inhibitory receptors, like $GABA_AR$, are activating for a period of time during embryonic development (Ben Ari., 2002; Owens and Kriegstein 2002; Gulledge and Stuarts, 2003; Chavas and Marty, 2003). This suggests that

switching the nature of the synapse may have little effect on development, in both invertebrates and mammals.

My studies described in Chapter III provide a proof of principle that synaptic engineering is a feasible approach to modulate behavior. The possibility that this same technique could be successful as a tool to re-engineer the activity, performance and coordination of the circuits is enticing. In *C. elegans*, the LGC-55 cation channel could be used to identify the role certain neurons have in behavior or activate specific cells/neural circuits without cross reactivity from their native neurotransmitter. Furthermore, since altering the ion selectivity loop of an LGIC does not seem to affect expression or trafficking of the channel, expressing a cation version of a receptor in muscle cells and looking for hypercontraction to the application of different molecules is a feasible approach to deorphanizing other LGCCs (See Appendix I). Additionally, by engineering cation versions of known LGCCs in *C. elegans* we might be able identify their roles in behavior. The cationic version of LGC-55 could also be useful to activate or modify neural circuits in other model systems like, the fruit fly or the mouse, where there are no known tyramine gated channels and the use of tyramine by the nervous system is limited.

In addition to directly affecting postsynaptic excitability, monoamines that act through metabotropic receptors can regulate neurotransmitter release though the inhibition of Ca_V2 channels. In particular the $G_{\beta\gamma}$ protein has been shown to

modulate the excitability of postsynaptic cells through direct interaction with Ca_V channels (Dascal, 2001; Zamponi and Snutch, 1998). In humans, mutations that alter calcium channel properties or interactions between Ca_V channles and G-protiens can result in many neurological disorders including ataxia, epilepsy, and migraine, underlining the importance of modulation of calcium channel activity (Caterall, 2000). In our genetic screen for tyramine signaling mutants we identified an invaluable gain-of-function allele (*zf35*) of the *unc-2* gene. *unc-2* encodes the sole *C. elegans* α1 subunit of the high voltage-gated calcium channel (Ca_V2). In mammals the N-, P/Q-and R-type Ca_V2 channels are the predominant voltage-gated calcium channels in presynaptic nerve terminals where channel opening and Ca^{2+} influx triggers synaptic release of neurotransmitter (Caterall, 2000).

In Chapter IV I showed that, while *unc-2* loss-of-function mutants are uncoordinated, *unc-2(zf35)* mutants are hyperactive in many motor programs, which are also involved with the escape response. In addition, the *unc-2(zf35)* mutants exhibit hyperactivity in egg laying, and are hypersensitive to aldicarb, which are indicators of increased neurotransmission. The electrophysiological data show that this mutation causes an increase in channel conductance and a shift in the activation potential of the channel to lower voltages, suggesting a heightened channel activity which is likely the cause of increased neurotransmitter release in the *unc-2(zf35)* animals.

The *unc-2(zf35)* mutation causes a glycine to arginine substitution in highly conserved intracellular linker between TM III-S6 and TM IV-S1. The intracellular linkers between TM domains have been implicated in association with the voltage sensing domains of the channel (S4), accessory subunits, and G-proteins, that regulate channel activity (Caterall, 2000). Similar gain-of-function mutations were identified in the human CACNA1A gene that encodes the pore forming α1 subunit of Ca_V2 in patients with the neurological disorder Familial Hemiplegic Migraine (FHM) (Hans et al., 1999; Tottene et al., 2005). This suggests that *unc-2(zf35)* could serve as an invertebrate model for this channelopathy. Furthermore, given their easily identifiable hyperactive phenotypes, these mutants are good candidates for drug screens to look for treatments for FHM and perhaps other disorders that are the result of increased calcium channel function.

Additionally, these mutants are also useful in suppressor screens to look for molecular components or mechanisms for calcium channel processing and expression. The pilot suppressor screen discussed in Chapter IV, was quite successful in identifying mutants and we found that the spectrum of isolated mutants was different from previous aldicarb-resistance screens (Nonet et al., 1993; Miller et al., 1996). We isolated several mutants, which represent novel alleles of genes known to function in calcium channel trafficking and localization. Some of the mutants we identified are represented by single alleles indicating that our screen is incomplete (Table IV-1). We should therefore increase the

number of genomes screened to isolate a comprehensive set of genes that play a role in calcium channel function. Mammalian studies indicate that the regulation of Ca_V2 channels is complex and can be modulated by multiple factors, many of which are likely unidentified (Caterall, 2000). The majority of these studies were performed using candidate gene approaches in cell culture, so an unbiased genetic screen would take *in vivo* approach that might uncover novel mechanisms for regulation of Ca_V2 channels.

The UNC-2 *gf* mutation also could be used as powerful new tool to hyperactivate neurons within a circuit. While optogenetics can reveal the direct behavioral consequences of neuronal activation, the stimulation occurs outside of the typical behavioral setting. Cell-specific expression of *unc-2(zf35)* would allow us to constitutively hyperactivate subsets of neurons or individual neurons, throughout the animal's life. By analyzing the behavior of transgenic animals that express *unc-2(zf35)* in specific cell types in combination with analysis of receptor expression, calcium imaging and electrophysiological data, we might also be able to shed light on how the nervous system maintains homeostasis of neuronal activity. Furthermore, these experiments would allow us to dissect how neuronal assemblies produce a coordinated behavioral output within the context of normal behavior.

My doctoral thesis work aimed to explore how an animal can coordinate motor programs in order to produce a complex behavioral output. To that end,

this work broadened the role for monoamines in fast synaptic transmission by identifying a ligand-gated chloride channel activated by the biogenic amine tyramine. Furthermore, identification of this receptor provided a new role for tyramine at the synapse as a genuine neurotransmitter. This work is also among the rare examples where the neural path from sensory input to motor output has been completed. The identification of this pathway lead to novel experiments in genetic engineering, where we found it is possible to alter behavioral outputs by simply changing the nature of synaptic activity. We also discovered an invaluable gain-of-function mutant that may lead to the discovery of treatments for calcium channelopathies, as well as further the understanding of calcium channel physiology and neural circuit function. Together, the work presented in this thesis has furthered the understanding of how neural circuit activity orchestrates complex behaviors and provides motivation for the advancement of the study of the interactions between monoamines and ion channels in behavior.

Figure V-1

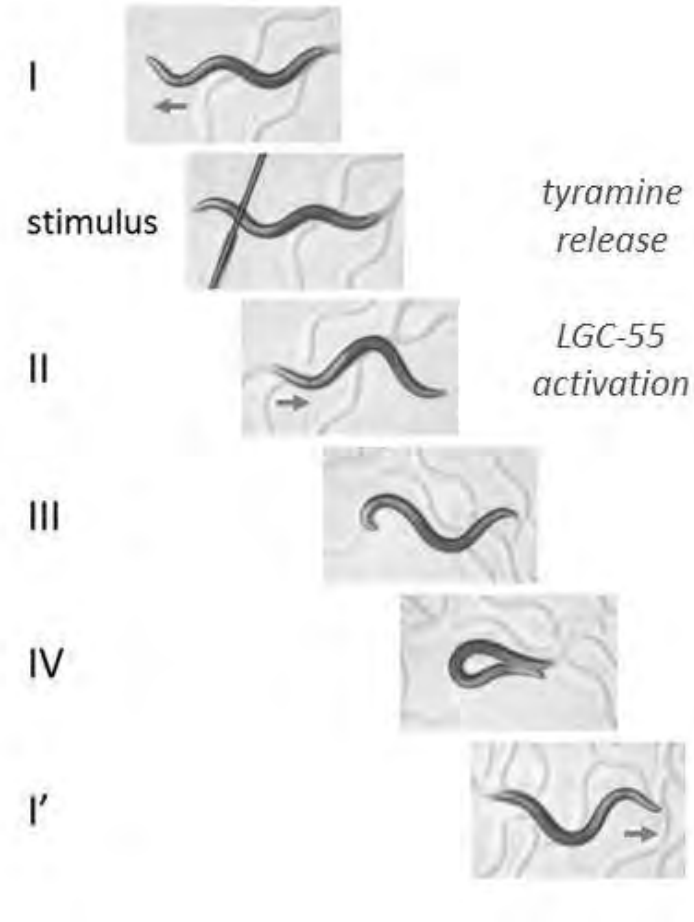

Phases of the *C. elegans* escape response.

Shown are still frames taken during the *C. elegans* escape response illustrating the four phases of the behavior. During normal locomotion the animal moves forward and displays exploratory head movements (I), after the animal is touched in the anterior portion of the body the animal executes a reversal during which these head movements are suppressed (II), after a long reversal the animal makes a deep ventral head bend (III) and slides its head along the ventral side of the body in and "omega turn" (IV) to reorient its locomotion trajectory in the opposite direction of the point of stimulus. It is at this point the animal moves forward and exploratory head movements are resumed (I').

Figure V-2

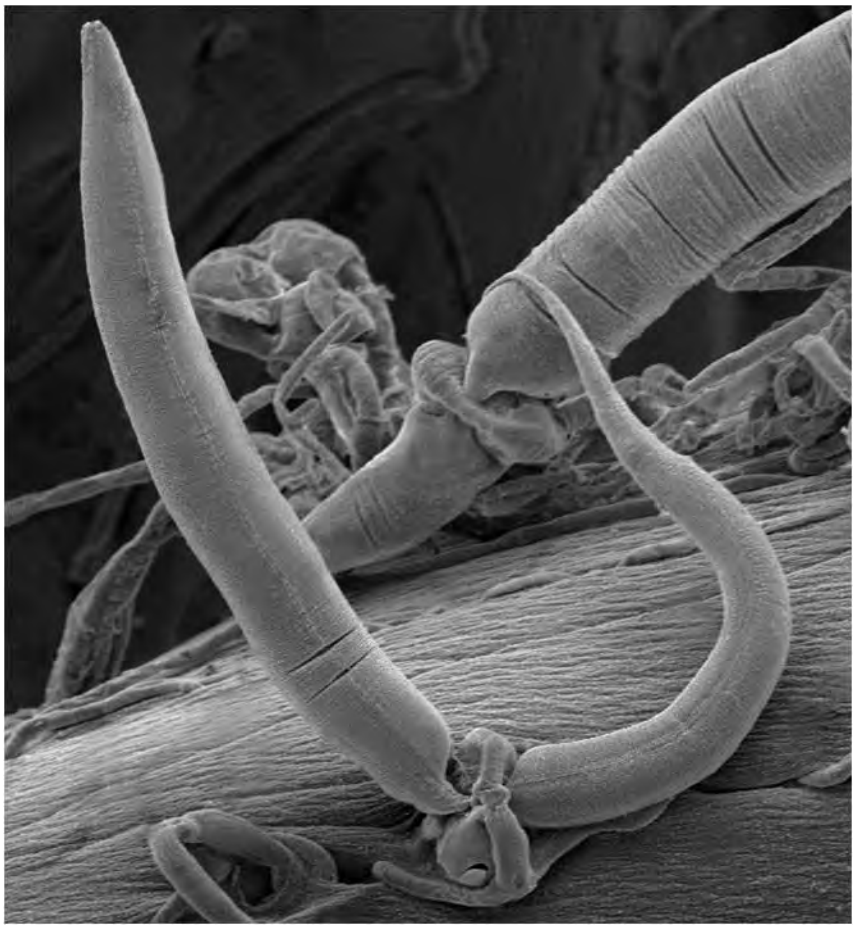

***C. elegans* caught by a constricting ring of a nematophagous fungus.**

Scanning electron micrograph of *C. elegans* L2 larvae caught in the constricting rings of the nematode trapping fungi, *Drechslerella doedycoides*. Image courtesy of Sean M. Maguire.

APPENDICES

APPENDIX I

Cloning and Characterization of Orphan Cys-Loop Ligand Gated Chloride Channels (LGCCs) In *C. elegans*

The work represented in this appendix is the preliminary data for a project which aims to deorphanize a group of predicted *C. elegans* ligand-gated chloride channels. I generated all the reagents including all constructs for *C. elegans* and *Xenopus* oocyte expression as well as the transgenic animals.

Introduction and Results

Cys-loop ligand gated ion channels (LGICs) play a major role in synaptic transmission, as activation of these channels directly alters excitability of neurons and can lead to excitation or inhibition of neural circuits. Like the mammalian genome, the C. elegans genome contains a large family of Cys-loop LGIC genes (Jones and Sattelle, 2008). Work from our laboratory and others has led to the identification of a novel class of Cys- loop ligand-gated chloride channels (LGCC) activated by biogenic amines (Figure AI-1). The Cys-loop ligand gated ion channel (LGIC) family consists of a group of neurotransmitter receptor subunits, such as the nicotinic acetylcholine (nAchR), γ-amniobutyric acid (GABA), glycine, and serotonin (5HT3a) receptors. Each subunit contains four transmembrane domains (M1-M4), an extracellular N-terminus and a large intracellular loop that connects transmembrane domains M3 and M4 (Betz, 1990).

Three LGCCs in *C.elegans*, MOD-1, LGC-53, and LGC-55 which are activated by the biogenic amines serotonin, dopamine, and tyramine respectively, have been elecrophsysologically characterized (Ranganathan et al., 2000; Ringstad et al., 2009; Pirri et al., 2009). MOD-1, LGC-53, and LGC-55 define a novel class of ligand-gated chloride channels (LGCC) that are gated by biogenic amines (Figure AI-1). There are eight closely related members of the novel LGCC group of subunits, five of which are uncharacterized, lgc-50, -51, -52, -54 and *ggr-3*. Each of these subunits is likely to form anion selective channels given the presence of a PAR motif in the cytoplasmic loop preceding

the M2 domain, which has been shown to play a major role in anion selectivity (Karlin and Akabas, 1995).

Using comparative genomic sequence alignments we found that the annotated gene finder predictions of the *C. elegans* sequences for three of these genes (*lgc-50, lgc-52* and *lgc-54*) were incorrect and identified the correct the 5' ends of the five orphan LGCCs. We performed RT-PCR based on these predictions, and isolated and cloned cDNA for the remaining five LGCC subunits (Table AI-1). To further characterize these genes, we generated fluorescent reporters to analyze the expression patterns for each of these putative chloride channels. Thus far, we have made transgenic animals that express a reporter for each of the following genes: *lgc-50, -51, 54* (Table AI-1). We found that *lgc-50* is expressed in a single pair of bilaterally symmetric neurons in the head, as well as in head and neck muscle. *lgc-51* is expressed in at least five pairs of neurons in the head as well as a pair in the tail. *lgc-54* is expressed in six pairs of neurons in the head of which we identified the RIC, RMED and RMEV (Figure AI-2). These results suggest that these LGCCs encode functional subunits that are expressed by the worm. Additionally, their expression in neurons indicates that they may a play a role in modulating *C. elegans* behavior.

To determine the ligands that activate these LGCCs we expressed each subunit individually in *Xenopus* oocytes for two-electrode voltage clamp (TEVC) electrophysiology. We found that bath application of dopamine, serotonin,

tyramine, octopamine or histamine at concentrations up to 100 μm did not produce detectable currents. Since, *Xenopus* oocyte TEVC is a heterologous expression system we also ectopically expressed each subunit in all *C. elegans* muscle cells, to mimic a more native environment. We exposed transgenic animals that expressed *lgc-50, -51, -52, -54* or *ggr-3* in all muscle cells to exogenous biogenic amines and found that the animals behaved similarly to wild type animals in the presence of dopamine, serotonin, tyramine, or octopamine (data not shown).

Materials and Methods

Cloning of *C. elegans* LGCCs

Comparative genomic sequence alignments of *C. elegans* LGCCs were carried out using MacVector software (Accelrys). Based on these alignments and gene finder predictions the following primers were designed to amplify LGCCs from first strand cDNA pools:

lgc-50: 5’ ATGCGATTTCTTCTTGTTCTTC, 3’ TTACATGGGACGATCCATTTTC; *lgc-51*: 5’ ATGTGCTTATTCCATTTCTTAGC; 3’ TTATTGAGAAATTCGTGAACAAG; *lgc-52*: 5’ ATGATCTACAGTATACAGGTGAG, 3’ TCAAGTGTAGACAGGATTCATG; *lgc-54*: 5’ ATGACAAACGTTACGGGATTC, 3’ TCAGGATGGTGGCGTCATTTG; *ggr-3:* 5’ ATGCTACACGATGTCATCTATATG, 3’ CATGTTTGCAGCTTTTAATGGTTAG

The oligo-dT primed cDNA pool was generated from whole worm RNA using the Super-Script (II) First Strand Synthesis System (Invitrogen). Isolated cDNAs were then sublcloned into pGEM-T using the pGEM-T Easy Vector System (Promega).

All transgenic strains were obtained by microinjection of plasmid DNA into the germline of *lin-15(n765s)*. At least three independent transgenic lines were obtained and data are from a single representative line. GFP reporter constructs were generated by cloning a genomic fragment containing 2 kb upstream, the first intron, first exon and part of the second exon relative to the predicted start site for each *lgc-50, -51, -52, -53, -54* and *ggr-3* in the GFP expression vector, pPD95.70. Constructs for muscle specific expression were generated by cloning *lgc-50, -51, -52, -53, -54* or *ggr-3* cDNA into pPD95.86 behind the *myo-3* promoter. GFP and *myo-3* constructs were microinjected along with the *lin-15ts* rescuing plasmid pL15EK at 80 ng/µl.

Cell Identification of *plgc-54::*GFP

Identifications of cells that expressed *plgc-54*::GFP reporter were based on cell body position, axon morphology and coexpression with previously described cell specific mCherry markers. Strains containing the following fusion genes were used to confirm cell identification: RIC: *zfIs25, ptdc-1::*mCherry, RMED/V: *ufIs34, punc-47::*mCherry

Electrophysiology of *C. elegans* LGCCs

Full length cDNA including 5' and 3' UTRs for each LGCC was cloned into the vector pSGEM or pTLNII for oocyte expression. Capped RNA was prepared the using T7 or SP6 polymerase from Promega. Stage V and VI oocytes from *X. laevis* were injected with ~50 ng of cRNA. Two electrode voltage clamp experiments were performed 2-3 days post injection at room temperature (22-24°C). The standard bath solution for recording was ND96: 96 mM NaCl, 2 mM KCl, 1.8 mM $CaCl_2$, 1 mM $MgCl_2$, 5 mM HEPES. Oocytes were voltage clamped at -60 mV and were subjected to a 10 second application of each neurotransmitter (100 μM, in ND96) with 2-3 minute washes between each application.

Discussion and Future Directions

Despite extensive study, how biogenic amines regulate outputs of neural networks to control behavior is still poorly understood. Biogenic amines are implicated in a large variety of neurological disorders including, substance abuse, depression, schizophrenia and migraine. Their signaling pathways have been the focus for development of treatments for these disorders. Better understanding of the functional roles of these channels will undoubtedly shed new light on how biogenic amines modulate neural circuits and behavior. Our work and that of others defined a new class of ligand-gated chloride channels (LGCCs) activated by biogenic amines, suggesting there are new mechanisms

for biogenic amine signaling in the nervous system (Ranganathan et al., 2000; Ringstad et al., 2009; Pirri et al., 2009; Jones and Sattelle, 2008).

Our phylogenetic comparison suggests there are eight closely related members of this group of LGCCs, five of which ligand specificity is unknown. We have cloned these genes and determined that at least three of them, *lgc-50, -51,* and *-54*, are expressed in the *C. elegans* nervous system (Figure AI-2). However, expression of these subunits individually in either the heterologous *Xenopus* expression system or endogenously in *C. elegans* muscle did not produce a functional channel that was activated by application of the biogenic amines dopamine, serotonin, tyramine, octopamine or histamine. Although based on previous experiments (Ranganathan et al., 2000; Ringstad et al., 2009; Pirri et al., 2009) we expected the putative LGCCs described here to also act as homomeric channels. However, it is possible that these subunits coassemble to form heteromeric complexes. Additionally, it is possible that that these channels interact with other compounds. In addition to the biogenic amines tested here, the responses to the classical neurotransmitters, acetylcholine, GABA and glycine as well as biosynthetic intermediates for biogenic amine synthesis should be determined.

To determine how LGCC subunits modulate behavioral outputs, it will be important to analyze the behaviors of mutant animals. We have obtained deletion mutants for all the remaining LGCCs through the *C. elegans* Knockout

Consortium and National Bioresource Project and each has been extensively backcrossed. In combination with the expression profiles, analysis of locomotory, egg laying, feeding, and defecation behaviors in these mutants might provide information on the neural circuits that are modulated by these LGCCs. Application of exogenous biogenic amines can reveal distinct phenotypes, and provide information on the type of behaviors being modulated by a particular receptor. These pharmacological assays can elicit typical behaviors, for example exogenous serotonin stimulates egg laying, pharyngeal pumping and inhibits locomotion. Additionally, there are mutations we can employ which can change the kinetics or reverse the polarity of the channel that could help identify the function of the LGCCs in the nervous system. These genetic and pharmacological studies may identify the effects of a single receptor on behavior and define new roles for biogenic amines and their corresponding ionotropic receptors in the regulation of *C. elegans* behavior.

Figure AI-1

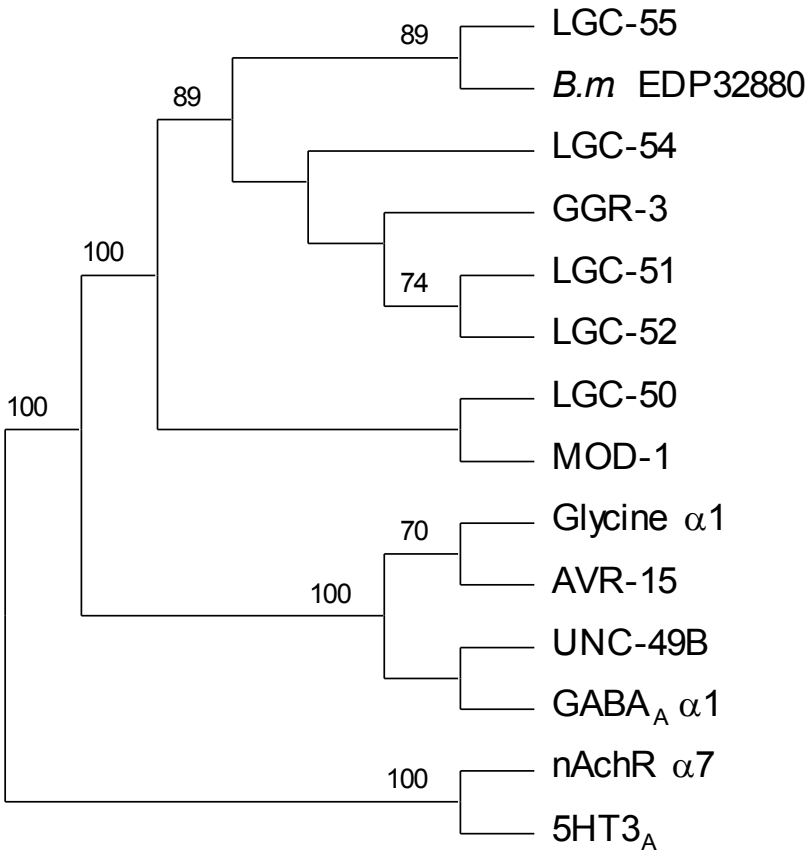

A novel class of cys-loop ligand gated chloride channels (LGCC).

Phylogenetic tree of LGC-55 and various ligand-gated ion channels. Shown are predicted *C. elegans* LGICs, including the 5HT receptor MOD-1, glutamate receptor AVR-15, GABA receptor UNC-49$_B$, the *Brugia malayi* predicted protein EDP32880, and the human GABA$_A\alpha$1, nAchRα7 and 5HT3a.

Table AI-1

Cloned cDNAs	Cloned promoters	*Xenopus* expression vectors	GFP transgenics	*myo-3* transgenics
lgc-50	*lgc-50*	*lgc-50*	*lgc-50*	*lgc-50*
lgc-51	*lgc-51*	*lgc-51*	*lgc-51*	*lgc-51*
lgc-52	*lgc-52*	*lgc-52*		*lgc-52*
lgc-54	*lgc-54*	*lgc-54*	*lgc-54*	*lgc-54*
ggr-3	*ggr-3*	*ggr-3*		*ggr-3*

LGCC reagents generated.

Each LGCC cDNA was isolated from oligo-dT primed cDNA pools and subcloned into the pGEM-T vector. Additionally each cDNA was subcloned into both pSGEM and pTLNII vectors for expression in *Xenopus* oocytes as well as behind the *myo-3* promoter for expression in all muscle cells. The genomic fragment containing each LGCC promoter was cloned into a GFP expression vector. The last two columns indicate which stable transgenic lines were produced for either GFP reporter or muscle cell expression. Stable lines expressing *plgc-52::*GFP*, pggr-3::*GFP*, myo-3::*LGC-51, and *myo-3::*LGC-52 still need to be generated as the time of this thesis publication.

Figure AI-2

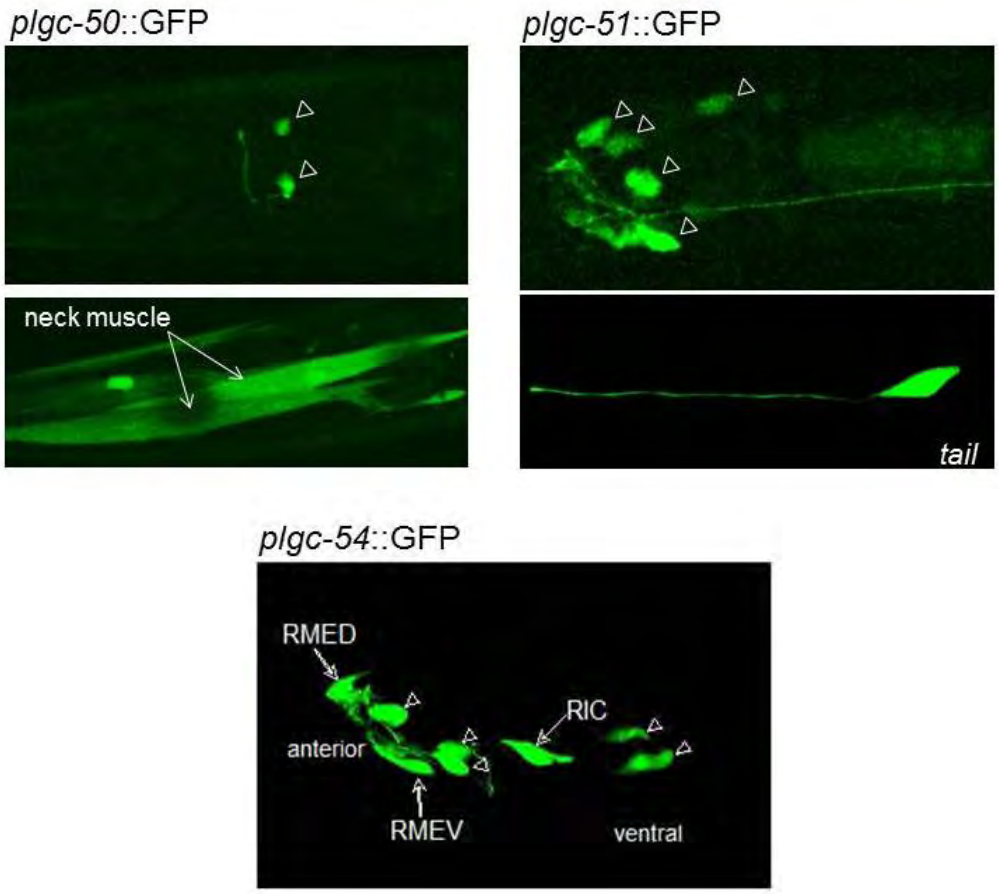

Expression Pattern of LGCCs.

Adult animals showing expression of fluorescent transcriptions reporters. *lgc-50* is expressed in a single pair of neurons in the head (top) as well as head and neck muscles (bottom). *lgc-51* is expressed in at least five pairs of neurons in the head (top) and a single neuron in the tail (bottom). *lgc-54* is expressed in six pairs of neurons in the head, of which we have identified the RIC, REMV and RMED. Anterior is to the left and ventral is down in all images. Muscle cells and identified neurons are indicated, open triangles indicate unidentified neurons. Scale bar, 10 μm.

APPENDIX II

Evolution of Nematode Escape Behavior

The work represented in this Appendix is the preliminary data for a project which aims to explore the evolutionary relationships of nematode escape responses. I performed all the behavioral analysis and isolation of wild soil nematodes and fungus described in this appendix. The introduction highlighting *C. elegans* predator-prey relationship is taken from the peer-reviewed Review article *The Neruoethology of C. elegans escape*, written by myself and Dr. Mark Alkema. This review was published in *Current Opinion in Neurobiology 22(2)* in April, 2012. The immunostaining in figure AII-3 was performed by Jasmim Abraham and Sean Maguire.

Introduction, Results and Discussion

Foraging can expose *C. elegans* to encounters with its natural predators. Nematophagous mites (Karagoz, M., et al., 2007), springtails (Read, D., et al., 2006), water bears (Hohnberg and Traunspurger, 2009) and other predacious nematodes like *Pristionchus pacificus* (Bento, G., et al., 2010) can actively kill and eat nematodes. Nematodes face another lurking foe in their habitat: predacious fungi. These carnivorous fungi, from the family of Orbiliales (Ascomycota), possess hyphal structures to trap nematodes in the soil and decaying organic debris (Duddington, 1951; Thorn and Barron, 1984). One method of capturing nematodes employs adhesive branches, knobs or hyphal nets that stick to, and entangle nematodes. By far the most sophisticated trapping mechanism is the constricting ring. When a worm crawls through the ring gentle friction induces the ring to rapidly inflate and lasso its prey. Predacious fungi form few, if any traps in the absence if nematodes. Trap formation is induced by the presence of nematodes, including *C. elegans* (Xie, et al., 2010), and stimulates the growth of a variety of hyphal traps. Once a nematode is caught by a hyphal trap, death does not come quickly. A prolonged struggle usually only ends when fungal hyphae perforate the cuticle, and absorb the contents of the nematode.

Work from our lab has shown that the escape response elicited by gentle anterior touch is critical for the worm's survival in the presence of these trap forming fungi (Maguire, et al., 2011). Our studies of predator-prey relationships

between *C. elegans* and the constricting ring fungus *Drechslerella doedycoides* showed that the fungus is extremely efficient in entrapping the early larval stages. Wild-type animals survive most encounters with the hyphal noose, while mutants that fail to sense touch or that cannot reverse, are trapped more frequently. Moreover, *lgc-55* mutants, which fail to suppress foraging head movements and execute a long reversal in response to touch, are caught more often than the wild type (Maguire, et al. 2011). We showed that coordination of these motor programs in the *C. elegans* escape response is vitally important to evade fungal predation.

To determine if this escape response was unique to *C. elegans* or if it was a behavior displayed by other soil nematoes we examined the escape responses of other rhabditid nematode species. We found that all rhabditid species tested responded robustly to anterior touch (Figure AII-1). Soil nematodes from the Eurhabditis clade, close relatives of *C. elegans*, display a similar escape response, suppressing head oscillations in response to anterior touch (Figure AII-2). Interestingly, several species from the Pleiorhabditis clade, *M. longespiculosa*, *T. palmarum*, and *P. strongyloides*, fail to coordinate head and body movements in their escape response (Figure AII-2). Furthermore, although these animals failed to suppress head oscillations in response to touch, immunohistochemistry experiments show they have cells that express TDC-1, suggesting they release either octopamine or tyramine (Figure AII-3 and data not shown, personal communication, J. Abraham, and M. Alkema). Further

experiments should be done to determine if these cells are tyraminergic as, it would be interesting to determine how these animals are using tyramine in a manner that is unique compared to other rhabditid nematodes. These Pleiorhabditis species do not exclusively inhabit the soil and are mostly found in parasitic association with insects or mammals. This may indicate that the touch-induced suppression of head movements has evolved from selective pressures imposed by predacious fungi.

Nematodes and predacious fungi that use rings as trapping devices have been found in 100 million year old amber indicating an ancient predator-prey relationship (Schmidt, et al., 2007). To determine if fungi that employ ring traps still inhabit the same soils as nematodes today, we isolated nematodes and fungi that were found in soil samples from the local environment. We took soil from locations in Massachusetts and Rhode Island that were high in decaying material such as, leaf litter and rotting fruits. From our samples, we isolated at least four different species of nematodes and three different species of fungus, including fungi that used trapping rings to capture nematodes (Figure AII-4). These results suggest that more extensive field studies to analyze the ecology of predatory fungi and cohabitating nematodes are possible. These studies will be critical to determine the dynamics of this unique predator-prey relationship. The phylogeny of predacious fungi and morphology of these trapping devices suggest that constricting rings have evolved from non-constricting rings (Li, et al., 2005). This raises the possibility that constricting rings and the suppression of head

movements are the result of an evolutionary arms race. Since we know the molecular and neuronal basis of the escape response in *C. elegans*, comparative studies with other nematodes should allow us to find the selection pressures that shape behavioral adaptation.

Materials and Methods

Nematode Maintenance

Nematodes of the Eurhabditis, Diplogastrids, and Pleiorhabditis clades were maintained at room temperature (19-21ºC) on nematode grow medium (NGM) and fed the *E.coli* strain OP50. *T. palmarum* was maintained on NGM made with 2% agar to prevent burrowing. *P. redivivus* was grown at room temperature room temperature (19-21ºC), in a 60% apple cider vinegar solution supplemented with a slice of apple.

Behavioral Assays

All behavioral assays were done at room temperature (19-21ºC) with young adult animals. Response to anterior touch was quantified by touching each animal in the anterior portion of the body 5 times with an ISI of approximately 5 seconds. A positive response was recorded if the animal stopped movement or accelerated in either direction in response to the touch. At least 30 animals of each species were scored, and shown is the mean % of positive responses.

Suppression of head movements was scored as described in Alkema et al., 2005. At least 50 animals of each species were scored.

Isolation of Wild Nematodes and Fungi

Soil samples were collected decaying debris or compost from Lincoln, Rhode Island and Shrewsbury, Princeton, and Bolton, Massachusetts. The samples were kept in containers at room temperature (19-21ºC) for no longer than 24 hours. To isolate nematodes, soil was sparsely spread on NGM plates seeded with OP50 and moistened with M9 buffer. The samples were incubated covered at room temperature (19-21ºC) for 1-3 days, in order to isolate fertile adult females or hermaphrodites. Animals were picked singly and those that could successfully produce offspring were propagated. Individual species were identified by morphological features and at least one isolate of each species recovered was kept. To isolate fungi, soil was sparsely spread on 1.7% water agar plates and moistened with M9 buffer. The samples were incubated at 20ºC for 3-5 days to allow fungi spores to germinate. Individual species of fungi were identified by morphological features of spores. To produce pure cultures spores from each identifiable species were picked to separate pates. To test if fungi could form traps, starved fungus was plated on water agar and allowed to grow for 7 days. Once the plate was filled with hyphae, nematode suspension was added and allowed to incubate at 20ºC for 24 hours.

Figure AII-1

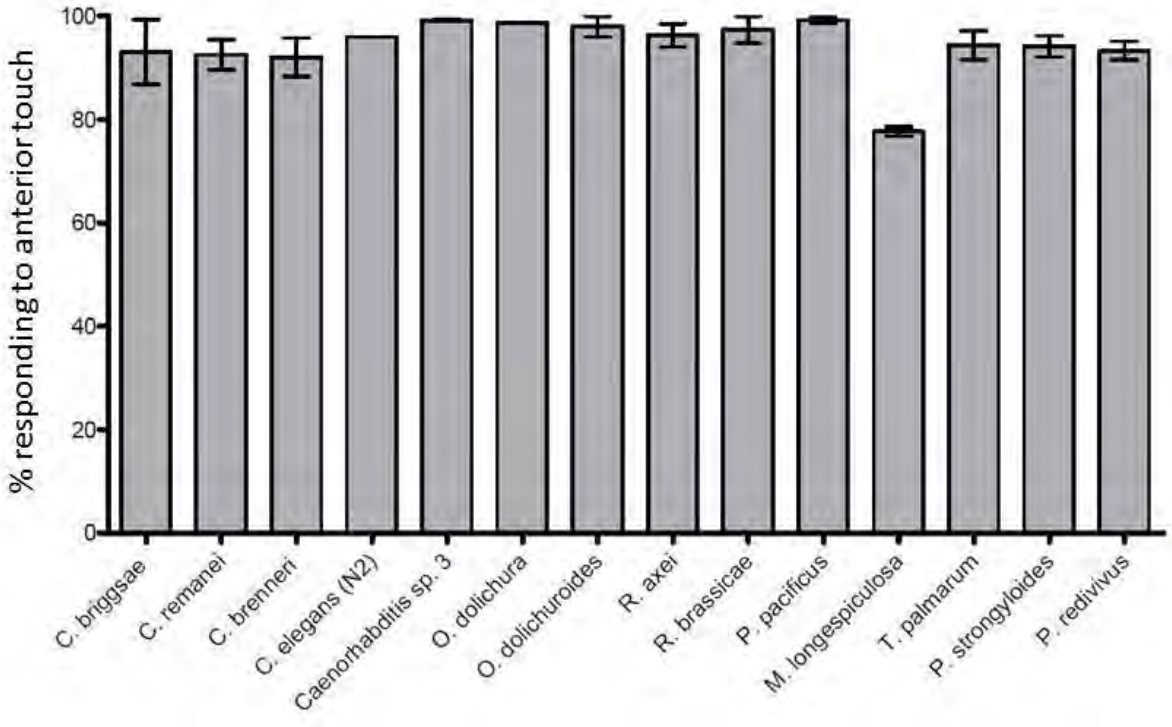

Rahbditid nematodes respond to anterior touch.

Shown is the mean response to five gentle touches to the anterior portion of the body of each species of rabditid nematodes for at least 30 or more animals. All animals respond by either stopping or attempting to escape from the point of stimulus.

Figure AII-2

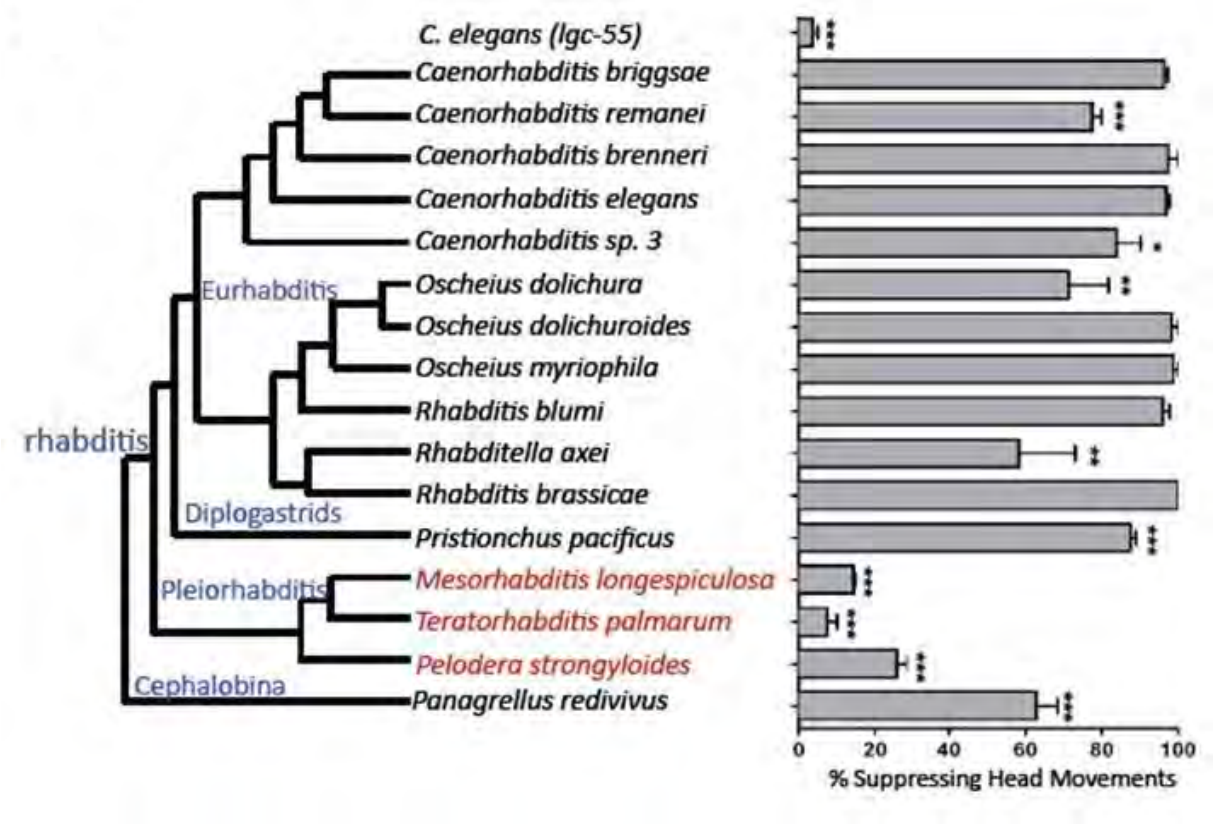

The Pleiorhabditis clade fails to suppress head oscillations during the escape response.

Left: Phylogenetic tree of Rhabditid nematodes. Highlighted in red are the species of the Pleiorhabditis clade that fail to suppress head movements in response to anterior touch. *Panagrellus redivivus* is most distantly related to *C. elegans.*

Right: Suppression of head oscillations in response to anterior touch was scored during the reversal response of at least 30 or more animals of each species. Error bars represent the SEM. Statistical difference from *C. elegans*, *p<0.01, **p<0.001, ***p<0.0001, two-tailed Student's t test.

Figure AII-3

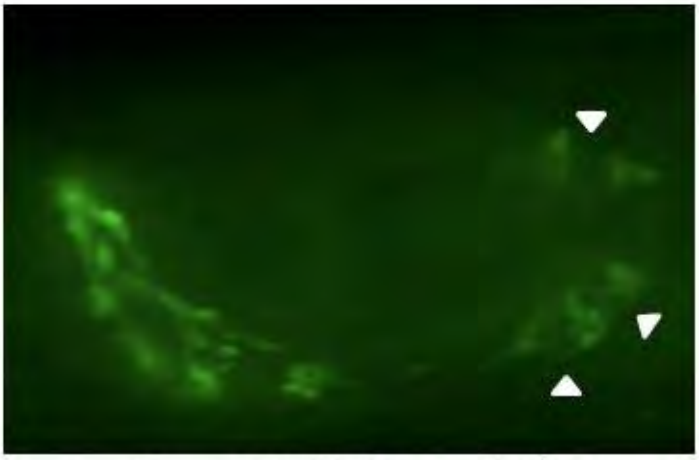

Mesorhabditis longespiculosa

The Pleiorhabditis species, *Mesorhabditis longespiculosa,* has cells that express TDC-1.

Shown is an image of whole mount staining of *Mesorhabditis longespiculosa* with TDC-1 antibodies. TDC-1 is expressed in at least three neurons which send projections to a structure similar to the *C. elegans* nerve ring. Image courtesy of Jasmin Abraham.

Figure AII-4

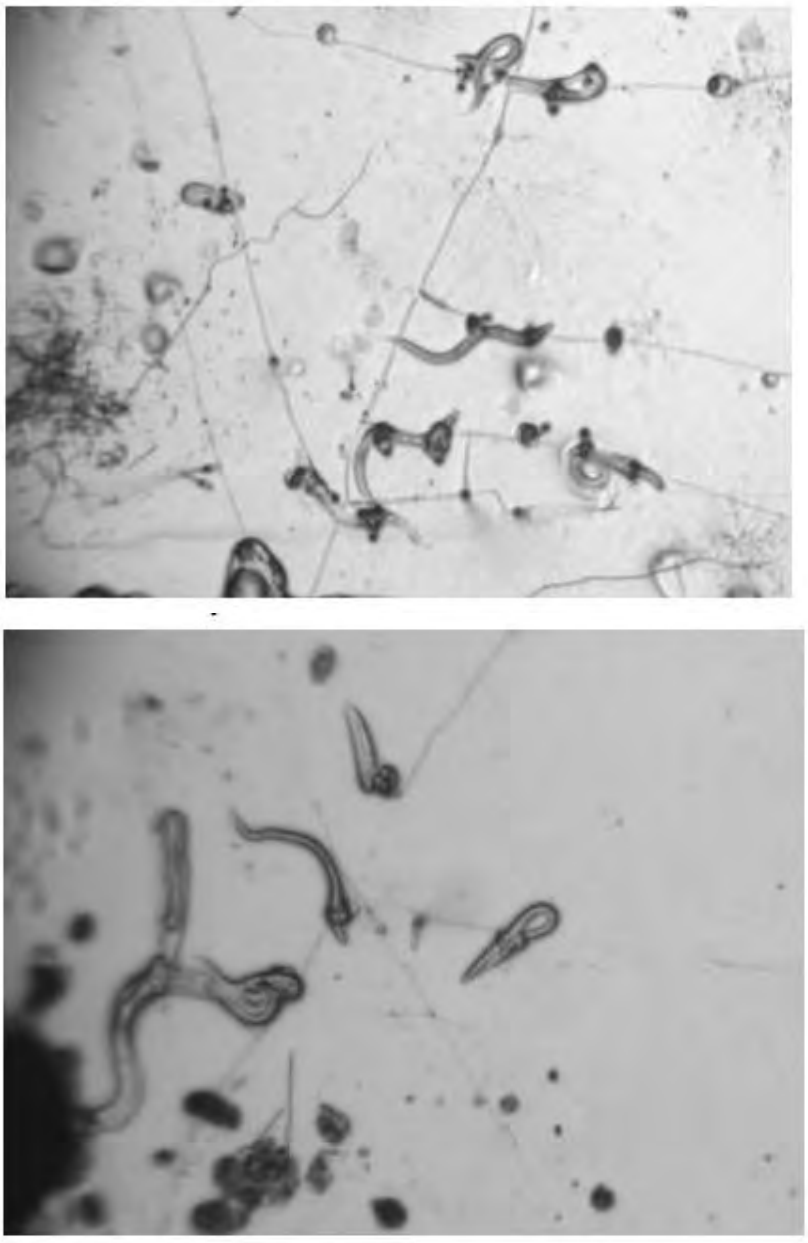

Figure AII-4.

Constricting ring fungi can be isolated from soil samples.

Images of constricting ring fungi and nematodes isolated from local soil samples. This illustrates the active predator-prey relationship between nematodes and fungi in the soil environment.

BIBLIOGRAPHY

Adamo, S. A., Linn, C. E., and Hoy, R. R. (1995). The role of neurohormonal octopamine during 'fight or flight' behaviour in the field crickets *Gryllus bimaculatus*. J Exp Biol *198*, 1691-1700.

Alkema, M. J., Hunter-Ensor, M., Ringstad, N., and Horvitz, H. R. (2005). Tyramine Functions independently of octopamine in the Caenorhabditis elegans nervous system. Neuron *46*, 247-260.

Allen, M. J., Godenschwege, T. A., Tanouye, M. A., and Phelan, P. (2006). Making an escape: development and function of the Drosophila giant fibre system. Semin Cell Dev Biol *17*, 31-41.

Altun-Gultekin, Z., Andachi, Y., Tsalik, E. L., Pilgrim, D., Kohara, Y., and Hobert, O. (2001). A regulatory cascade of three homeobox genes, ceh-10, ttx-3 and ceh-23, controls cell fate specification of a defined interneuron class in C. elegans. Development *128*, 1951-1969.

Avila, F. W., Bloch Qazi, M. C., Rubinstein, C. D., and Wolfner, M. F. (2012). A requirement for the neruomodulators octopamine and tyramine in *Drosophila melanogaster* female sperm storage. Proc Natl Acad Sci USA *109*, 4562-4567.

Bamber, B. A., Beg, A. A., Twyman, R. E., and Jorgensen, E. M. (1999). The Caenorhabditis elegans unc-49 locus encodes multiple subunits of a heteromultimeric GABA receptor. J Neurosci *19*, 5348-5359.

Barrett, C. F., Cao, Y. Q., and Tsien, R. W. (2005). Gating deficiency in a familial hemiplegic migraine type 1 mutant P/Q- type calcium channel. J Biol Chem *280(25)*, 24064-24071.

Barron, G. L. (1977). The Nematode-Destroying Fungi: Topics in Mycobiology. Canadian Biological Publications.

Beg, A. A., and Jorgensen, E. M. (2003). EXP-1 is an excitatory GABA-gated cation channel. Nat Neurosci *6*, 1145-1152.

Beltramo, M., Krieger, M., Calas, A., Franzoni, M. F., and Thibault, J. (1993). Aromatic amino acid decarboxylase (AADC) immunohistochemistry in vertebrate brainstem with an antiserum raised against AADC made in *E. coli*. Brain Res Bull *32(2)*, 123-32.

Ben Ari, Y. (2002). Excitatory actions of GABA during development: the nature of nurture. Nat Rev Neurosci. *3(9)*, 728-739.

Ben Arous, J., Tanizawa, Y., Rabinowitch, I., Chatenay, D., and Schafer, W. R. (2010). Automated imaging of neuronal activity in freely behaving *Caenorhabditis elegans*. J Neurosci Methods *187*, 229-234.

Bendesky, A., Tsunozaki, M., Rockman, M. V., Kruglyak, L., and Bargmann, C. I. (2011). Catecholamine receptor polymorphisms affect decision-making in *C. elegans*. Nature *472*, 313-318.

Bento, G., Ogawa, A., and Sommer, R. J. (2010). Co-option of the hormone-signaling module dafachronic acid-DAF-12 in nematode evolution. Nature *466*, 494-497.

Berry, M. D. (2004). Mammalian central nervous system trace amines. Pharmacologic amphetamines, physiologic neruomodulators. J. Neurochem *90*, 257-271.

Betz, H. (1990). Ligand-gated ion channels in the brain: the amino acid receptor superfamily. Neuron *5*, 383-392.

Blenau, W., and Baumann, A. (2001). Molecular and pharmacological properties of insect biogenic amine receptors: lessons from *Drosophila* melanogaster in *Apis melifera*. Arch Insect Biochem Physiol *48*, 13-38.

Blenau, W., Balfanz, S., and Baumann, A. (2000). Amtyr1: characterization of a gene from honeybee (Apis mellifera) brain encoding a functional tyramine receptor. J Neurochem *74*, 900-908.

Blumenthal, E. M. (2003). Regulation of chloride permeability by endogenously produced tyramine in the *Drosophila* Malpighian tubule. Am J Physiol Cell Physiol *284*, C718-728.

Blumenthal, E. M. (2005). Modulation of tyramine signaling by osmolality in an insect secretory epithelium. Am J Physiol Cell Physiol *289*, C1261-7.

Borowsky, B., Adham, N., Jones, K. A., Raddatz, R., Artymyshyn, R., Ogozalek, K. L., Durkin, M. M., Lakhlani, P. P., Bonini, J. A., Pathirana, S., Boyle, N., Pu, X., Kouranova, E., Lichtblau, H., Ochoa, F. Y., Branchek, T. A., and Gerald, C. (2001). Trace amines: identification of a family of mammalian G protein-coupled receptors. Proc Natl Acad Sci USA *98*, 8966-8971.

Boulton, A. A. (1980). Trace amines and mental disorders. Can J Neurol Sci *7(3)*, 261-263.

Branchek, T. A., and Blackburn, T. P. (2003). Trace amine receptors as targets for novel therapeutics: legend, myth and fact. Curr Opin Pharmacol *3(1)*, 90-97.

Brede, M., Philipp, M., Kanus, A., Muthig, V., and Hein, L. (2004). alpha2-adrenergic receptor subtypes-novel functions uncovered in gene-targeted mouse models. Biol Cell *96*, 343-348.

Brembs, B., Christiansen, F., Pfluger, H. J., and Duch, C. (2007). Flight initiation and maintenance deficits in flies with genetically altered biogenic amine levels. J Neurosci *27*, 11122-11131.

Brenner, S. (1974). The genetics of Caenorhabditis elegans. Genetics *77*, 71-94.

Bunzow, J. R., Sonders, M. S., Arttamangkul, S., Harrison, L. M., Zhang, G., Quigley, D. I., Darland, T., Suchland, K. L., Pasumamula, S., Kennedy, J. L., Olson, S. B., Magenis, R. E., Amara, S. G., and Grandy, D. K. (2001). Amphetamine, 3,4-methylenedioxymethamphetamine, lysergic acid, diethylamine and metabolites of the catecholamine neurotransmitters are agonists of a rat trace amine receptor. Mol Pharmacol *60*, 1181-1188.

Burrell, B. D., and Smith, B. H. (1995). Modulation of the honey bee (*Apis mellifera*) sting response by octopamine. J Insect Physiol *41*, 671-680.

Card, G. and Dickinson, M. (2008). Performance trade-offs in the flight initiation of *Drosophila*. J Exp Biol *211*, 341-353.

Catterall, W. A. (2000). Structure and regulation of voltage-gated Ca^{2+} channels. Annu Rev Cell Dev Biol *16*, 521-555.

Certel, S. J., Savella, M. G., Schlegel, D. C., and Kravitz, E. A. (2007). Modulation of *Drosophila* male behavioral choice. Proc Natl Acad Sci USA *104*, 4706-4711.

Chalfie, M., and Sulston, J. (1981). Developmental genetics of the mechanosensory neurons of Caenorhabditis elegans. Dev Biol *82*, 358-370.

Chalfie, M., Sulston, J. E., White, J. G., Southgate, E., Thomson, J. N., and Brenner, S. (1985). The neural circuit for touch sensitivity in *Caenorhabditis elegans*. J Neurosci *5*, 956-964.

Chalfie, M., Tu, Y., Euskirchen, G., Ward, W. W., and Prasher, D. C. (1994). Green fluorescent protein as a marker for gene expression. Science *263*, 802-805.

Chavas, J., and Marty, A. (2003). Coexistence of excitatory and inhibitory GABA synapses in the cerebellar interneuron network. J Neurosci. *23(6)*, 2019-2031.

Christensen, M., Esteves, A., Yin, X., Fox, R., Morrison, R., McDonnell, M., Gleason, C., Miller, D. M. 3rd, and Strange, K. (2002). A primary cluture system

for functional analysis of *C. elegans* neurons and muscle cells. Neuron *33(4)*, 503-514.

Chronis, N., Zimmer, M., and Bargmann, C. I. (2007). Microfluidics for *in vivo* imaging of neuronal and behavioral activity in *Caenorhabditis elegans*. Nat Methods *4*, 727-731.

Cole, S. H., Carney, G. E., McClung, C. A., Willard, S. S., Taylor, B. J., and Hirsh, J. (2005). Two functional but noncomplementing *Drosophila* tyrosine decarboxylase genes: distinct roles for neural tyramine and octopamine in female fertility. J Biol Chem *280*, 14948-14955.

Cowan, W. M., Südhof, T. C., and Stevens, C. F. (2001). Synapses, Johns Hopkins University Press.

Croll, N. A. (1975a). Behavioural analysis of nematode movement. Adv Parasitol *13*, 71-122.

Croll, N. A. (1975b). Integrated behavior in the feeding phase of *Ceanorhabditis elegans* (Nematoda). J. Zool., Lond. *176*, 159-176.

Cully, D. F., Vassilatis, D. K., Liu, K. K., Paress, P. S., Van der Ploeg, L. H., Schaeffer, J. M., and Arena, J. P. (1994). Cloning of an avermectin-sensitive glutamate-gated chloride channel from *Caenorhabditis elegans*. Nature *371*, 707-711.

D'Andrea, G., Terrazzino, S., Leon, A., Fortin, D., Perini, F., Granella, F., and Bussone, G. (2004). Elevated levels of circulating trace amines in primary headaches. Neurology *62(10)*, 1701-1705.

Dascal, N. (2001). Ion-channel regulation by G-proteins. Trends Endocrinol Metab *12*, 391-398.

Davis, M. W., Hammarlund, M., Harrach, T., Hullett, P., Olsen, S., and Jorgensen, E. M. (2005). Rapid single nucleotide polymorphism mapping in C. elegans. BMC Genomics *6*, 118.

Dent, J. A., Davis, M. W., and Avery, L. (1997). avr-15 encodes a chloride channel subunit that mediates inhibitory glutamatergic neurotransmission and ivermectin sensitivity in *Caenorhabditis elegans*. EMBO J *16*, 5867-5879.

Derkach, V., Surpernant, A., and North, R. A. (1989). 5-HT3 receptors are membrane ion channels. Nature *339*, 706-709.

Donini, A., and Lange, A. B. (2004). Evidence for a possible neurotransmitter/neuromodulator role of tyramine on the locust oviducts. J Insect Physiol *50*, 351-361.

Donnelly, J. L.*, Clark, C. M.*, Leifer, A., Haburcak, M., Pirri, J. K., Francis, M. M., Samuel, A. D., Alkema, M. J. (2013). Monoaminergic orchestration of motorprograms in a complex C. elegans behavior. PLoS Biol, *In Press.*

Duddington, C. L. (1951). The ecology of predacious fungi. I. Preliminary survey. Trans Br Mycol Soc *34*, 322-331.

Dyck, L. E. (1989). Release of some endogenous trace amines from rat striatal slices in the presence and absence of a monoamine oxidase inhibitor. Life Sci *44*, 1149-1156.

Eaton, R.C. (1984). Neural Mechanisms of Startle Behavior, New York: Plenum Press.

Edwards, D. H., Heitler, W. J., and Krasne, F. B. (1999). Fifty years of a command neuron: the neurobiology of escape behavior in the crayfish. Trends Neruosci *22*, 153-161.

Edwards, D. H., Yeh, S. R., Musolf, B. E., Antonsen, B. L., and Krasne, F. B. (2002). Metamodulation of the crayfish escape circuit. Brain Behav Evol *60*, 360-369.

Foreman, M. B., and Eaton, R. C. (1993). The direction change concept for reticulospinal control of goldfish escape. J Neurosci *13*, 4101-4113.

Francis, M. M., and Maricq, A. V. (2006). Electrophysiological analysis of neuronal and muscle function in *C. elegans*. Methods Mol Biol. *351*, 175-192.

Frøkjær-Jensen, C., and Jorgensen, E. M. (2009). Calcium: an insignificant thing. Nat Neurosci *12*, 1213-1214.

Frøkjær-Jensen, C., Kindt, K. S., Kerr, R. A., Suzuki, H., Melnik-Martinez, K., Gerstberih, B., Driscol, M., and Schafer, W. R. (2006). Effects of voltage-gate calcium channel subunit genes on calcium influx in cultured *C. elegans* mechanosensory neurons. J Neurobiol *66(10)*, 1125-1139.

Gally, C., and Bessereau, J. L. (2003). GABA is dispensable for the formation of junctional GABA receptor clusters in *Caenorhabditis elegans*. J Neurosci. *23(7)*, 2591-2599.

Galzi, J. L., Devillers-Thiéry, A., Hussy, N., Bertrand, S., Changeux, J. P., and Betrand, D. (1992). Mutations in the channel domain of a neuronal nicotinic receptor convert ion selectivity from cationic to anionic. Nature *359*, 500-505.

Gargus, J. (2009). Genetic calcium signaling abnormalities in the central nervous system: seizures, migraine and autism. Ann N Y Acad Sci *1151*, 133-156.

Geffeney, S. L., Cueva, J. G., Glauser, D. A., Doll, J. C., Lee, T. H., Montoya, M., Karania, S., Garakani, A. M., Pruitt, B. L., and Goodman, M. B. (2011). DEG/ENaC but not TRP channels are the major mechanoelectrical transduction channels in a *C. elegans* nociceptor. Neuron *71*, 845-857.

Gracheva, E. O., Hadwiger, G., Nonet, M. L., and Richmond , J.E. (2008). Direct interactions between C. elegans RAB-3 and Rim provide a mechanism to target vesicles to the presynaptic density. Neruosci Lett *444(2)*, 137-142.

Gray, J. M., Hill, J. J., and Bargmann, C. I. (2005). A circuit for navigation in Caenorhabditis elegans. Proc Natl Acad Sci USA *102*, 3184-3191.

Green, W. N., and Wanamaker, C. P. (1997). The role of the cystine loop in acetylcholine receptor assembly. J Biol Chem *272*, 20945-20953.

Grutter, T., de Carvalho, L. P., Dufresne, V., Taly, A., Edelstein, S. J., and Changeux, J. P. (2005). Molecular tuning of fast gating in pentameric ligand-gated ion channels. Proc Natl Acad Sci USA *102*, 18207-18212.

Gulledge, A. T., and Stuart, G. J. (2003). Excitatory actions of GABA in the cortex. Neuron *37(2)*, 299-309.

Gunthorpe, M. J., and Lummis, S. C. (2001). Conversion of the ion selectivity of the 5-HT(3a) receptor from cationic to anionic reveals a conserved feature of the ligand-gated ion channel superfamily. J Biol Chem. *276(24)*, 10977-10983.

Guo, Z. V., Hart, A. C., and Ramanathan, S. (2009). Optical interrogation of neural circuits in *Caenorhabditis elegans*. Nat Methods *6*, 891-896.

Hall, D. H., and Russell, R. L. (1991). The posterior nervous system of the nematode *Caenorhabditis elegans*: serial reconstruction of identified neurons and complete pattern of synaptic interactions. J Neruosci *11*, 1-22.

Hall, D., and Altun, Z. F. (2007). C. elegans Atlas, Cold Spring Harbor Laboratory Press).

Hammarlund M, Palfreyman MT, Watanabe S, Olsen S, and Jorgensen EM. (2007). Open syntaxin dock synaptic vesicles. PLoS Biol *5(8)*.

Hammond, S., and O'Shea, M. (2007). Escape flight initiation in the fly. J Comp Physiol A Neuortehol Sens Neural Behav Physiol *193(4)*, 471-476.

Hans, M., Luvisetto, S., Williams, M. E., Spagnolo, M., Urrutia, A., Tottene, A., Brust, P. F., Johnson, E. C., Harpold, M. M., Stauderman, K. A., and Pietrobon, D. (1999). Functional consequences of mutation in the human alpha1A calcium channel subunit linked to familial hemiplegic migraine. J Neurosci *19(5)*, 1610-1619.

Hart, A. C., Sims, S., and Kaplan, J. M. (1995). Synaptic code for sensory modalities revealed by C. elegans GLR-1 glutamate receptor. Nature *378*, 82-85.

Hatton, G. I., and Yang, Q. Z. (2001). Ionotropic histamine receptors and H2 receptors modulate supraoptic oxytocin neuronal excitability and dye coupling. J Neurosci *21*, 2974-2982.

Henwood, R. W., Boulton, A. A., and Phillis, J. W. (1979). Iontophoretic studies of some trace amines in the mammalian CNS. Brain Res *164*, 347-351.

Herberholz, J., Sen, M. M., and Edwards, D. H. (2004). Escape behavior and escape circuit activation in juvenile crayfish during prey-predator interactions. J Exp Biol *207*, 1855-1863.

Hohnberg, K., and Traunspurger, W. (2009). Foraging theory and partial consumption in a tardigrad-nematode system. Behav Ecol *20*, 884-890.

Hombert, U., Seyfarth, J., Binkle, U., and Alkema, M. J. *In Press.* Identification of distinct tyraminergic and octopaminergic neurons innervating the central complex of the desert locust, *Schistocerca gregaria*. J. Com. Neurology.

Hua, J. Y., and Smith, S. J. (2004). Neural activity and the dynamics of central nervous system development. Nature Neuroscience *7*, 327-332.

Imoto, K., Busch, C., Sakmann, B., Mishina, M., Konno, T., Junichi, N., Bujo, H., Mori, Y., Fukuda, K., and Numa, S. (1998). Rings of negatively charged amino acids determine the acetylcholine receptor channel conductance. Nature *335*, 645-648.

Isaac, R. E., MacGregor, D., and Coates, D. (1996). Metabolism and inactivation of neurotransmitters in nematodes. Parasitology *113* Suppl, S157-73.

Jaeger, C. B., Ruggiero, D. A., Albert, V. R., Park D. H., Joh, T. H., and Reis, D. J. (1984). Aromatic L- amino acid decarboxylase in the rat brain: immunocytochemical localization in neurons of the brain stem. Neuroscience *11*, 691-713.

Ji, F., Kanbara, N., and Obata, K. (1999). GABA and histogenesis in fetal and neonatal mouse brain lacking both the isoforms of glutamic acid decarboxylase. Neurosci Res. *33(3)*, 187-194.

Jones, A. K., and Sattelle, D. B. (2004). Functional genomics of the nicotinic acetylcholine receptor gene family of the nematode, *Caenorhabditis elegans*. Bioessays *26*, 39-49.

Jones, A. K., and Sattelle, D. B. (2008). The cys-loop ligand-gated ion channel gene superfamily of the nematode, Caenorhabditis elegans. Invert Neurosci *8*, 41-47.

Kaeser, P. S., Deng, L., Wang, Y., Dulubova, I., Liu, X., Rizo, J., and Südhof, T. C. (2011). RIM proteins tether Ca2+ channels to presynaptic active zones via a direct PDZ-domain interaction. Cell *144(2)*, 282-295.

Karagoz, M., Gulcu, B., Cakmak, I., Kaya, H. K., and Hazir, S. (2007). Predation of entomopathogenic nematodes by Sancassania sp (Acari: Acaridae). Exp Appl Acarol *43(2)*, 85-95.

Karlin, A., and Akabas, M. H. (1995). Toward a structural basis for the function of nicotinic acetylcholine receptors and their cousins. Neuron *15*, 1231-1244.

Katz, P. S. (1998). Neuromodulation intrinsic to the central pattern generator for escape swimming in *Tritonia*. Ann N Y Acad Sci *860*, 181-188.

Katz, P. S., Getting, P. A., and Frost, W. N. (1994). Dynamic neuromodulation of synaptic strength intrinsic to a central pattern generator circuit. Nature *367*, 729-731.

Kawano, T., Po, M. D., Gao, S., Leung, G., Ryu, W. S., and Zhen M. (2011). An imbalancing act: gap junctions reduce the backward motor circuit activity to bias *C. elegans* for forward locomotion. Neuron *72*, 572-586.

Keramidas, A., Moorhouse, A. J., French, C. R., Schofield, P. R., and Barry, P. H. (2000). M2 pore mutations convert the glycine receptor channel from being anion- to cation- selective. Biophys J. *79(1)*, 247-249.

Kitahama, K., Araneda, S., Geffard, M., Sei, H., and Okamura, H. (2005). Tyramine-immunoreactive neuronal structures in the rat brain: abundance in the median eminence of the mediobasal hypothalamus. Neurosci Lett *383*, 215-219.

Koelle, M. R., and Horvitz, H. R. (1996). EGL-10 regulates G protein signaling in the C. elegans nervous system and shares a conserved domain with many mammalian proteins. Cell *84(11)*, 115-125.

Korn, H., and Faber, D. S. (2005). The Mauthner cell half a century later: a neurobiological model for decision-making? Neuron *47*, 13-28.

Kravitz, E. A. (1988). Hormonal control of behavior: amines and the biasing of behavioral output in lobsters. Science *241*, 1775-1781.

Kutsukake, M., Komatsu, A., Yamamoto, D., and Ishiwa-Chigusa, S. (2000). A tyramine receptor gene mutation causes a defective olfactory behavior in *Drosophila melanogaster*. Gene *245*, 31-42.

Lackner, M. R., Nurrish, S. J., and Kaplan, J. M. (1999). Facilitation of synaptic transmission by EGL-30 Gqalpha and EGL-8 PLCbeta: DAG binding to UNC-13 is required to stimulate acetylcholine release. Neuron *24(2)*, 335-346.

Lainé, V., Frøkjær-Jensen, C., Couchoux, H., and Jospin, M. (2011). The alpha1 subuint EGL-19, the alpha2/delta subunit UNC-36, and the beta subunit CCB-1 underlie voltage-depenent calcium currents in *Caenorhabditis elegans* striated muscle. J Biol Chem *286(41)*, 36180-36187.

Langosch, D., Laube, B., Rundström, N., Schmieden, V., Bormann, J., and Betz, H. (1994). Decreased agonist affinity and chloride conductance of mutant glycine receptors associated with human hereditary hyperekplexia. EMBO *13(18)*, 4223-4228.

Lee, R. Y., Lobel, L., Hengartner, M., Horvitz, H. R., and Avery, L. (1997). Mutations in the alpha1 subunit of an L-type voltage-activated Ca^{2+} channel cause myotonia in *Caenorhabditis elegans*. EMBO *16(20)*, 6066-6076.

Leifer, A. M., Fang-Yen, C., Gershow, M., Alkema, M. J., and Samuel, A. D. (2011). Optogenetic manipulation of neural activity in freely moving *Caenorhabditis elegans*. Nat Methods *8*, 147-152.

Li, Y., Hyde, K. D., Jeewon, R., Cai, L., Vijaykrishna, D., and Zhang, K. (2005). Phylogenetics and evolution of nematode-trapping fungi (Orbiliales) estimated from nuclear and protein coding genes. Mycologia *97*, 1034-1046.

Lin, X. G., Ming, M., Chen, M. R., Niu, W. P., Zhang, Y. D., Liu, B., Jiu, Y. M., Yu, J. W., Xu, T., and Wu, Z. X. (2010). **UNC-31**/CAPS docks and primes dense core vesicles in *C. **elegans*** neurons. Biochem Biophys Res Commun. *397(3)*, 526-531.

Maguire, S. M., Clark, C. M., Nunnari, J., Pirri, J. K., and Alkema, M. J. (2011). The *C. elegans* touch response facilitates escape from predacious fungi. Curr Biol *21*, 1326-1330.

Mahoney, T. R., Luo, S., and Nonet, M. L. (2006). Analysis of synaptic transmission in *Caenorhabditis elegans* using an aldicarb-sensitivity assay. Nat Protoc *1(4)*, 1772-1777.

Marder, E., and Bucher, D. (2001). Central pattern generators and the control of rhythmic movements. Curr Biol *11*, R986-96.

Marella, S., Fischler, W., Kong, P., Asgarian, S., and Scott, K. (2006). Imaging taste responses in the fly brain reveals a functional map of taste category and behavior. Neuron *49(2)*, 285-295.

Maricq, A. V., Peckol, E., Driscoll, M., and Bargmann, C. I. (1995). Mechanosensory signalling in C. elegans mediated by the GLR-1 glutamate receptor. Nature *378*, 78-81.

Maricq, A. V., Peterson, A. S., Brake, A. J., Myers, R. M., and Julius, D. (1991). Primary structure and functional expression of the 5HT3 receptor, a serotonin-gate ion channel. Science *254*, 432-437.

Mathews, E. A., García, E., Santi, C. M., Mullen, G. P., Thacker, C., Moerman, D. G., and Snutch, T. P. (2003). Critical residues of the *Caenorhabditis elegans unc-2* voltage-gated calcium channel that affect behavioral and physiological properties. J Neurosci *23(16)*, 6537-6545.

McClung, C., and Hirsh, J. (1999). The trace amine tyramine is essential for sensitization to cocaine in *Drosophila*. Curr Biol *9*, 853-860.

McIntire, S. L., Jorgensen, E., Kaplan, J., and Horvitz, H. R. (1993). The GABAergic nervous system of Caenorhabditis elegans. Nature *364*, 337-341.

Mellem, J. E., Brockie, P. J., Madsen, D. M., and Maricq, A. V. (2008). Action potentials contribute to neuronal signaling in C. elegans. Nat Neurosci *11*, 865-867.

Menard, C., Horvitz, H. R., and Cannon, S. (2005). Chimeric mutations in the M2 segments of the 5-hydroxytrptamine- gated chloride channel MOD-1 define a minimal determinant of anion/cation permeability. J Biol Chem. *280(30)*, 27502-27507.

Mendel, J. E., Korswagen, H. C., Liu, K. S., Hajdu-Cronin, Y. M., Simon, M. I., Plasterk, R. H., and Sternberg, P. W. (1995). Participation of the protein Go in multiple aspects of behavior in *C.elegans.* Science *267*, 1652-1655.

Mennerick, M., and Zourmski, C. F. (2000). Neural activity and survival in the developing nervous system. Molecular Neruobiology *22*, 41-54.

Miller, G. M., Verrico, C. D., Jassen, A., Konar, M., Yang, H., Panas, H., Bahn, M., Johnson, R., and Madras, B. K. (2005). Primate trace amine receptor 1 modulation by the dopamine transporter. J Pharmacol Exp Ther *313*, 983-994.

Miller, K. G., Alfonso, A., Nguyen, M., Crowell, J. A., Johnson, C. D., and Rand, J. B. (1996). A genetic selection for *Caenorhabditis elegans* synaptic transmission mutants. PNAS *93(22)*, 12593-12598.

Miller, K. G., Emerson, M. D., and Rand, J. B. (1999). Goalpha and diacylglycerol kinase negatively regulate the Gqalpha pathway in *C. elegans*. Neuron *24(2)*, 323-333.

Miller, K. G., Emerson, M. D., McManus, J. R., and Rand, J. B. (2000). RIC-8 (Synembryn): a novel conserved protein that is required for G(q)alpha signaling in the C. elegans nervous system. Neruon *27(2)*, 289-299.

Misgeld, T., Burgess, R. W., Lewis, R. M., Cunningham, J. M., Lichtman, J. W., and Sanes, J. R. (2002). Roles of neurotransmitter in synapse formation: development of neuromuscular junctions lacking choline acetyltransferase. Neuron *36(4)*, 635-648.

Monastrioti, M., Linn, C. E. Jr., and White, K. (1996). Characterization of *Drosophila* tyramine beta-hydroxylase gene and isolation of mutant flies lacking octopamine. J Neurosci *16*, 3900-3911.

Mueller, K. L., Hoon, M. A., Erlenbach, I., Chandrashekar, J., Zuker, C. S., and Ryba, N. (2005). The receptors and coding logic for bitter taste. Nature *434*, 225-229.

Mullen, G. P., Mathews, E. A., Saxena, P., Fields, S. D., McManus, J. R., Moulder, G., Barstead, R. J., Quick, M. W., and Rand, J. B. (2006). The Caenorhabditis elegans snf-11 gene encodes a sodium-dependent GABA transporter required for clearance of synaptic GABA. Mol Biol Cell *17*, 3021-3030.

Nagaya, Y., Kutsukake, M., Chiqusa, S. I., and Komatsu, A. (2002). A trace amine, tyramine, functions as a neuromodulator in *Drosophila melanogaster*. Neurosci Lett *329*, 324-328.

Nonet, M. L., Grundahl, K., Meyer, B. J., and Rand, J. B. (1993). Synaptic function is impaired but not eliminated in C. elegans mutants lacking synaptotagmin. Cell *73(7)*, 1291-1305.

Nusbaum, M. P., and Beenhakker, M. P. (2002). A small-systems approach to motor pattern generation. Nature *417*, 343-350.

O'Hagan, R., Chalfie, M., and Goodman, M. B. (2005). The MEC-4 DEG/ENaC channel of *Caenorhabditis elegans* touch receptor neurons transduces mechanical signals. Nat Neurosci *8*, 43-50.

Ohta, H., Utsumi, T., and Ozoe, Y. (2003). B96Bom encodes a Bombyx mori tyramine receptor negatively coupled to adenylate cyclase. Insect Mol Biol *12,* 271-223.

Okkema, P. G., Harrison, S. W., Plunger, V., Aryana, A., and Fire, A. (1993). Sequence requirements for myosin gene expression and regulation in *Caenorhabditis elegans*. Genetics *135*, 385-404.

Ortells, M. O., and Lunt, G. G. (1995). Evolutionary history of the ligand-gated ion-channel superfamily of receptors. Trends Neurosci *18*, 121-127.

Owens, D. F., and Kriegstein, A. R. (2002). Is there more to GABA than synaptic inhibition? Nat Rev Neurosci. *3(9)*, 715-727.

Paton, W. D. (1958). Central and synaptic transmission in the nervous system; pharmacological aspects. Annu Rev Physiol *20*, 431-470.

Phelan, P., Nakagawa, M., Wilkin, M. B., Moffat, K. G., O'Kane, C. J., Davies, J. A., and Bacon, J. P. (1996). Mutations in shaking-B prevent electrical synapse formation in the Drosophila giant fiber system. J Neurosci *16*, 1101-1113.

Piedras-Renteria, E. S., Watase, K., Harata, N., Zhuchenko, O., Zoghbi, H. Y., Lee, C. C., and Tsien, R. W. (2001). Increased expression of alpha 1A Ca2+ channel currents arising from expanded trinucleotide repeats in spinocerebellar ataxia type 6. J Neurosci *21(23)*, 9185-9193.

Pirri, J. K., McPherson, A. D., Donnelly, J. L., Francis, M. M., and Alkema, M. J. (2009). A tyramine-gated chloride channel coordinates distinct motor programs of a *Caenorhabditis elegans* escape response. Neuron *62(4)*, 526-538.

Putrenko, I., Zakikhani, M., and Dent, J.A. (2005). A family of acetylcholine-gated chloride channel subunits in *Caenorhabditis elegans*. J Biol Chem *280*, 6392-6398.

Ranganathan, R., Cannon, S. C., and Horvitz, H. R. (2000). MOD-1 is a serotonin-gated chloride channel that modulates locomotory behaviour in C. elegans. Nature *408*, 470-475.

Rao, V. T., Accardi, M. V., Siddigui, S. Z., Beech, R. N., Prichard R. K., and Forrester, S. G. (2010). Characterization of a novel tyramine-gated chloride channel from *Haemonchus contortus*. Mol Biochem Parasitol *173*, 64-68.

Read, D. S., Sheppard, S. K., Bruford, M. W., Glen, D. M., and Symondson, W. O. (2006). Molecular detection of predation by soil micro-arthropods on nematodes. Mol Ecol *15*, 1963-1972.

Rex, E., and Komuniecki, R. W. (2002). Characterization of a tyramine receptor from *Caenorhabditis elegans*. J Neurochem *82*, 1352-1359.

Rex, E., Hapiak, V., Hobson, R., Smith, K., Xiao, H., and Komuniecki, R. (2005). TYRA-2 (F01E11.5): a *Caenorhabditis elegans* tyramine receptor expressed in the MC and NSM pharyngeal neurons. J Neurochem *94, 181-191.*

Ringstad, N., Abe, N., and Horvitz, H. R. (2009). Ligand-gated chloride channels are receptors for biogenic amines in *C. elegans*. Science *325*, 96-100.

Roeder, T. (1999). Octopamine in invertebrates. Prog Neurobiol *59*, 533-561.

Roeder, T. (2005). Tyramine and octopamine: ruling behavior and metabolism. Annu Rev Entomol *50*, 447-477.

Roeder, T., Seifert, M., Kähler, C., and Gewecke, M. (2003). Tyramine and octopamine: antagonistic modulators of behavior and metabolism. Arch Insect Biochem Physiol *54*, 1-13.

Sagasti, A., Hobert, O., Troemel, E. R., Ruvkun, G., and Bargmann, C. I. (1999). Alternative olfactory neuron fates are specified by the LIM homeobox gene lim-4. Genes Dev *13*, 1794-1806.

Saheki, Y., and Bargmann, C. I. (2009). Presynaptic CaV2 calcium channel traffic requires CALF-1 and the alpha(2)delta subunit UNC-36. Nat Neurosci *12(10)*, 1257-1265.

Saudou, F., Amlaiky, N., Plassat, J. L., Borrelli, E., and Hen, R. (1990). Cloning and characterization of a *Drosophila* tyramine receptor. EMBO J *9,* 3611-3617.

Schafer, W. R., and Kenyon, C. J. (1995). A calcium-channel homologue required for adaptation to dopamine and serotonin in *Caenorhabditis elegans*. Nature *375*, 73-78.

Schafer, W. R., Sanchez, B. M., and Kenyon, C. J. (1996). Genes affecting sensitivity to serotonin in *Caenorhabditis elegans*. Genetics *143(3)*, 1219-1230.

Schmidt, A. R., Dorfelt, H., and Perrichot, V. (2007). Carnivorous fungi from Cretaceous amber. Science *318*, 1743.

Schneider, A., Ruppert, M., Hendrich, O., Giang, T., Ogueta, M., Hampel, S., Vollbach, M., Büschges, A., and Scholz, H. (2012). Neuronal basis of innate olfactory attraction to ethanol in *Drosophila*. PLoS One *doi:10.1371/journal.pone.0052007*.

Schuske, K., Beg, A. A., and Jorgensen, E. M. (2004). The GABA nervous system in *C. elegans*. Trends Neurosci *27*, 407-414.

Ségalat, L., Elkes, D. A., and Kaplan, J. M. (1995). Modulation of serotonin-controlled behaviors by Go in *Caenorhabditis elegans*. Science *267*, 1648-1651.

Serra, S. A., Fernàndez-Castillo, N., Macaya, A., Cormand, B., Valverde, M. A., and Fernàndez- Fernàndez, J. M. (2008). The hemiplegic migraine-associated Y1245C mutation in CACNA1A results in a gain of channel function due to its effect on the voltage sensor and G-protein-mediated inhibition. Eur J Physiol *458(3)*, 489-502.

Shaner, N. C., Campbell, R. E., Steinbach, P. A., Giepmans, B. N., Palmer, A. E., and Tsien, R. Y. (2004). Improved monomeric red, orange and yellow fluorescent proteins derived from Discosoma sp. red fluorescent protein. Nat Biotechnol *22*, 1567-1572.

Shatz, C. J., and Stryker, M. P. (1988). Prenatal tetrodotoxin infusion blocks segregation of retinogeniculate afferents. Science *242*, 87-89.

Shtonda, B., and Avery, L. (2005). CCA-1, EGL-19, and EXP-2 currents shape action potentials in the *Caenorhabditis elegans* pharynx. J Exp Biol *208*, 2177-2190.

Singer, D., Biel, M., Lotan, I., Flokerzi, V., Hofmann, F., and Dascal, N. (1991). The roles of the subunits in the function of the calcium channel. Science *253*, 1553-15557.

Splawski, I., Timothy, K. W., Sharpe, L. M., Decher, N., Kumar, P., Bloise, R., Napolitano, C., Schwartz, P. J., Joseph, R. M., Condouris, K., Tager-Flusberg, H., Priori, S. G., Sanquinetti, M. C., and Keating, M. T. (2004). Ca(V)1.2 calcium channel dysfunction causes a multisystem disorder including arrhythmia and autism. Cell *119(1)*, 19-31.

Steger, K. A., Shtonda, B. B., Thacker, C., Snutch, T. P., and Avery, L. (2005). The *C. elegans* T-type calcium channel CCA-1 boosts neuromuscular transmission. J Exp Biol *208*, 2191-2203.

Stevenson, P. A., Dyakonova, V., Rillich, J., and Schildberger, K. (2005). Octopamine and experience-dependent modulation of aggression in crickets. J Neurosci *25*, 1431-1441.

Stirman, J. N., Crane, M. M., Husson, S. J., Wabnig, S., Schultheis, C., Gottschalk, A., and Lu, H. (2011). Real-time multimodal optical control of neurons and muscles in freeling behaving *Caenorhabditis elegans*. Nat Methods *8*, 153-158.

Tanouye, M. A., and Wyman, R. J. (1980). Motor outputs of giant nerve fiber in Drosophila. J Neurophysiol *44*, 405-421.

Thorn, R. G., and Barron, G. L. (1984). Carnivorous Mushrooms. Science *224*, 76-78.

Tottene, A., Pivotto, F., Fellin, T., Cesetti, T., van den Maagdenberg, A. M., and Pietrobon, D. (2005). Specific kinetic alterations of human CaV2.1 calcium channels produced by mutation S218L causing familial hemiplegic migraine and delayed cerebral edema and coma after minor head trauma. J Biol Chem *280(18)*, 17678-17686.

Troemmel, E. R, Kimmel, B. E., and Bargmann, C. I. (1997). Reprogramming chemotaxis responses: sensory neurons define olfactory preferences in *C. elegans.* Cell *91(2)*, 161-169.

Tsalik, E. L., Niacaris, T., Wenick, A. S., Pau, K., Avery, L., and Hobert, O. (2003). LIM homeobox gene-dependent expression of biogenic amine receptors in restricted regions of the C. elegans nervous system. Dev Biol *263*, 81-102.

Varsheny, L. R., Chen, B. L., Paniagua, E., Hall, D. H., Chklovskii, D. B. (2011). Structural properties of the *Caenorhabditis elegans* neuronal network. PLoS Comput Biol, doi: 10.1371/journal.pcbi.1001066.

Weber, W. (1999). Ion currents of Xenopus laevis oocytes: state of the art. Biochim Biophys Acta *1421*, 213-233.

Weimer, R.M., Gracheva, E.O., Meyrignac, O., Miller, K. G., Richmond ,J. E., and Bessereau, J. L. (2006). UNC-13 and UNC-10/rim localize synaptic vesicles to specific membrane domains. J Neruosci *26(31)*, 8048-8047.

Wes, P. D., and Bargmann, C. I. (2001). *C. elegans* odour discrimination requires asymmetric diversity in olfactory neurons. Nature *410*, 698-701.

White, J. G., Southgate, E., Thomson, J. N., and Brenner, S. (1986). The structure of the of the nervous system of the nematode Caenorhabditis elegans. Philos Trans R Soc Lond B Biol Sci *314*, 1-340.

Wicks, S. R., Yeh, R. T., Gish, W. R., Waterston, R. H., and Plasterk, R. H. (2001). Rapid gene mapping in Caenorhabditis elegans using a high density polymorphism map. Nat Genet *28*, 160-164.

Willows, A. O., Dorsett, D. A., and Hoyle, G. (1973). The neuronal basis of behavior in Tritonia: Neuronal mechanisms of a fixed action pattern. J Neurobiol *4*, 255-285.

Wotring, V. E., Miller, T. S., and Weiss, D. S. (2003). Mutations at the GABA receptor selectivity filter: a possible role for effective charges. J Physiol. *548*, 527-540.

Wragg, R. T., Hapiak, V., Miller, S. B., Harris, G. P., Gray, J., Komuniecki, P. R., and Komuniecki, R. W. (2007). Tyramine and octopamine independently inhibit serotonin-stimulated aversive behaviors in Caenorhabditis elegans through two novel amine receptors. J Neurosci *27*, 13402-13412.

Xie, H., Aminuzzaman, F. M., Xu, L., Lai, Y., Li, F., and Liu, X. (2010). Trap induction and trapping in eight nemaptode-trapping fungi (Orbiliaceae) as affected by juvenile stage of *Caenorhabditis elegans*. Mycopatologia *169*, 467-473.

Yamamoto, N., and López-Bendito, G. (2012). Shaping brain connections through spontaneous neural activity. Eur J Neruosci *35(10)*, 1595-15604.

Zamponi, G. W., and Snutch, T. P. (1998). Modulation of voltage-dependent calcium channels by G proteins. Curr Opin Neurobiol *8*, 351-356.

Zhao, B., Khare, P., Feldman, L., and Dent, J. A. (2003). Reversal frequency in Caenorhabditis elegans represents an integrated response to the state of the animal and its environment. J Neurosci *23*, 5319-5328.

Zhao, G. Q., Zhang, Y., Hoon, M. A., Chandrashekar, J., Erlenbach, I., Ryba, N. J., and Zuker, C. S. (2003). The receptors for mammalian sweet and umami taste. Cell *115(3)*, 255-266.

Zheng, Y., Brockie, P. J., Mellem, J. E., Madsen, D. M., and Maricq, A. V. (1999). Neuronal control of locomotion in *C. elegans* is modified by a dominant mutation in the GLR-1 ionotropic glutamate receptor. Neuron *24*, 347-361.

Zhou, C., Rao, Y., Rao, Y. (2008). A subset of octopaminergic neurons are important for *Drosophila* aggression. Nat Neurosci *11*, 1059-1067.

Zhu, Z. T., Munhall, A. C., and Johnson, S. W. (2007). Tyramine excites rat subthalamic neurons in vitro by a dopamine-dependent mechanism. Neuropharmacology *52*, 1169-1178.

Zumstein, N., Forman, O., Nongthomba, U., Sparrow, J. C., and Elliott, C. J. (2004). Distance and force production during jumping in wild-type and mutant Drosophila melanogaster. J Exp Biol *207*, 3515-3522.